uOttawa

L'Université canadienne
Canada's university

FACULTÉ DES ÉTUDES SUPÉRIEURES ET POSTOCTORALES

uOttawa

L'Université canadienne
Canada's university

FACULTY OF GRADUATE AND POSDOCTORAL STUDIES

Purva Wagh

AUTEUR DE LA THÈSE / AUTHOR OF THESIS

M.Sc. (Cellular and Molecular Medicine)

GRADE / DEGREE

Department of Cellular and Molecular Medicine

FACULTÉ, ÉCOLE, DÉPARTEMENT / FACULTY, SCHOOL, DEPARTMENT

Functional Analysis of Two Novel Zebrafish Genes Involved in the Formation of Actinotrichia During Fin Development and Regeneration

TITRE DE LA THÈSE / TITLE OF THESIS

Dr. M-A. Akimenko

DIRECTEUR (DIRECTRICE) DE LA THÈSE / THESIS SUPERVISOR

CO-DIRECTEUR (CO-DIRECTRICE) DE LA THÈSE / THESIS CO-SUPERVISOR

EXAMINATEURS (EXAMINATRICES) DE LA THÈSE / THESIS EXAMINERS

Dr. M. Ekker

Dr. K. Turksen

Gary W. Slater

Le Doyen de la Faculté des études supérieures et postdoctorales / Dean of the Faculty of Graduate and Postdoctoral Studies

FUNCTIONAL ANALYSIS OF TWO NOVEL ZEBRAFISH GENES INVOLVED IN THE FORMATION OF ACTINOTRICHIA DURING FIN DEVELOPMENT AND REGENERATION

By

Purva Wagh

Thesis submitted to the
Faculty of Graduate and Postdoctoral Studies
in partial fulfillment of the requirements for the degree of

Master of Science

In Cellular and Molecular Medicine

Department of Cellular and Molecular Medicine
Faculty of Medicine
University of Ottawa

Your file Votre référence
ISBN: 978-0-494-50933-3
Our file Notre référence
ISBN: 978-0-494-50933-3

ABSTRACT

In a screen for genes differentially expressed during fin regeneration in adult zebrafish, two novel genes, *2-H06* and *2-F11*, belonging to the same family coding for secreted proteins with unknown function, were identified. Besides their expression during fin regeneration, they are specifically expressed in the embryonic fins of zebrafish. During development, their expression is restricted to the developing fin folds of both paired and unpaired fins. Searches of the current genomic databases did not reveal any orthologs of *2-H06* or *2-F11* genes in tetrapods, plants and invertebrates species. However, orthologs of the genes are found in other teleost fish like the puffer fish *Takifugu rubripes* (fugu), *Tetraodon nigroviridis* and the Medaka fish (*Oryzias latipes*), and in the cartilaginous fish, elephant shark (*Callorhinchus milii*). In zebrafish embryos, around hatching time, the first component of the fin exoskeleton is seen. It is made of two layers of collagenous fibrils called actinotrichia. These fibrils are only present in fish fins and their appearance correlates with the onset of the developmental divergence between fish paired fin buds and higher vertebrate limb buds. Functional analysis was performed using the gene "knock-down" approach by injection of morpholino oligonucleotides in 1-cell-stage zebrafish embryos. It revealed no significant defects when the morpholino of each gene was injected individually but co-injection of both of the morpholinos induced a complete absence of the actinotrichia, which led to the fin fold losing its structural integrity. Moreover, rescue analysis performed by co-injecting single stranded mRNA (*2-H06* or *2-F11*) with the two morpholinos in embryos confirmed that the absence of actinotrichia was a defect specific to the knockdown of the *2-H06* and *2-F11* genes. The results of this

study suggest that these two genes encode structural proteins of the actinotrichia and loss of this gene family in species other than fish maybe one of the causes or consequences of the evolutionary transition from fins to limbs.

TABLE OF CONTENTS

LIST OF FIGURES AND TABLES

LIST OF ABBREVIATIONS

2-F11-MO	2-F11 morpholino
2-H06-MO	2-H06 morpholino
aa	Amino acids
AB	Avidin-Biotin-Peroxidase complex
AER	Apical ectodermal ridge
AP	Alkaline Phosphatase
BAC	Bacterial artificial chromosomes
BCIP	5'-bromo-4'-chloro-3'-indolyl phosphate
bmp2b	Bone morphogenetic protein 2b
BSA	Bovine serum albumin
cDNA	Complementary deoxyribonucleic acid
C-ter	C-terminal end
DAB	3,3'-diaminobenzidine
DDRT-PCR	Differential display reverse transcriptase polymerase chain reaction
DEPC	Diethyl pyrocarbonate
dpa	Days post amputation
dpf	Days post fertilization
ECM	Extra cellular matrix
EDTA	Ethylenediaminetetraacetic acid
EGFP	Enhanced green fluorescent protein
EST	Expressed sequence tag
ff	Fin fold
fgf	Fibroblast frowth factor
GAG	Glycosaminoglycans
hox	Homeobox containing gene
hpf	Hours post fertilization
ISH	*In situ* hybridization
kD	Kilo Daltons
lfc	Lepidotrichia forming cells
LG	Linkage group
mff	Median fin fold
MO	Morpholino

mpf	Months post fertilization
mRNA	Messenger ribonucleic acid
NBT	Nitroblue tetrazolium
N-ter	N-terminal end
PAC	P1-based artificial chromosome
PBS	Phosphate buffered saline
PBST	Phosphate buffered saline tween
PFA	Paraformaldehyde
ptc-1	Patched-1, gene
PZ	Progress zone
RA	Retinoic acid
RNA	Ribonucleic acid
RT-PCR	Reverse transcription polymerase chain reaction
SDS-PAGE	Sodium dodecyl sulfate polyacrylamide gel electrophoresis
SHH	Sonic hedgehog, protein
shh	Sonic hedgehog, gene
SSH	Suppression subtractive hybridization
TBST	Tris-HCl-buffered saline tween
YAC	Yeast artificial chromosome
ZPA	Zone of polarizing activity

ACKNOWLEDGEMENTS

I would like to sincerely thank my supervisor Dr. Marie-Andrée Akimenko for having given me the opportunity to do my master's studies in her laboratory. Thank you for your patience, financial support and ideas. I would like to give special thanks to Dr. Bhaja Padhi for being a very good teacher and mentor. I will be forever grateful to you for introducing me to scientific research, having the patience to teach me and also helping me with thesis writing. I am very thankful to the members of my advisory committee Dr. Cristofre Martin and Dr. Margaret Sonnenfeld for all their advice and help. I am grateful for all the help provided by Dr. Micheline Paulin-Levasseur, Dominique Vaillant and Dr. Luc Poitras and for teaching me immunoblotting. I would also like to thank everyone from the Ekker Lab, Loeb Institute, the Department of Cellular and Molecular Medicine (in particular Donna Hooper) and the Faculty of Graduate and Postgraduate Studies (in particular Christine Hendley) for all their help.

I would like to thank Bitapi Ray, Danielle Guay, Daniel Kolczinsky, Amanda Smith, Fabien Avaron and Jing Zhang for all their help and for all the laughs we shared in the lab. To my friends, thank you for all the fun times. My best friends, Shree Joshi and Ashwin Jain, thank you for always being there. My one and only, beautiful sister, Vaibhavi Wagh, thank you for everything, I wish you all the happiness in the world.

Above all, I would like to dedicate this work to my parents. I am who I am because of them. Mom and dad, thank you for your constant support, encouragement and prayers.

1. INTRODUCTION

1.1. Zebrafish as a model organism

In recent years, the teleost zebrafish (*Danio rerio*) has become an important model in the study of the genetics underlying development, normal body function and disease. These hardy, freshwater fish originate in India and they have become more widely used in research since the early 1980s. The growing interest in zebrafish research was paralleled by an increase in tools and methods available to study these fish.

The *Danio rerio* combine several characteristics that facilitate genetic analysis. Since the adults are fairly small in size, only about 4cm in length, a large number of fish can be housed in a relatively small space. They are highly prolific and adults lay up to a few hundred eggs per clutch. The resulting embryos are optically clear, easily accessible and grow very rapidly; within 24 hours post fertilization (hpf) the basic body structure is established and within 3 days post fertilization (dpf), embryogenesis is complete (Figure 1). Moreover, zebrafish embryos remain transparent up to 2dpf, therefore observation of early developmental processes and organ systems deep within the living embryo, such as cell movements during gastrulation or in later stages, can be easily followed with the aid of a basic dissecting microscope (Figure 1), and gene expression patterns can be observed directly within the whole mount embryo through *in situ* hybridization (ISH) using labeled antisense RNA probes (Strähle *et al.*, 1994; Nüsslein-Volhard & Dahm, 2002).

The external development of zebrafish offspring allows embryos to be manipulated genetically or through cell transplantation experiments useful in studying cell fates during early embryogenesis (Thisse *et al.*, 2004). The transient functional

Figure 1. The early developing wild type *Danio rerio* embryo.

The figure shows the various stages of development of the zebrafish embryo and larva starting from 1hpf to 5dpf. Lateral view, anterior to the left.

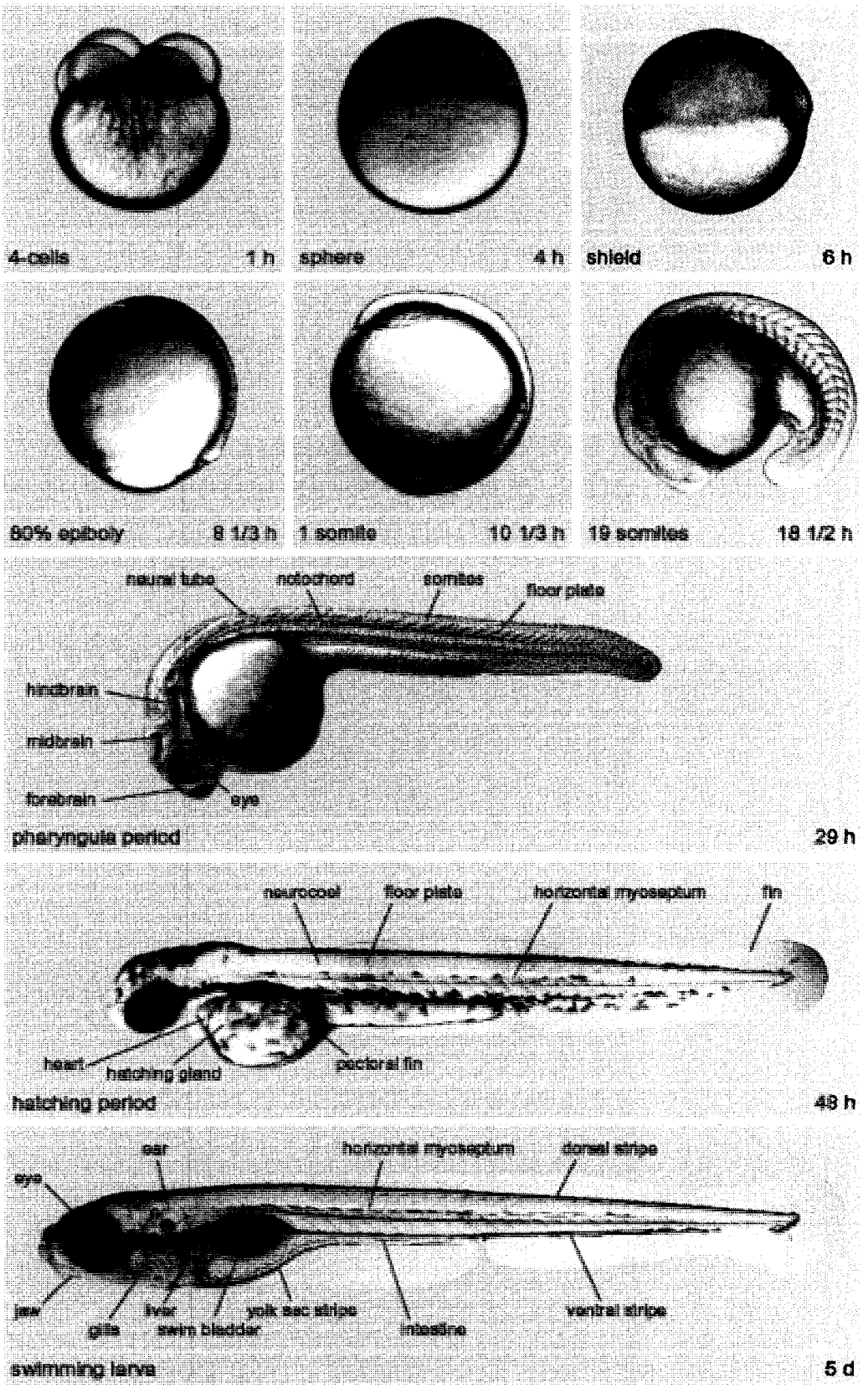

(Haffter *et al.*, 1996)

inhibition of a specific gene can be carried out in vivo by injecting antisense morpholino oligonucleotides (MO) into 1-celled zebrafish embryos (Figure 2A) (Nasevicius & Ekker, 2000; Ekker & Larson, 2001). MOs are chemically modified antisense oligonucleotides that provide complete resistance to nucleases, have high target affinity, high knockdown efficacy and very little non-antisense activity (Summerton, 1999; Nasevicius & Ekker, 2000). The morpholinos are designed to bind to the translation initiation site (Figure 2B) or intron-exon boundary and block translation initiation or mRNA splicing, respectively, creating a functional knockdown for the designated gene (Thorpe *et al.*, 2005). They function through an RNase-H-independent mechanism by hindering translation (Summerton & Weller, 1997; Summerton, 1999) and are not subject to endogenous degradation activity. Following injection, they are effective over a period of 4 to 5 days that is they are effective through the entire process of embryogenesis. Another advantage is the relatively easy generation of transgenic lines by microinjection of DNA constructs into one- or two-celled embryos, allowing lineage analysis of different cell types.

In addition, important genomic resources have been developed in zebrafish. Genomic libraries in BAC (bacterial artificial chromosomes), PAC (P1-based artificial chromosomes) and YAC (Yeast artificial chromosomes) vectors have been constructed (http://zfin.org/zf_info/zfprbs.html, March 13th, 2007).

Moreover, zebrafish genomics are greatly enhanced by the creation of genomic mapping panels as well as the current genome sequencing project undertaken by the Sanger Institute in Cambridge, United Kingdom, in February, 2001. The sequencing of the zebrafish genome is on the verge of completion and the Sanger Institute aims to

Figure 2. Functional analysis using morpholino oligonucleotides.

Gene knock-down approach using injection of morpholinos in one-cell stage zebrafish embryos. **A.** Microinjection of a morpholino into a one-celled zebrafish embryo with the needle still in the cell. **B.** The diagram depicts the microinjection of a morpholino oligonucleotide designed to bind to the translation initiation site of the mRNA and the subsequent inhibition of gene function.

A

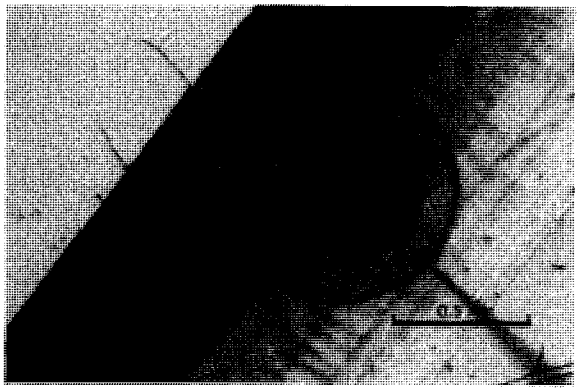

B

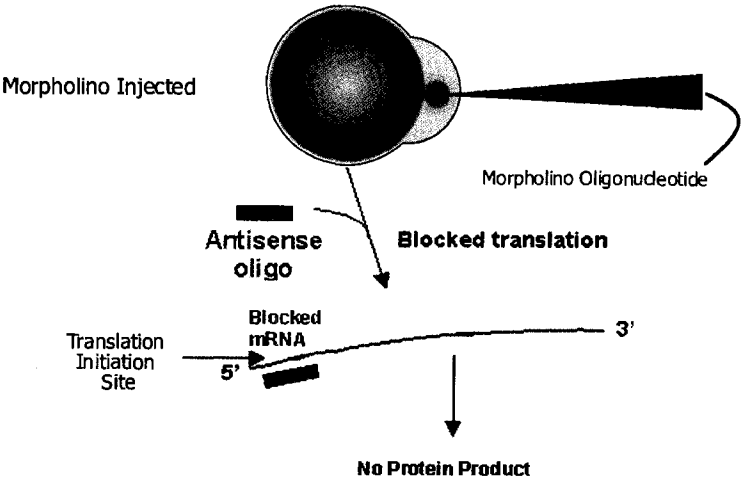
Morpholino Injected
Morpholino Oligonucleotide
Antisense oligo
Blocked translation
Translation Initiation Site
Blocked mRNA
5'
3'
No Protein Product

complete it by the end of 2008. Furthermore, the meiotic (Knapik *et al.*, 1998) and radiation hybrid (Geisler *et al.*, 1999; Hukriede *et al.*, 1999) maps allow for the placement of sequences on zebrafish chromosomes or linkage groups. Analysis of these sequences has and will lead to the discovery of a large number of genetic elements and a rapidly growing number of genes many of which are novel.

Several other tools are being explored further in zebrafish such as inducible expression of transgenes, conditional knockdown systems and imaging techniques to monitor late organogenesis (Beis & Stainier, 2006).

1.2. An overview of fin and limb development

Adult zebrafish have five different fins that differ in function and morphology (Figure 3A). These fins can be classified into two different groups: paired and median fins. The paired fins comprise of the pectoral and the pelvic fins and the median fins include the dorsal, caudal and anal fins (Figure 3A). Each fin, paired or median, develops in a sequential order characteristic of each teleost species.

During embryonic development a single sagittal fold termed the median fin fold (mff), developing around the posterior part of the embryo will give rise to the median fins, while the pectoral and pelvic fin buds give rise to paired fins (Figure 3B). The pelvic fins start to develop at three weeks post fertilization independently from the pectoral fins which start to develop during embryogenesis.

As the zebrafish pectoral fin bud is homologous to the tetrapod forelimb bud (Grandel & Schulte-Merker, 1998), paired fin development has been extensively

Figure 3. The adult and embryonic fins in a wild type zebrafish.

A. The paired and median fins in a wild type adult zebrafish. The fins of the zebrafish are classified into two groups, the paired fins which comprise of the pectoral and pelvic fins, and the median fins which include the dorsal, anal and caudal fins. **B.** Lateral view of a WT 3dpf larva showing the embryonic fins. The figure shows the median fin fold around the posterior end of the trunk region. The median fin fold gives rise to the dorsal, anal and caudal fins at around 1 month post fertilization. The arrow points to the position of the pectoral fin bud over the yolk sac. The ventral fin fold that will give rise to the ventral fin is posterior to the anal region. Anterior is to the left.

A

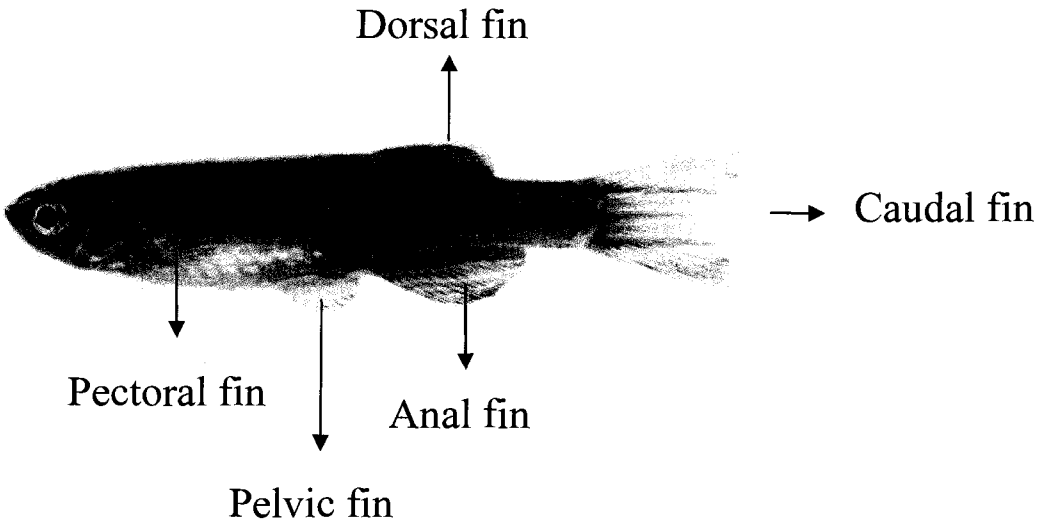
Dorsal fin
Caudal fin
Pectoral fin
Anal fin
Pelvic fin

B

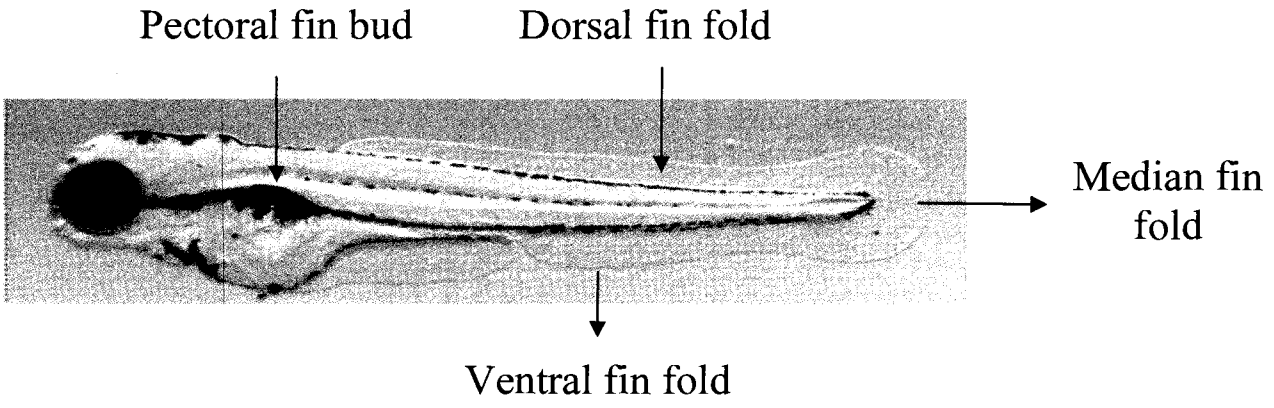
Pectoral fin bud
Dorsal fin fold
Median fin fold
Ventral fin fold

investigated, including several studies previously done in our lab (Akimenko & Ekker, 1995; Akimenko *et al.*, 1995; Grandel & Schulte-Merker, 1998; Pillai *et al.*, 2004; Yan *et al.*, 2005). Remarkable similarities of developmental and genetic mechanisms between fin buds and limb buds have been found (Grandel & Schulte-Merker, 1998; Neumann *et al.*, 1999; Ng *et al.*, 1999; Ahn *et al.*, 2002; Ng *et al.*, 2002; Kawakami *et al.*, 2004; Norton *et al.*, 2005; Abe *et al.*, 2007). Discussing the importance of the apical epidermis and of the underlying mesenchymal cells during the growth of the fin and limb buds is essential, since the two novel genes studied in this work are specifically expressed in these tissues during development.

The Apical Ectodermal Ridge (AER) is a major signaling center for limb outgrowth. It is induced by the mesoderm of the limb bud, as a thickening of the distal ectoderm, at the boundary between the dorsal and ventral domains of the lateral ectoderm (Altabef *et al.*, 1997; Michaud *et al.*, 1997). In the tetrapod limb bud, the AER provides growth factors required for the proximo-distal outgrowth of the bud from the Progress Zone (PZ), a region of mesenchymal proliferation located at the distal end of the bud underlying the AER (Niswander & Martin, 1992; Suzuki *et al.*, 1992; Riley *et al.*, 1993) (Diagram 4A). If the AER is removed, cells of the progress zone cease to proliferate and die, and the limbs are truncated (Summerbell, 1974; Johnson *et al.*, 1994; Saunders, 1998). In return, maintenance of the AER depends on signals emanating from cells of the progress zone (Summerbell *et al.*, 1973; Johnson *et al.*, 1994). The Zone of Polarizing Activity (ZPA), located in the mesenchyme of the posterior margin of the limb bud is responsible for the anterior-posterior patterning of the limb bud.

Cues from both the ZPA and the AER of the limb bud are required for each others maintenance as well as the subsequent growth of the bud (Riddle *et al.*, 1993; Vogel & Tickle, 1993). Thus, continued growth of the limbs depends on cell interactions between the AER and the progress zone and the AER keeps the underlying mesenchyme undifferentiated and in a proliferative state (Michaud *et al.*, 1997).

1.3. Early similarities between fin and limb development

The pectoral fin buds develop first during embryonic development as a protuberance of the epidermal tissue as two bilateral buds over the yolk sac on each side of the trunk, at the level of the third somite at 28hpf (Diagram 4B). The pelvic fins, the homologues of the posterior tetrapod limbs, form later during larval development on both sides of the ventral median fin fold anterior to the anus approximately one month post fertilization (mpf).

At around 31 hpf, as the fin buds develop, a thickened epidermal cap termed the pseudo apical ectodermal ridge becomes prominent at their tips (Géraudie & François, 1973) (Diagram 4B). This pseudo apical ectodermal ridge rims the buds in an antero-posterior direction. This apical epidermis in zebrafish is morphologically homologous to the AER of the tetrapod limb buds (Grandel & Schulte-Merker, 1998).

These observations suggest that the early stages of formation of teleost fins and tetrapod limbs are controlled by similar molecular mechanisms. Another significant connection between the zebrafish fin bud and the tetrapod limb bud is the presence of a posterior mesenchymal domain in the bud, corresponding to the ZPA which is thought to

Diagram 4. The different signaling centers of the tetrapod limb bud and the pectoral fin bud.

Diagram 4A. The limb bud possesses three organizing centers- the Apical Ectodermal Ridge (AER), the Progress Zone (PZ) and the Zone of Polarizing Activity (ZPA). These zones are closely inter-related; signals from these centers interact with each other in order to pattern the axes of the limb. The AER is a thickened ectodermal layer which supports the proliferation of undifferentiated mesenchymal cells in the Progress Zone (PZ), allowing the limb to grow proximo-distally. The Zone of Polarizing Activity (ZPA) polarizes the anterior-posterior axis of the limb bud and is dependent on the presence of the AER.

Diagram 4B. The apical epidermis or the "pseudo apical ridge" of the pectoral fin buds is an AER-like tissue that folds on itself and generates an outgrowth, to form the apical fin fold (ff). This is the first clear morphological divergence between the fin and limb buds.

A

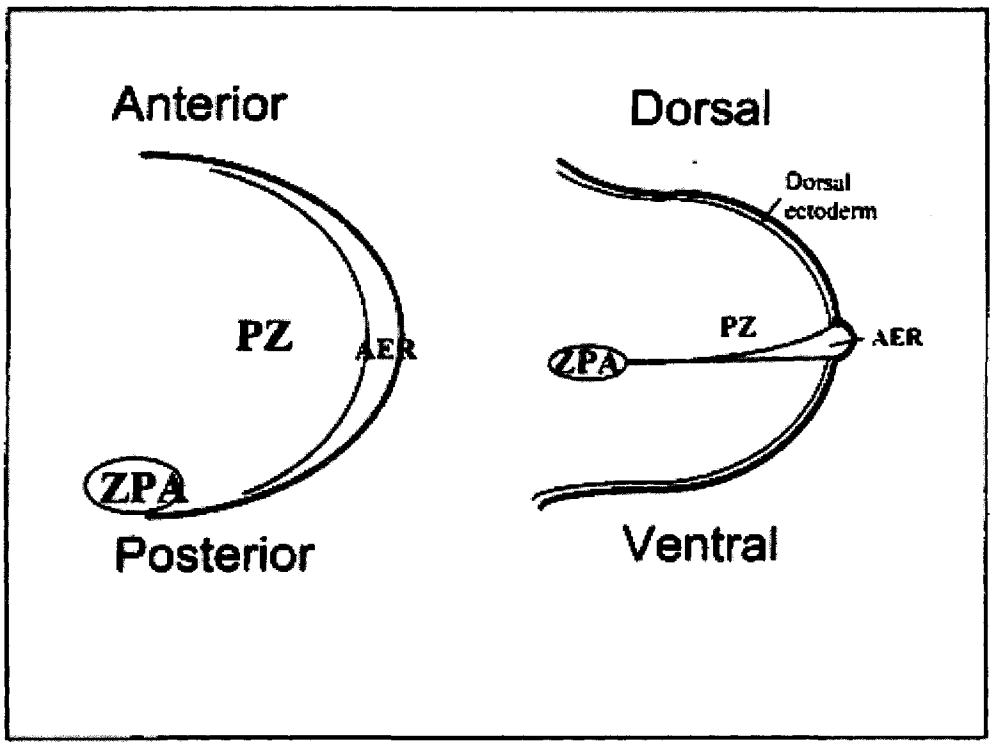
Anterior
Dorsal
Dorsal ectoderm
PZ
AER
ZPA
PZ
AER
ZPA
Posterior
Ventral

B

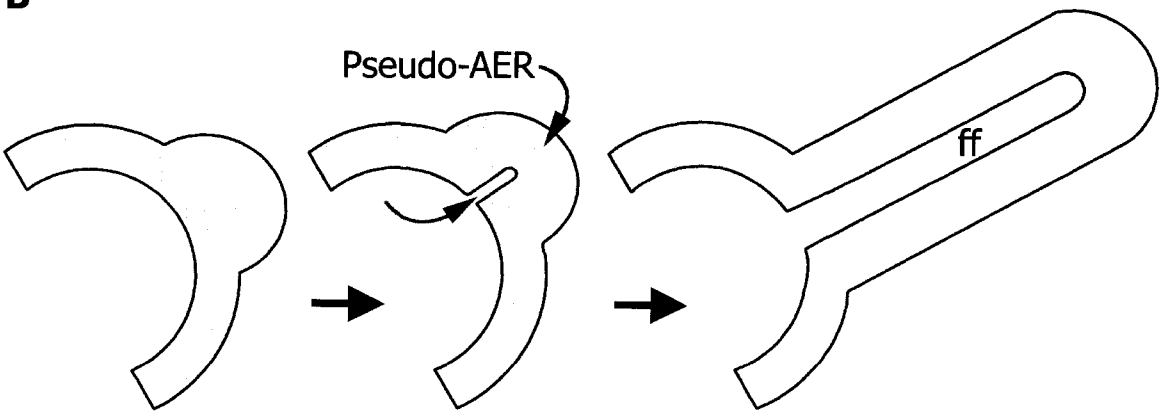
Pseudo-AER
ff

play a role in polarizing the posterior mesenchyme and thereby patterning the antero-posterior axis of the limb bud (Saunders & Gasseling, 1968).

Sonic Hedgehog (*Shh*) is one of the signaling molecules which mediate the antero-posterior patterning of tetrapod limb buds. The zebrafish homolog is expressed during the development of the fin bud in a region analogous to the ZPA in tetrapods (Krauss *et al.*, 1993), suggesting the presence of a signaling center similar to the ZPA is present in the pectoral fin buds. This hypothesis is further supported by the finding that global administration of retinoic acid (RA) induces ectopic expression of *shh* in the mesenchymal cells at the anterior margin of the bud (Akimenko *et al.*, 1995) in the same way as local application of RA to the anterior part of the chicken limb bud induced expression of *Shh* in an anterior subset of mesenchymal cells. Furthermore, at least part of the Shh signaling cascade is conserved during both tetrapod limb and pectoral fin bud development since *patched1 (ptc-1)* the Shh receptor and a downstream gene of hedgehog signaling pathway *bmp2b* (bone morphogenetic protein 2b) are expressed in a similar fashion (Marigo *et al.*, 1996; Laforest *et al.*, 1998). Moreover, *fgf8* (fibroblast growth factor-8) (Fürthauer *et al.*, 1997; Reifers *et al.*, 1998) and *en1* (engrailed1) (Ekker *et al.*, 1992) are each active in the expected tissues in the zebrafish fin buds and thus probably exert an equivalent function as in the chick (Crossley *et al.*, 1996) or mouse (Crossley & Martin, 1995).

1.4. Divergence between fin and limb development

The AER and the apical epidermis of the zebrafish fin buds are both transient structures. However, in contrast to the AER of developing limb bud of tetrapod species

that regresses and disappears as the bud elongates (stage 28 in chick embryo) (Yamaguchi *et al.*, 2004), the apical epidermis of fish fin buds folds on itself, to form the apical fold (Diagram 4B). This is the first major morphological difference observed between fin and limb buds. The major part of the adult fin, containing the exoskeleton (the fin rays) will develop from this elongating fin fold. The actinotrichial fibrils are first observed at this crucial point of divergence between fin bud and limb bud development.

Unlike the vertebrate limbs, adult fish fins present two different kinds of skeleton: endoskeleton (cartilage bones) and exoskeleton (dermal bones or fin rays). The endoskeleton results from endochondral ossification of cartilage and the second from the mineralization of a proteoglycan matrix synthesized by scleroblasts. As the fin buds grow, the first skeletal elements start to condensate by 37hpf in the center of the fin bud and will give rise a few hours later to the cartilaginous endochondral disc which gives rise to the larval endoskeletal girdle and the fin endoskeleton. The exoskeleton of teleost fins is formed by two different skeletal elements, the lepidotrichia and the actinotrichia. Specialized cells from the distal mesenchyme, the scleroblasts, intercalate between the actinotrichia and the basement membrane and start to secrete the bone matrix in a proximal to distal fashion, forming the exoskeleton or the fin rays called the lepidotrichia (Grandel & Schulte-Merker, 1998). During fin fold elongation the lepidotrichia fin rays, push the actinotrichia to distal part of each fin ray (details on fin ray morphology will be described later).

The actinotrichia are collagenous fibrils forming two (dorsal and ventral) arrays along the proximo-distal axis within the fin fold (Wood & Thorogood, 1984). Shortly after ridge-to-fold transition the space between the actinotrichial arrays is invaded by

cells migrating distally from the base of the fin bud. These cells encounter the actinotrichial fibrils and move between them, using the actinotrichial fibrils as a substratum (Wood & Thorogood, 1984) (Diagram 5). Hence, these fibrils form the first support of the fin fold and facilitate the migration of mesenchymal cells located at the base of the buds within the fin fold.

Median fin fold development

In contrast to the mechanisms underlying the development of paired appendages, very little is known about the formation of the median fins. The median fins, the caudal, dorsal and anal fins arise from a unique median epidermal fin border called the median fin fold (mff) which runs dorsally and ventrally along the trunk and around the tip of the tail of the embryos (Figure 3B). Median and paired fin development is controlled by a common set of molecular mechanisms (Akimenko *et al.*, 1994; Akimenko *et al.*, 1995). The fins are formed by the rapid expansion of the mesenchyme underlying the ectodermal layer of the mff during embryogenesis. The mff expresses many genes (*dlxs*, *fgfs*, *msxs*, etc.) which are also expressed in the apical fold in paired fin buds (Akimenko *et al.*, 1994; Akimenko *et al.*, 1995; Reifers *et al.*, 1998; Draper *et al.*, 2003; Fischer *et al.*, 2003; Kawakami *et al.*, 2004; Nomura *et al.*, 2006). Morphogenesis of the mff starts at around 18hpf (Dane & Tucker, 1985; Kimmel *et al.*, 1995). The structure originates at the anal/cloaca area on the ventral midline encircling the tail (Abe *et al.*, 2007). Posterior to the anal area there is a ventral fin fold that will give rise to the ventral fin (Figure 3B). The morphologically distinct wedge-shaped

Diagram 5. Schematic representation of the development of the fin fold.

Fin bud begins as an outgrowth of the epidermal tissue that folds at its apex forming the "pseudo-apical ridge". The actinotrichia, first component of the dermal skeleton of the fin ray, are polymerized beginning at the apex of the sub-epidermal space of the fold. The actinotrichia made of elastoidin, are used by mesenchymal cells as a substrate for migration during distal growth of the bud.

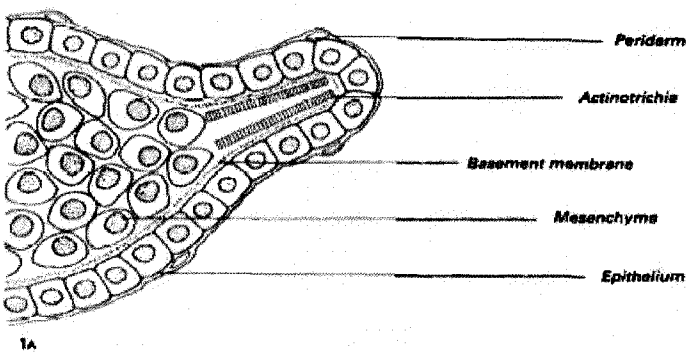

Beginning of the formation of the fin fold

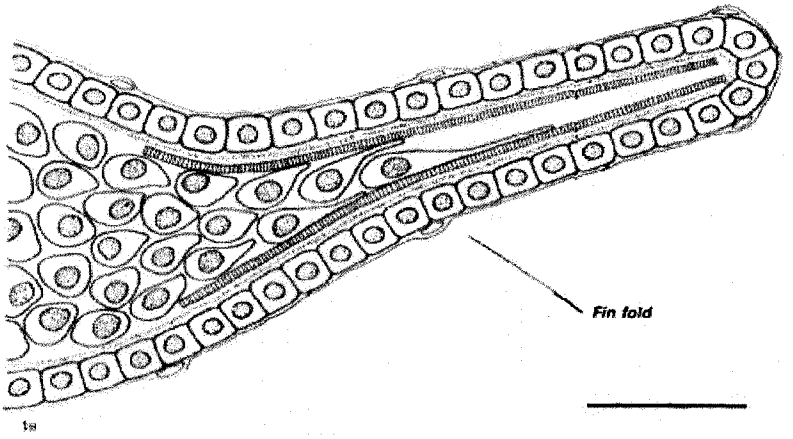

Elongation of the fin fold at a later stage

Fig. 1

ANDREW WOOD AND PETER THOROGOOD
J. Cell Sci. 66, 205-222 (1984) 205

epidermal cells characteristic of the mff appear at the dorsal midline at around 18hpf. The mff cells emerge from the tail bud region and extend anteriorly toward the head on the ventral and dorsal midlines as the tail elongates. Anterior extension in the dorsal midline reaches the final border of the mff at the 8th somite level at 25hpf, the entire mff structure continually elongates distally and radially (Abe *et al.*, 2007).

During larval development, starting around the third week of life the different median fins start to form from this median fin fold and are concomitant to the formation of the fin ray structures. This second phase of development occurs in a sequential order, starting with the caudal fin, followed successively by the anal and the dorsal fins.

1.5. Teleost fish fins as a model of regeneration

It is a well documented fact since the eighteenth century that some fish are able to regenerate their fins but only recently has more detailed information on the process through histological and molecular studies emerged. Teleost fish have been used as a model for fin regeneration studies since the end of the eighteenth century (Morgan, 1900, 1902) and complete fin regeneration has been documented in species such as *Fundulus heteroclitus* (Goss, 1969), *Salaria pavo* (Bernhard & Wagner, 1992), *Tilapia melanopleura, Cyprinus carpio, Carassius auratus* (Santamaria & Becerra, 1991; Santamaria *et al.*, 1992; Becerra *et al.*, 1996; Marí-Beffa *et al.*, 1996; Santamaria *et al.*, 1996a; Marí-Beffa *et al.*, 1999) and of course the zebrafish, *Danio rerio* (Géraudie *et al.*, 1994; White *et al.*, 1994; Akimenko *et al.*, 1995; Ferretti & Géraudie, 1995; Géraudie *et al.*, 1995). This, together with the relative simplicity of the structure of the fins, makes the fin an ideal system for the studies of the regeneration process. However, so far only

very little is known about the regeneration process and many fundamental questions concerning the diverse processes causing and involved with regeneration remain unanswered.

Diseases or injuries that cause tissue damage or organ failure could be cured by thoroughly understanding the mechanism of regeneration. Many studies have shown that many of the genes and developmental pathways involved during development are similar to those involved in the process of regeneration (Muneoka & Bryant, 1982; Muneoka & Sassoon, 1992; Simon *et al.*, 1997).

Urodele amphibians also have the capability to regenerate different tissues of their bodies, such as the lens of the eye, limbs, tail and jaws. The most intensively studied aquatic urodeles in terms of adult limb regeneration are newts (*Notophthalmus* and *Pleurodeles*) and the axolotl (*Ambystoma*) (Roy & Levesque, 2006). One feature that strongly differs between regeneration in urodele amphibians and in fish is the speed at which it occurs. In fish, the process takes place much quicker with some fishes (zebrafish) forming well developed fin components only a week after partial fin amputation. In contrast, the establishment of limb structures in urodeles can take several weeks (Brockes & Kumar, 2002; Nye *et al.*, 2003).

1.6. Zebrafish as a model for studies on regeneration

As many other teleost fishes, the zebrafish has the capability to fully regenerate its fins after partial amputation, that is, when amputation is performed at the level of the dermoskeleton. This is a three stage process involving wound healing, blastema formation and the fin ray formation/distal outgrowth (Bernhard & Wagner, 1992;

Akimenko *et al.*, 2003; Poss *et al.*, 2003) stages similar to those seen during limb regeneration (Géraudie & Singer, 1992). (The process of caudal fin regeneration in the zebrafish is described in further detail in the next section).

Zebrafish as a genetic system allows for large-scale genetic screens, hence a rapidly growing number of genes have been described in this species (Mullins & Nüsslein-Volhard, 1993; Driever *et al.*, 1994). This offers a useful tool to study fin regeneration and the expression of a number of genes in regenerating zebrafish fins has been reported (White *et al.*, 1994; Akimenko *et al.*, 1995; Jones *et al.*, 1995; Laforest *et al.*, 1998). Moreover, zebrafish has become a very popular model to analyze vertebrate embryonic development and an increasing amount of data on gene expression during embryonic development is now available (http://zfin.org/; April, 2007) that greatly aids regeneration studies in the adult fish.

Using key genes known to play a fundamental role during fin and limb development, and studying their expression patterns during fin regeneration, may provide some insight into the mechanism of fin regeneration. For example, the homeobox gene *msxB* is expressed in the AER and the PZ of the developing fin buds of zebrafish embryos (Akimenko *et al.*, 1995) and during caudal fin regeneration its expression is re-activated in the blastema (Akimenko *et al.*, 1995). Other genes, such as *shh*, *ptc-1*, encoding for the *shh* receptor (Laforest *et al.*, 1998) as well as *col10a1* (Avaron *et al.*, 2006) are expressed during zebrafish fin development and are subsequently expressed during fin regeneration (although they may not have the same function as seen during development).

1.7. Caudal fin regeneration

Fins of adult zebrafish are comprised of epithelium, mesenchyme, bony fin rays, blood vessels, nerves, connective tissue, and pigment (Akimenko *et al.*, 2003; Poss *et al.*, 2003). The dermal skeleton of the teleost fins is composed of 18 major bony rays separated by interray tissue (Akimenko *et al.*, 2003; Poss *et al.*, 2003). Each ray, formed by a dermal bone named lepidotrichia, is composed of two symmetrical and concave hemi-rays surrounding the connective tissue, nerves and blood vessels (Becerra *et al.*, 1983). The hemi-rays are segmented and form a number of bifurcations along the proximo-distal axis of the ray. Both paired and unpaired fins undergo similar fin ray development and regeneration processes. When the caudal fin is amputated below the first bifurcation, replacement of the missing part occurs in an apparently faithful phenotype. However, a defect is observed in the pattern of the branching forks which form more distal than in the non amputated ray (Géraudie *et al.*, 1995).

After amputation or injury, the fin regenerates through a process involving successive events similar to those observed during the epimorphic regeneration of urodele amphibian limbs (Tsonis *et al.*, 1996): wound healing, blastema formation, outgrowth and progressive differentiation of the blastema cells (Goss & Stagg, 1957; Becerra *et al.*, 1996; Johnson & Bennett, 1999; Akimenko *et al.*, 2003).

1.7.1. Wound healing

Like a limb regenerate, a fin regenerate comprises of a wound epidermis (consisting of migrating epidermal cells) that close the wound and covers the stump within 6 hours in the zebrafish (Poleo *et al.*, 2001) and between 12 to 24 hours in other

teleosts (Bullock *et al.*, 1978; Géraudie & Singer, 1992; Becerra *et al.*, 1996). This initial phase of wound healing is independent of proliferation (Poleo *et al.*, 2001). Overtime the epithelium builds up multiple layers and forms the wound epidermis or apical epidermal cap (AEC) (Becerra *et al.*, 1996). The AEC is believed to fulfill a similar essential role as the apical ectodermal ridge during development, secreting patterning factors for the developing limbs (Capdevila & Izpisua Belmonte, 2001). Blood lost after amputation is minimal and healing begins immediately after injury (Becerra *et al.*, 1996). Blood from the injured capillaries accumulate at the wound, forming a temporary closure. The lack of formation of a basement membrane between epidermis and the mesenchyme allows for the epidermal cap to lay in direct contact with the underlying mesenchyme. This close contact is thought to play a role in patterning and positional identity similar to that of the pseudo-apical ectodermal ridge in developing fin buds (Géraudie & François, 1973; Géraudie, 1980; Wood, 1982). As in urodele amphibians, a decrease in contact between the blastema and the epidermal cap attenuates the regenerative process (Marí-Beffa *et al.*, 1996a; Marí-Beffa *et al.*, 1996b). This lack of regeneration is due to the inhibition of blastema proliferation, suggesting that the state of mesenchymal cell differentiation and proliferation is controlled by the epidermis in the regenerating fin (Becerra *et al.*, 1996; Santos Ruiz *et al.*, 1996).

1.7.2. Blastema formation

Ray regeneration is possible because of the formation, shortly after amputation, of a mass of undifferentiated and proliferating cells called a blastema, distal to the stump of each ray (Becerra *et al.*, 1996; Poleo *et al.*, 2001; Akimenko *et al.*, 2003; Poss *et al.*,

2003). Blastema formation in zebrafish is apparent 48 hours post amputation (hpa) (Géraudie *et al.*, 1995; Poleo *et al.*, 2001). This blastema proliferates beneath the wound epidermis which is composed of a well defined basal layer of cuboidal epithelial cells covered by a multilayered epidermis (Becerra *et al.*, 1996; Akimenko *et al.*, 2003). The zebrafish blastema is characterized by the expression of two *msx* genes (*msxB* and msx*C*), transcriptional repressors that presumably maintain the dedifferentiated stage of blastemal cells (Akimenko *et al.*, 1995; Odelberg *et al.*, 2000). As blastemal cells leave this area, they differentiate to give rise to all the cell types necessary to reestablish the amputated tissues (Becerra *et al.*, 1996; Géraudie & Ferretti, 1997, 1998). As the dermal bone matrix accumulates, it will progressively mineralize, beginning in the proximal (more mature) region of the regenerate (Géraudie & Landis, 1982; Géraudie & Singer, 1992; Becerra *et al.*, 1996; Marí-Beffa *et al.*, 1996b; Akimenko *et al.*, 2003).

The next phase of fin regeneration is termed "regenerative outgrowth" (48 hpa until completion of regeneration). The actual re-growth of the fin tissue takes place during this phase. The blastema subdivides into a distal and a proximal part, with different cell proliferation profiles (Nechiporuk & Keating, 2002). It has been demonstrated that teleost fins fail to regenerate if deprived of their nerve supply (Goss & Stagg, 1957), implying the trophic influence of nerves as another factor in controlling teleost fin regeneration (Becerra *et al.*, 1996). The relatively rapid dedifferentiation, followed by a continuous cycle of proliferation and re-differentiation of the blastema, occurs until the amputated fin is restored to its original form within 3 weeks (Santamaría *et al.*, 1992).

Outlining the above regenerative process has made obvious the essential role and interaction of both the epidermal cap and the blastema that is required for the regenerative process.

1.8. Background on fin rays

1.8.1. Lepidotrichia

The caudal fin of the zebrafish is composed of 5 minor rays located on the lateral sides of the fin, and a series of 18 major rays separated by soft tissue. The skeleton of the rays consists of dermal bones (Moss, 1963); these dermal rays are called lepidotrichia and are composed of two concave, parallel and symmetrical segmented elements defined as the hemi-rays, facing each other forming a tube-like structure (Diagram 6). These hemirays occupy a subepidermal position and are attached to the endoskeleton by striated muscle (Géraudie *et al.*, 1994).

Each hemiray is the product of the mineralization of collagen basal lamella and sulphate glycosaminoglycans (GAG), synthesized and secreted by scleroblasts or lepidotrichia forming cells (LFC), cells of mesenchymal origin. The rays originate at the base of the fin in the subepidermal location, grow distally by progressive addition of segments joined end to end by ligaments that once formed cannot elongate but increase in diameter and bifurcate along the proximo-distal axis of the fin. The segmented structure of the lepidotrichia gives the flexibility to the fin ray. Blood vessels, nerve bundles, pigment cells and fibroblasts are in the mesenchymal compartment between the rays in the inter-ray tissue, as well as in the intra-ray space (Nechiporuk & Keating, 2002).

Distally, each lepidotrichium ends in a double palisade of the unmineralized, long rigid actinotrichia that line the internal surface of the last segment of each lepidotrichia and give support to the edge of the tip of the fin (Chandross & Bear, 1979; Géraudie & Landis, 1982; Becerra *et al.*, 1983) (Diagram 6).

1.8.2. Actinotrichia

The actinotrichia appear before lepidotrichia, as the first component of the fin exoskeleton in fin development and regeneration (Géraudie & Singer, 1992; Becerra *et al.*, 1996). During development, collagenous fibrils up to 2μm in diameter are deposited along the proximo-distal axis in two (dorsal and ventral) arrays (Wood & Thorogood, 1984) maintaining the embryonic fin fold stretched. During fin regeneration, the long hyper-polymerized actinotrichial fibrils extend from the distal end of the lepidotrichia into the blastema and have been proposed to guide the localization of the scleroblasts and thus the site of ray formation and outgrowth (Géraudie & Landis, 1982). They remain always distally located in a constant polymerization-depolymerization balance and the elastoidin depolymerization and turnover are thought to be controlled by scleroblasts (Marí-Beffa *et al.*, 1989).

The origin of the actinotrichia is still a subject of controversy. Some observations suggest that they could be synthesized by epidermal cells at the tip of the fin (Géraudie, 1980). However, only cells of mesenchymal origin surrounding the actinotrichia immuno-react with anti-actinotrichia antiserum suggesting that connective cells, and not epidermal cells, synthesize actinotrichia (Santamaria *et al.*, 1996b).

Diagram 6. Schematic representation of one bifurcating fin ray.

The rays, called lepidotrichia, are composed of two parallel and symmetrical segmented elements defined as the hemi-rays. Caudally, each lepidotrichium forms a few dichotomous branches along the proximo-distal axis of the fin. Each lepidotrichia ends with a row of long rigid elastoidin rods called actinotrichia. The segmented structure of the lepidotrichia gives the flexibility to the fin ray.

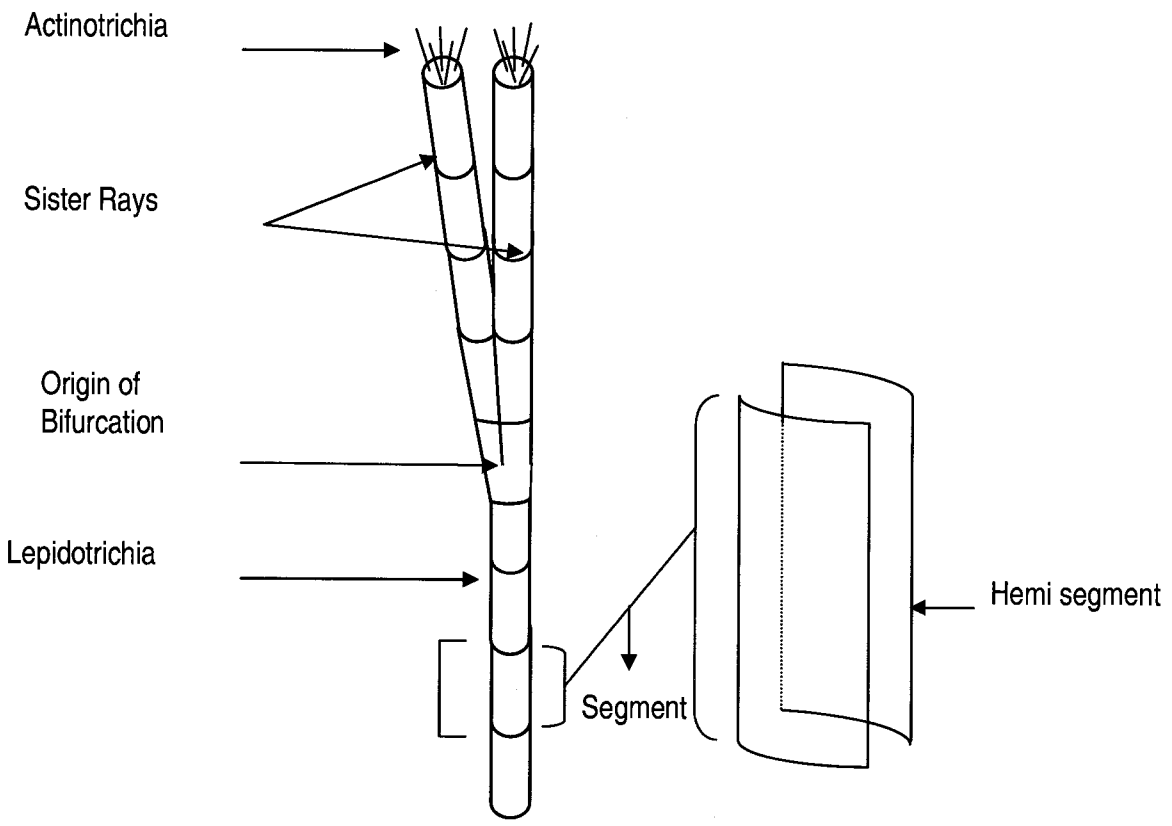
Actinotrichia
Sister Rays
Origin of
Bifurcation
Lepidotrichia
Segment
Hemi segment

1.9. Background on Actinotrichial Elastoidin

Actinotrichia are soft, unmineralized fibrils made of elastoidin (Bechara *et al.*, 2000). The name elastoidin was given to the fibrous protein of the ceratotrichia or fin rays of the elasmobranch, *Mustelus Laevis* by Krukenberg in 1885 as elastoidin had intermediate properties between elastin and collagen (Damodaran *et al.*, 1956). In selachian (elasmobranchs) fish, ceratotrichia are the only skeletal structure of the fins. Ceratotrichia have a chemical composition very similar to teleost actinotrichia (Santamaria *et al.*, 1996b). Based on x-ray diffraction patterns and banding in electron microscopy it was initially though that elastoidin was a type of collagen (Ramachandran, 1962; Chandross, 1982).

Very little is known about the composition of the actinotrichia as most of the studies performed on elastoidin fibrils were in the 1950's and 60's. Many studies (Damodaran *et al.*, 1956; Ramachandran, 1962; Sastry & Ramachandran, 1965; Kimura & Kubota, 1966, 1969) were performed to find the chemical composition of the elastoidin fibrils obtained from the dorsal fin of the sharks *Carcharinus melanopterus* and *Prionace glauca.* Various biochemical analyses on elastoidin fibrils were performed to demonstrate that they are not made solely of collagen and that elastoidin, though similar to fibrillar collagens, is a distinct protein complex.

Protein analysis showed that the tyrosine content of elastoidin is 7.15% by weight as compared to the 1% for collagens (Damodaran *et al.*, 1956). A difference noted between elastoidin and collagen was the 0.35% cysteine content of elastoidin which is only present in insignificant amounts in collagens (Damodaran *et al.*, 1956). Upon autoclaving, the elastoidin was broken down to two components, one collagenous and the

other a non-collagenous tyrosine-rich fraction (Kimura & Kubota, 1966) with relatively little hydroxy-proline content similar to that of fish collagens (Damodaran *et al.*, 1956).

The shrinkage temperature is defined as "a measure of the structural stability of collagen expressed in a temperature unit" (Stringer, 1960). The shrinkage temperature (hydrothermal stability) of the elastoidin fiber as measured in the Theis Shrinkage Tester (an apparatus designed by Theis in 1945) was found to be 63-64°C in water, the fiber contracting to about 30% of its original length. On cooling and applying longitudinal tension, the shrunk fiber became re-elongated to about 85% of its initial length (Damodaran *et al.*, 1956). This reversibility of thermal shrinkage shown by elastoidin in its natural state indicates the possibility of the presence of cross-linkage that do not occur in collagens, since collagen fibrils manifest reversible shrinkage only after treatment with formaldehyde. It is possible that the non-collagenous portion of the elastoidin complex may be involved in the cross-linking of the collagenous fibrils. It is now known that the collagenous component of elastoidin is collagen type 1 α1 (col1a1) (Montes *et al.*, 1982; Kimura *et al.*, 1986) while the non-collagenous component has not yet been characterized.

1.10. Project background

To isolate and identify genes that are up-regulated or differentially expressed during fin regeneration, suppression subtractive hybridization (SSH; (Diatchenko *et al.*, 1996)) and differential display reverse transcriptase polymerase chain reaction (DDRT-PCR; (Liang & Pardee, 1992; Bauer *et al.*, 1993)) analyses were carried out in our laboratory (Padhi *et al.*, 2004). Only cDNAs that are up-regulated during the initiation (1

day post amputation (dpa)) and during the outgrowth and differentiation steps (4 dpa) of fin regeneration but are not expressed in the intact, non-regenerating caudal fins of wild-type (WT) zebrafish were isolated. Identified genes were systematically mapped to zebrafish chromosomes and the expression patterns of some of these genes were determined by in situ hybridization to validate their differential expression between intact and regenerating fins as well as during embryonic development (Padhi *et al.*, 2004).

In situ gene expression screening identified two novel genes (*2-F11* and *2-H06*) without any known function, which are involved during both fin development and regeneration. One of them, *2-F11*, obtained from the 4 dpa SSH library, showed a strong expression at 4 dpa which persisted, at least, until 7 dpa. Expression was restricted to the blastema and the basal epithelial layer except for the most distal cells in both cases, whereas expression of *2-H06* was restricted to the blastema (more details in the Results section). Transcripts of both genes were undetectable at 1 dpa or in intact fins. Expression of *2-F11* and *2-H06* in embryos was observed in the caudal fin fold at 1 dpf and, then at 3 dpf, their expression was specifically restricted to the pectoral fin folds and the median fin fold.

1.11. Project objectives

The two genes, *2-H06* and *2-F11*, code for two novel secreted proteins with unknown functions and present highly restricted expression patterns in developing fin buds and regenerating fins. The objective of this work was to perform a functional analysis of the zebrafish *2-H06* and *2-F11* genes, using the gene knockdown approach by injecting morpholino oligonucleotides, to investigate their role during fin development and regeneration.

2. MATERIALS AND METHODS

2.1. Fish maintenance and breeding

Fish were raised and kept under standard laboratory conditions at 28.5°C with a photo period of 14 hours of light and 10 hours of darkness, and fed regularly (Westerfield, 1995). In order to obtain embryos, one male and one female fish was placed in a breeding tank (Aquatic Habitats) over night. Breeding tanks consist of two stacked plastic containers where the base of the top container has a wire mesh with holes large enough to allow fertilized eggs to fall in the space between. Eggs were collected shortly after spawning the next morning induced by the onset of the photoperiod. The embryos were staged at specific hours or days post fertilization by microscopic examination as described by Kimmel *et al.* (1995). Embryos collected were stored in Petri dishes containing embryo media (5mM NaCl, 0.17mM KCl, 0.33mM $CaCl_2$, 0.33mM $MgSO_4$) and 3 x 10^{-5}% methylene blue. In order to better visualize internal structures, whole mount in situ hybridized embryos were incubated with 200 mM 1-phenyl-2-thiourea (PTU, Sigma) to inhibit pigment formation. They were then anaesthetized in tricaine (ethyl-maminobenzoate, Sigma) (Westerfield, 1995), and fixed in 4% paraformaldehyde (PFA) in phosphate-buffered saline (PBS; 137 mM NaCl, 2.7 mM KCl, 10 mM Na_2HPO_4, 2 mM KH_2PO_4 (pH: 7.4)) at specific hours or days after fertilization as described by Kimmel *et al.* (1995).

2.2. Fin amputations

Adult zebrafish of at least 10 weeks of age were anesthetized by immersion in

system water containing 0.17 mg/ml tricaine (ethyl-aminobenzoate) (Westerfield, 1995) to immobilize the fish and minimize possible pain and discomfort caused by the procedure. Caudal fins of adult fish were amputated, using a scalpel, proximal to the first branch point of the lepidotrichia, and fish were then returned to their tanks where they recover rapidly with very little bleeding and no sign of obvious pain. At various time points afterwards, the regenerating fins were processed for excision, injection, ISH or cryo-sectioning, depending on the experiments.

2.3. *In vitro* transcription of antisense RNA probes

We purchased zebrafish ESTs clones from the German Human Genome Resource Center (RZPD), Germany. Whole mount ISH was carried out using digoxigenin-labeled antisense riboprobes synthesized *in vitro* from a linearized plasmid DNA template. The DNA was linearized using various restriction enzymes (see table below). The probe-synthesizing transcription reaction, containing 1 μg linearized DNA, 2 μl NTP labeling mix (10mM ATP, 10mM CTP, 10mM GTP, 6.5mM UTP, 3.5mM DIG-11-UTP (Roche), 10X transcription buffer, 20 Units RNase Inhibitor (Promega), 20 Units RNA polymerase (T7, T3, SP6; Roche), was incubated at 37°C for 2 hours. The synthesized probe was then precipitated with lithium chloride (500mM) and 100% ethanol and incubated for 30 minutes at –80°C. The precipitated probe was pelleted for 30 minutes in a microcentrifuge (Heraeus Instruments) at high speed, washed with 70% ethanol, respun for 5-10 minutes and air dried. The probe was resuspended in DEPC treated water (0.1% Diethyl pyrocarbonate (DEPC) in water stirred overnight) to a final concentration of approximately 100ng/μl.

The following probes were used:

Clone names	RNA polymerase	Restriction endonucleases used for linearization
2-H06	T7	*Eco*R1
2-F11	T7	*Sal*1
Col1a1	T7	*Eco*R1
Col1a3	T7	*Eco*R1
2-J	T7	*Sal*1

2.4. *In vitro* mRNA synthesis

mMESSAGE mMACHINE® kit (Ambion, TX, USA) was used to synthesize 5'-capped RNA which mimics eukaryotic mRNAs found *in vivo* according to the manufacturer's instructions. The 20μl transcription mixture (1μg of linear DNA template, 2μl of enzyme mix, 2μl of 10X reaction buffer, 10μl of 2X NTP/CAP, nuclease-free water) was incubated at 37°C for 1 hour. The RNA was extracted using an equal volume of phenol/chloroform, then with an equal volume of chloroform and was precipitated with one volume of isopropanol. The RNA solution was centrifuged at 4°C for 15 minutes; the pellet was resuspended in DEPC water and stored at -80°C.

2.5. cDNA cloning

Total RNA was extracted from 48hpf embryos. Approximately 100 embryos were

dechorionated and fixed in 1 ml TRIzol (Sigma) overnight. Samples were homogenized with an insulin syringe and centrifuged at 12,000 x g for 10 minutes at 4°C. The supernatant was chloroform extracted and precipitated with isopropanol. The dried pellet was resuspended in DEPC-treated deionized water.

Messenger RNA (mRNA) was isolated by adding 2 volumes of dilution buffer (Promega) to the total RNA preparation and 1 µl oligo (dT)n (Promega). The mixture was incubated for 5 minutes at 70°C and left to cool to room temperature for 10 minutes. The cooled RNA solution was incubated for 5 minutes in a 200 µl magnetic bead solution (Promega) washed with 0.5X SSC. A magnetic stand was used to capture and wash beads three times with 200 µl 0.5X SSC. mRNA was eluted with 300 µl DEPC-treated deionized water and precipitated with 3M sodium acetate and isopropanol. The dried mRNA pellet was stored in -80°C and used for first strand cDNA synthesis.

First strand cDNA synthesis from mRNA pellet was carried out by standard Reverse Transcriptase-PCR (RT-PCR) (Sambrook & Russell, 2001) using random hexanucleotides. The synthesized single strand cDNA was then stored at -20°C. Amplification of the *2-H06*, *2-F11* and *2-J* cDNA was accomplished through PCR on these first strand preps using the following primers:

cDNA	Forward primer	Reverse primer
2-H06	5'-ATGGCCAGACTCATTAAGATC-3'	5'-TCATTTCTTGTAGCCACCCAC-3'
2-F11	5'-ATGGCTCATTTGAGAGGATATTCC-3'	5'-TTATTTCTTTCTGTAGTCTCC-3'
2-J	5'-CGTCAGAGGAGATCTGTGGAT-3'	5'-TTAGTGAGCTGGAGCAGCATG-3'

Reactions were carried out on a PTC-225 Peltier Thermal Cycler (MJ Research) for 30 cycles with the following cycling parameters: denaturing at 94°C for 30 seconds, primer annealing at 50°C for 30 seconds, elongation at 72°C for 3 minutes. RT-PCR products were immediately ligated into the pDrive TA-cloning vector (Qiagen kit). Resulting clones were screened for inserts of the correct size by PCR with the above primers. Clean plasmid preparation of the positive clone was obtained using a Promega Wizard plus SV mini preps DNA purification system. The clone was then sent for sequencing on an Applied Biosystems 3730 DNA analyzer at the Ottawa Health Research Institute Sequencing Service. Sequence analysis and multi-transcript alignments were done through SeqWeb (**http://www.uottawa.bioinformatics.org**, 2006).

2.6. *In situ* hybridization on whole mount embryos, larvae and fin regenerates

In situ hybridization experiments on whole mount fin regenerates were performed as described in Laforest *et al.* (1998). Following amputation, the regenerating fin samples were fixed overnight in a solution of PBS containing 4% PFA at 4°C. While embryos were manually dechorionated using fine forceps and fixed overnight in PFA at 4°C. The samples, both fins and embryos, were then washed in PBS/0.1% Tween-20 (PBST), dehydrated sequentially in 25%, 50%, 75% and 100% methanol and stored at least overnight at -20°C in 100% methanol. The samples were subsequently rehydrated in a series of 5-minute washes in dilutions of methanol and PBS (75% MeOH:25% PBS, 50% MeOH:50% PBS, 25% MeOH:75% PBS). The samples were washed 3 times for 5 minutes each in PBST. Fins were permeabilized in 20µg/ml proteinase K (Invitrogen) for

30 min, while after rehydration, embryos older than 24 hpf were digested with proteinase K (10 μg/ml) for varying times depending on the developmental stage. The samples were then washed twice for 5 minutes in PBST, fixed for 20 minutes in 4% PFA and washed twice for 5 minutes in PBST. For fins, samples were then incubated in acetylation solution consisting of 125μl triethanolamine and 27μl acetic anhydride in 10ml of water for 10 minutes, followed by two 10-minute washes in PBST.

Next, the samples were prehybridized at 65°C for 3-4 hours in a solution containing 50% deionized formamide, 5x SSC (20x SSC stock solution; 3.0 M NaCl, 0.3 M citric acid), 0.1% Tween-20, 50 μg/ml heparin, 9.2mM citric acid and 200 μg/ml yeast tRNA. After incubation for 3-4 hours, the hybridization solution was replaced with a fresh prehybridization solution containing 1 ng/μl DIG-labelled antisense RNA probe and the samples were allowed to hybridize overnight at 65°C.

The next day, the hybridized samples were washed at 65°C for 15 minutes in a series of dilutions of hybridization mix (hyb mix) and 2x SSC (75% hyb mix:25% 2x SSC, 50% hyb mix:50% 2x SSC, 25% hyb mix:75% 2x SSC and 100% 2x SSC). This was followed by two 30-minute washes in 0.2x SSC. The samples were successively washed at room temperature in serial dilutions of 0.2x SSC and PBST (75% 0.2x SSC:25% PBST, 50% 0.2x SSC:50% PBST, 25% 0.2x SSC:75% PBST and 100% PBST) for 10 minutes each. The samples were then preincubated for 1 hour at room temperature in PBST containing 10% calf serum and 40mg/ml bovine serum albumin (BSA) (Sigma). Samples were subsequently incubated at room temperature for 2-4 hours in a solution consisting of a preabsorbed anti-DIG antibody conjugated to Alkaline Phosphatase (AP) (Roche). Preabsorption of the antibody was performed during the first

day of the in situ hybridization where 2-3 of nonhybridized fins were placed in a solution containing 20µl calf serum, 20µl BSA, and 2µl antibody and 960µl PBST for 2-4 hours at room temperature and then placed at 4°C overnight. Following incubation with the preabsorbed anti-DIG AP antibody the hybridized samples were washed twice for 5 minutes and then placed at 4°C overnight.

The hybridized samples were subsequently put through 6 washes of 15 minutes each in PBST. Prior to the chromogenic reaction, the samples were equilibrated in three 5-minute washes in equilibration buffer (100mM Tris pH 9.5, 50mM $MgCl_2$, 100mM NaCl) plus 0.1% Tween-20 and 1mM levamisol (Sigma) at room temperature. Samples were then stained in a solution containing 0.175 mg/ml 5-Bromo-4-Chloro-3-Indolyl phosphate (BCIP) (Sigma) and 0.337mg/ml Nitro Blue Tetrazodium (NBT) (Sigma) in the equilibration buffer at room temperature until a suitable staining intensity was visualized. After staining, the samples were washed multiple times in PBST and post fixed in 4% PFA for 2 hours. Samples were then washed in PBS and stored at 4°C in PBS containing 5mM EDTA. The entire in situ hybridization procedure was carried out in six well plates (NUNC Brand Products) with the samples placed in plastic "baskets". The prehybridization and hybridization steps were however performed in eppendorf tubes (Diamed). Samples were observed and photographed using a Leica microscope equipped with Eclipse software.

2.7. Cryostat Sectioning

The embryos previously fixed and dehydrated in methanol (see 'whole mount *in situ* hybridization' protocol) were rehydrated in graded solutions in a series of 5 minute

washes of methanol/PBS dilutions (75% MeOH:25% PBS, 50% MeOH:50% PBS, 25% MeOH:75% PBS) and finally two 5 minute washes in 100% PBST. Embryos were embedded in a liquefied 5% sucrose/1.5% agarose solution containing PBS. The solidified sucrose/ agarose blocks with the enclosed specimen were cut for the desired size and orientation with scalpel and placed in a 30% sucrose PBS solution overnight at 4°C. Blocks to be sectioned were mounted on a cryostat chuck, covered in cryomatrix (VWR) and frozen in 2-methyl butane (-80°C) for sectioning on a cryostat (Leica CM 3050S; ON, Canada). 5 to12 μm sections were collected on coated glass slides (VWR), dried overnight at 42°C, and stored at -20°C until use.

2.8. *In situ* hybridization on cryostat sections

Sections were defrosted at room temperature for at least one hour prior to use. DIG-labelled antisense RNA probe was diluted (1:200) in the hybridization buffer consisting of 1x Salt solution (10x Salt stock solution; 1.95M NaCl, 0.12M Tris HCl, 0.01M Tris base, 0.05M NaH_2PO_4-H_2O, 0.05M Na_2HPO_4, 0.5M EDTA, pH 7.5), 50% deionized formamide, 10% dextran sulphate, 1mg/ml yeast tRNA and 1x Denhardt's solution (50x stock Denhardt's solution contains 1% Ficoll type 400, 1% polyvinylpyrolidone and 1% bovine serum albumin). The solution was sterile filtered. The hybridization solution was denatured at 70°C for 5-10 minutes and 500μl of this solution was added to each slide. Sections were subsequently hybridized overnight at 65°C in a sealed plastic container containing a Whatman paper soaked with 1x salt solution/50% formamide.

The next day the slides were transferred to a Coplin jar containing solution A (1x

SSC, 50% formamide, 0.1% Tween-20) that was heated to 65°C. The slides were washed twice for 30 minutes in solution A at 65°C, followed by two 30-minute washes at room temperature in 1x TBST (10x TBST stock solution: 1.4M NaCl, 27mM KCl, 0.25M Tris HCl pH 7.5, 1% Tween-20). Next, the slides were blocked in 10% heat-inactivated calf serum in 1x TBST for one hour at room temperature. Following incubation, the slides were dried one slide at a time making sure the area around the sections was dry. To each slide 500µl of 1:2000 dilution of anti-Dig AP Fab fragment (Roche) in 10% heat-inactivated calf serum and 1x TBST was added. Slides were incubated overnight in a humidified chamber at 4°C.

The following day the slides were washed 4-5 times for 20 minutes in 1x TBST. The slides were then washed twice for 10 minutes at room temperature in 1x NTMT (100mM NaCl, 100mM Tris HCl pH 9.5, 50mM $MgCl_2$, 0.1% Tween-20). Sections were stained in NTMT containing 0.175 mg/ml BCIP and 0.337mg/ml NBT at room temperature. Once a suitable color was visualized the reaction was stopped in 2 washes in 1x PBS. Sections were then fixed in 4% PFA for 20 minutes after which they were washed with distilled water. Slides were dried and then mounted by applying 3 drops of aquatex (VWR) along each slide and placing a glass cover over the sections. Slides were allowed to dry overnight and observed using a Zeiss Axioskop compound microscope.

2.9. Picrosirius Red Staining

The larvae were fixed overnight in 4% PFA at 4°C and then washed in PBST, dehydrated sequentially in 25%, 50%, 75% and 100% methanol and stored at least overnight at -20°C in 100% methanol.

They were then incubated for 1 hour in a 0.2% solution of Sirius Red (Direct Red 80, Aldrich, Milwaukee, WI) dissolved in saturated Picric acid (Sigma). This was followed by rapid rinsing in water. Once the water ran clear and without any red staining, the larvae were sequentially dehydrated into methanol and were stored in 80% glycerol/20%PBS.

2.10. Antisense morpholinos

Antisense morpholino oligonucleotides were ordered from Gene Tools, LLC (Philomath, USA). The *2-H06* morpholino (2-H06-MO) (5'-GCCATTTTTCTCGATTAGCTGAG-3') and *2-F11* morpholino (2-F11-MO) (5'-GGAAGATCCTCTCAAATGAGCCATG-3') were targeted to block the translation initiation of the *2-H06* and *2-F11* mRNAs, respectively. A non-specific standard control morpholino (5'-CCTCTTACCTCAGTTACAATTTATA-3') injected at the same concentration as the *2-H06* and *2-F11* morpholinos was used to account for non-specific morpholino effects. Stock solutions were prepared by solubilizing the morpholinos in 1X Danieau buffer (58mM NaCl, 0.7 mM KCl, 0.4 mM MgSO4, 0.6 mM Ca(NO3)2, 5mM HEPES pH 7.6) to a concentration of 2mM. Working concentrations were determined for each morpholino by diluting stock solutions to concentrations yielding low mortality rates, showing minimal phenotypic perturbations. Morpholinos were injected together with 0.1% phenol red into the yolk of 1-4 cell stage wild type zebrafish embryos at volumes ranging from 4-8nL. Injected embryos were raised in Petri dishes containing embryo media (5mM NaCl, 0.17mM KCl, 0.33mM CaCl2, 0.33mM MgSO4) and 3 x 10-5% methylene blue at 28°C.

2.11. Microinjection of morpholinos and mRNAs

Male and female adult fish were separated at night and bred the next morning. The embryos were collected soon after they were laid and fertilized and placed in 5-6 rows of 10-15 embryos in a Petri dish containing a cushion of solidified agar at the bottom. Microinjection needles were prepared from borosilicate glass filaments (O.D. of 1.2mm from Sutter Instrument Co., CA, USA) using a micropipette puller (Flaming/ Brown, Model P-87). The tip of the needles was broken with a scalpel. The needle was back-filled with 1-2µl of the injection material (morpholinos or mRNAs). A PV830 Pneumatic PicoPump microinjector was used to inject 4- 8 nl of the injection solution in embryos at the 1 cell stage using a Nikon SMZ-1B microscope. The injected embryos were raised in Petri dishes containing embryo media (5mM NaCl, 0.17mM KCl, 0.33mM $CaCl_2$, 0.33mM $MgSO_4$) and 3 x 10^{-5}% methylene blue in fish system water at 28°C. They were visualized using a Leica MZ FLIII microscope and photographed at various stages of development using AxioCam H Rm camera and AxioVision AC (version 4.2) software.

2.12. Antibodies

A polyclonal antibody anti-2-F11 (DVECLQYHLRAAYGYR) synthesized against a peptide from a region conserved in both the zebrafish proteins (2-H06 and 2-F11) as well as both the fugu proteins was ordered from *Open biosystems*. It was produced using amino acids 331-346 of 2-F11 as an immunogen in a rabbit. It was used at a dilution of 1:100 for immunohistochemistry and 1:10,000 for immunoblotting.

2.13. Whole mount immunohistochemistry

Whole mount immunostaining experiments were carried out as per Nuesslein-Volhard and Dahm (Nüesslein-Volhard & Dahm, 2002). Fixed and dehydrated embryos were rehydrated into PBST with graded MeOH:PBS dilutions. Embryos were then blocked 1 hour at room temperature in blocking solution (10% goat serum, 40 mg/ml BSA in PBT). Embryos were incubated over night at 4°C in a 1:100 dilution of the primary antibody diluted in blocking solution. The next day, specimens were washed four times 30 minutes in blocking solution and the avidin/biotinylated horseradish peroxidase (AB) complex substrate (from ABC Vecta Stain kit, Vector Laboratories) as well as the secondary antibody (anti-rabbit antibody from the Vecta Stain kit, Vector Laboratories) was added to embryos and incubated 45 minutes at room temperature. Embryos were subsequently washed again in blocking solution and finally PBST. Bound antibody was visualized using 1 mg/ml 3,3'-diaminobenzidine (DAB) (Sigma) in PBST plus 2µl 0.3% H_2O_2 for approximately 15-30 minutes. After rinsing in PBST, embryos were stored in 4% PFA or 80% glycerol/20%PBS.

2.14. SDS-PAGE and immunoblotting

Zebrafish embryos, larvae and fin samples were obtained at the desired stages as described by Kimmel *et al.* (1995). The embryos were dechorionated and the head and yolk region were amputated. The embryos as well as fins were directly homogenized in 2X sodium dodecyl sulfate sample buffer (SB) (Nili *et al.*, 2001) (125 mM Tris-HCl, 4% SDS, 20% glycerol, 10% 2-mercaptoethanol, 0.004% bromophenol blue) using the following concentrations: 40 embryo tails/80µl SB and 3 3dpa regenerating fin tips/100µl

SB. 10µl of the homogenized sample was loaded in the SDS-polyacrylamide gel electrophoresis (PAGE) gel (5% stacking and 12% resolving gel) (Schoft *et al.*, 2003) using BIO-RAD minigel apparatus. 10µl of broad range SDS-PAGE standard (BIO-RAD, ON, Canada) were loaded for molecular weight determination. The protein profile of the embryos was visualized by Coomassie Blue staining or electrophoretically transferred from gels to nitrocellulose membranes and processed for immunoblotting according to the Western Blotting Kit (Amersham, Canada). Membranes were incubated in 5% milk (w/v) in PBS for 1 hour at room temperature followed by washes in PBST (Tween-1:200; 5% stock). The nitrocellulose membrane was incubated with the primary antibody, anti-2-F11 (1:10,000) for 2 hours at room temperature and washed with PBST. The immunoblots were then incubated with HRP-anti-rabbit IgG (Amersham, Canada) (1:5,000) in 5% milk in PBST for 1 hour at room temperature. Blots were then developed using enhanced chemiluminescence (ECL) kit (Amersham, Canada) and visualized on Hyperfilm ECL (Amersham, Canada).

2.15. Peptide competition

The 2-F11 antibody was diluted at 1:10,000 in PBS in two tubes. In one tube 20µg of 2-F11 peptide (50 times anti-2-F11 antibody) was added. Both tubes were incubated at 37°C for 2 hours. The tubes were then centrifuged at 4°C in a microfuge to pellet any immune complexes. The solution was removed from the tubes leaving 5-10µl at the bottom to avoid disturbing invisible complexes. Both the tubes containing the antibodies, antibody with and without peptide, were used for immunoblotting.

2.16. Fluorescent microscopy and photography using fluorescence imaging

A dissection microscope (Leica MZ FLIII) with an integrated FLUOIII filter system is used to visualize the samples. A digital camera (Sony 3CCD Color Video Camera) and Eclipse software were used to photograph the samples. Fluorescent pictures of whole-mount caudal fin and larvae require an average exposure time of 55 msec.

3. RESULTS

3.1. Sequence analyses

A screen for genes differentially expressed during fin regeneration in adult zebrafish was performed in our lab (Padhi *et al.*, 2004). Two different but complementary approaches, Suppression Subtractive Hybridization (SSH; (Diatchenko *et al.*, 1996)) and differential display reverse transcription PCR (DDRT-PCR; (Liang & Pardee, 1992; Bauer *et al.*, 1993)) were used to isolate cDNAs whose expression is up-regulated during the initiation (1dpa) and during the outgrowth and differentiation (4dpa) steps of fin regeneration (Padhi *et al.*, 2004). Two cDNA fragments corresponding to two novel genes, *2-H06* and *2-F11* were isolated during this screen. They were found to be expressed exclusively in the regenerating fins but not in the intact, non-regenerating caudal fins of wild type zebrafish. They were also found to be expressed in the developing fin folds during embryonic development.

The *2-H06* (340bp) and *2-F11* (473bp) cDNA fragments were used to search the EST databases. An EST is considered identical to an SSH or to a DDRT-PCR clone, if it shares at least 95% identity in a window of at least 100 bases (Coimbra *et al.*, 2002; Padhi *et al.*, 2004). Two ESTs, fa96e08 and fa99d09, were found corresponding to the *2-H06* and *2-F11* cDNA fragments. The cDNAs characterized from the SSH libraries were mapped to zebrafish linkage groups (LG) by using the LN54 hybrid panel (Hukriede *et al.*, 2001; Padhi *et al.*, 2004). The expressed sequence tag (EST) for *2-H06* cDNA, fa96e08, was mapped to LG 2 while the EST for *2-F11* cDNA, fa99d09, was mapped to

LG 24. The translations of these cDNAs are not similar to proteins from previously described families.

3.2. Alignment of the sequences of the two proteins, 2-H06 and 2-F11, and details on their structure

Database searches (http://zfish.wustl.edu/, 2006), allowed us to find zebrafish EST assemblies (wz10432.1 and wz7326.1) that correspond to larger cDNA sequences, spanning the entire coding regions of each of the two genes. The predicted proteins are 508 amino acids (aa) and 570 aa-long, for 2-H06 and 2-F11, respectively. The two proteins resemble each other with a domain of 90 aa showing 73% identity and an overall 37.2% identity (Figure 7). Amino acid sequence analysis revealed that both 2-H06 and 2-F11 contain a signal peptide (http://www.cbs.dtu.dk/services/SignalP/) suggesting that the two proteins may be secreted. Furthermore, both proteins contain two potential cleavage sites (RXRR) for convertases (shown in green in Figure 7), enzymes catalyzing the maturation of pro-protein substrates in the secretory pathway (van de Loo *et al.*, 1997). The cleavage sites are located close to the N-terminal (N-ter) and C-terminal (C-ter) regions of the proteins (Figure 7). The molecular weight of the complete proteins is 56.1kD for 2-H06 while it is 65.5kD for 2-F11. The molecular weight of the two proteins after their potential cleavage is 45.6kD for 2-H06 and 46.2kD for 2-F11.

Search for the zebrafish genomic sequences in the Sanger Institute zebrafish genome database (http://www.sanger.ac.uk/Projects/D_rerio/) revealed that the *2-H06* and *2-F11* genes are made of 5 exons separated by 4 introns. Interestingly, the two genes

Figure 7. Alignment of the two zebrafish protein sequences of 2-H06 and 2-F11.

Figure 7 shows the alignment of the two peptide sequences. The putative cleavage sites for convertases are depicted in green. The identical amino acids are in red and the signal peptide is depicted in blue. The two proteins show an overall identity of 37.2% and a 90 aa domain with 73% identity, this domain is shown in a box. The positions of the 9 aa repeats conserved between both the sequences are underlined in each sequence. There are 2 more repeats in 2-H06 (also underlined) which are not conserved in the 2-F11 peptide sequence.

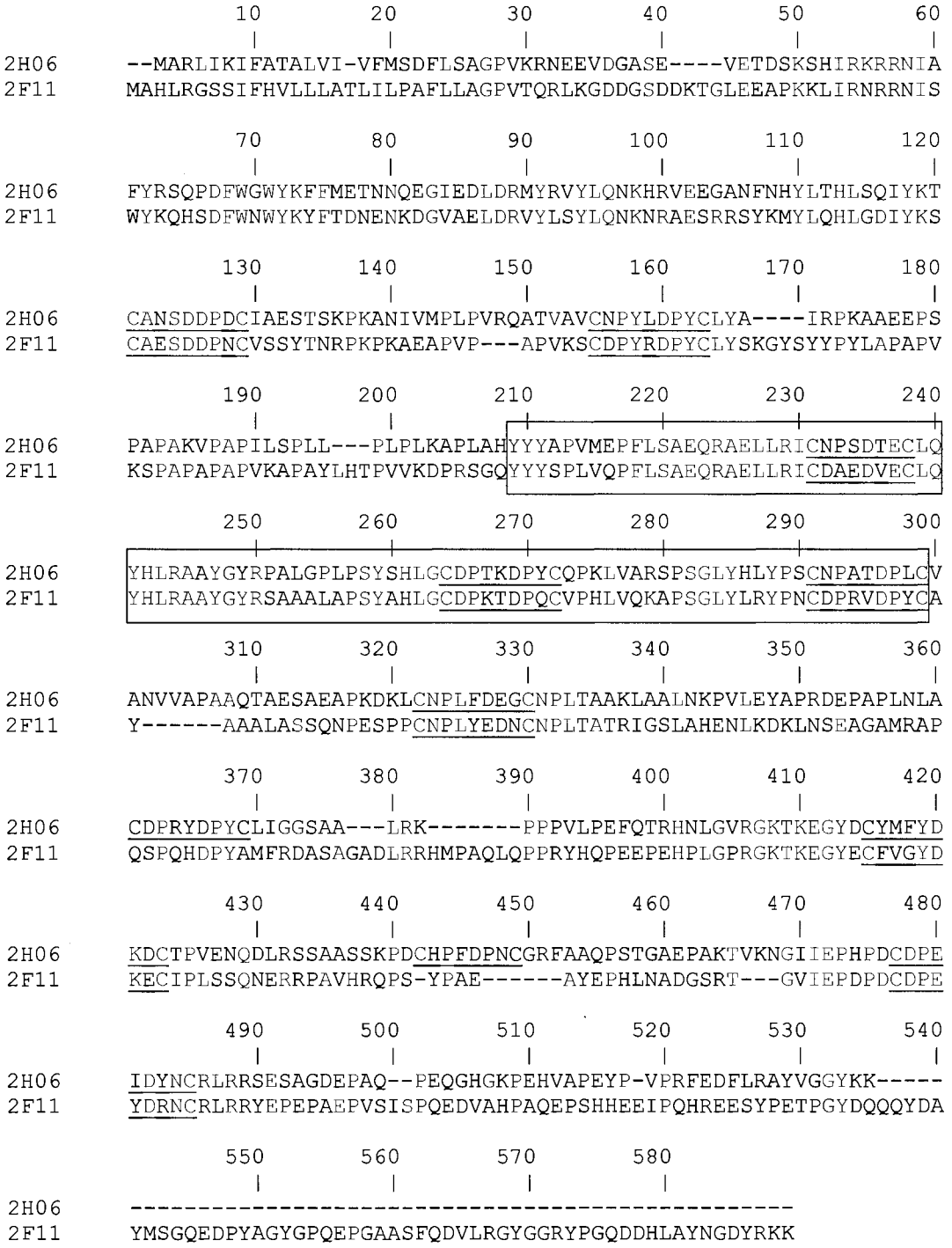
10 20 30 40 50 60
2H06 --MARLIKIFATALVI-VFMSDFLSAGPVKRNEEVDGASE----VETDSKSHIRKRRNIA
2F11 MAHLRGSSIFHVLLLATLILPAFLLAGPVTQRLKGDDGSDDKTGLEEAPKKLIRNRRNIS
70 80 90 100 110 120
2H06 FYRSQPDFWGWYKFFMETNNQEGIEDLDRMYRVYLQNKHRVEEGANFNHYLTHLSQIYKT
2F11 WYKQHSDFWNWYKYFTDNENKDGVAELDRVYLSYLQNKNRAESRRSYKMYLQHLGDIYKS
130 140 150 160 170 180
2H06 CANSDDPDCIAESTSKPKANIVMPLPVRQATVAVCNPYLDPYCLYA----IRPKAAEEPS
2F11 CAESDDPNCVSSYTNRPKPKAEAPVP---APVKSCDPYRDPYCLYSKGYSYYPYLAPAPV
190 200 210 220 230 240
2H06 PAPAKVPAPILSPLL---PLPLKAPLAHYYYAPVMEPFLSAEQRAELLRICNPSDTECLQ
2F11 KSPAPAPAPVKAPAYLHTPVVKDPRSGQYYYSPLVQPFLSAEQRAELLRICDAEDVECLQ
250 260 270 280 290 300
2H06 YHLRAAYGYRPALGPLPSYSHLGCDPTKDPYCQPKLVARSPSGLYHLYPSCNPATDPLCV
2F11 YHLRAAYGYRSAAALAPSYAHLGCDPKTDPQCVPHLVQKAPSGLYLRYPNCDPRVDPYCA
310 320 330 340 350 360
2H06 ANVVAPAAQTAESAEAPKDKLCNPLFDEGCNPLTAAKLAALNKPVLEYAPRDEPAPLNLA
2F11 Y------AAALASSQNPESPPCNPLYEDNCNPLTATRIGSLAHENLKDKLNSEAGAMRAP
370 380 390 400 410 420
2H06 CDPRYDPYCLIGGSAA---LRK-------PPPVLPEFQTRHNLGVRGKTKEGYDCYMFYD
2F11 QSPQHDPYAMFRDASAGADLRRHMPAQLQPPRYHQPEEPEHPLGPRGKTKEGYECFVGYD
430 440 450 460 470 480
2H06 KDCTPVENQDLRSSAASSKPDCHPFDPNCGRFAAQPSTGAEPAKTVKNGIIEPHPDCDPE
2F11 KECIPLSSQNERRPAVHRQPS-YPAE------AYEPHLNADGSRT---GVIEPDPDCDPE
490 500 510 520 530 540
2H06 IDYNCRLRRSESAGDEPAQ--PEQGHGKPEHVAPEYP-VPRFEDFLRAYVGGYKK-----
2F11 YDRNCRLRRYEPEPAEPVSISPQEDVAHPAQEPSHHEEIPQHREESYPETPGYDQQQYDA
550 560 570 580
2H06 ----------
2F11 YMSGQEDPYAGYGPQEPGAASFQDVLRGYGGRYPGQDDHLAYNGDYRKK

show similar exon / intron organization. All these strong similarities seen between the two genes suggest that they belong to the same gene family.

3.3. Alignment of the sequences of 2-H06 and 2-F11 with 2-J, a third zebrafish protein of the same family

More recently, Basic Local Alignment Search Tool (BLAST) searches performed with the help of Dr. Miguel Andrade, from the bioinformatics group (OHRI), revealed that a third zebrafish protein, 2-J, similar to 2-H06 and 2-F11 shows a 39% identity with these two proteins (Figure 8). Although this third sequence is much shorter there is a domain of highly conserved amino acids when compared with the 2-F11 and 2-H06 sequences. Moreover, one of the two convertases cleavage sites is also conserved in this protein (Figure 8).

3.4. 2-H06 and 2-F11 peptide sequence analysis

With the help of Dr. Miguel Andrade it was found that the two proteins, 2-H06 and 2-F11, show a central region of repeats composed of 9 amino acids flanked by two cysteines (Figure 7 and Figure 9). 2-H06 has 10 such repeats, 2-F11 has 8 and 2-J has 3 repeats. Based on the structure as well as composition of the sequence each repeat is hypothesized to form a loop and the repeats may stack upon each other and form rod-like structures.

Sequence analyses reveal that both 2-F11 and 2-H06 are very rich in proline which is present at a percentage higher than all other amino acids. After putative cleavage by convertases 2-H06 protein sequence has a 12.9% proline content while 2-F11 has

Figure 8. Regions of alignment between the three zebrafish proteins.

The alignment of the novel zebrafish proteins reveals a 39% identity between the three sequences. Only the highly conserved amino acids from 1 to 320 are shown. One of the two putative convertases cleavage sites is conserved between the three sequences and is highlighted in the green box. Identical amino acids are shown in red and the amino acids shown in blue are semi-conserved substitutions. The 9 aa repeats in 2-J are underlined.

```
                10        20        30        40        50        60
                 |         |         |         |         |         |
2-H06     -------------MARLIKIFATA-LVI-VFMSDFLSAGPVKRNEEVDGASE----VETD
2-F11     RFTPPHPNTGIMAHLRGSSIFHVL-LLATLILPAFLLAGPVTQRLKGDDGSDDKTGLEEA
2-J       ------MDEAVCEVISLLCLFGALQCLINLPVSQATSLAKISNDQASNPAINIDSKHAHD

                70        80        90       100       110       120
                 |         |         |         |         |         |
2-H06     SKSHI[   ]NI--AFYRSQPDFWGWYKFFMETNNQEGIEDLDRMYRVYLQNKHRVEEGAN
2_F11     PKKLI[   ]NI--SWYKQHSDFWNWYKYFTDNENKDGVAELDRVYLSYLQNKNRAESRRS
2-J       FLAHA[   ]SVDPNWYRKNPDFQSYYRYYNSIGHTEGLYEIDKIRMLYQQMRHLELT---

               130       140       150       160       170       180
                 |         |         |         |         |         |
2-H06     FNHYLTHLSQIYKTCANSDDPDCIAESTSKPKANIVMPLPVRQATVAVCNPYLDPYCLYA
2-F11     YKMYLQHLGDIYKSCAESDDPNCVSSYTNRPKPKAEAPVP---APVKSCDPYRDPYCLYS
2-J       ---YGPDASKYQNTLGLKPTP----PPTTQPPPPTLPPVS-KMNVIYLCNS-KDPQC---

               190       200       210       220       230       240
                 |         |         |         |         |         |
2-H06     ----IRPKAAEEPSPAPAKVPAPILSPLL---PLPLKAPLAHYYYAPVMEPFLSAEQRAE
2-F11     KGYSYYPYLAPAPVKSPAPAPAPVKAPAYLHTPVVKDPRSGQYYYSPLVQPFLSAEQRAE
2-J       -----KPHIVYLPAGGVPVLCDPRYHPNCKLSPAQNSPSPPVIVPEPVTTVPLPPTQKST

               250       260       270       280       290       300
                 |         |         |         |         |         |
2-H06     LLRICNPSDTECLQYHLRAAYGYRPALGPLPSYSHLGCDPTKD--PYCQPKLVARSPSGL
2-F11     LLRICDAEDVECLQYHLRAAYGYRSAAALAPSYAHLGCDPKTD--PQCVPHLVQKAPSGL
2-J       PPPPPPPIMVVKGMEYDCDPYWDPDCLIDNPPRPVKMVEPSSELPDEKVKKEIPVDPVPT

               310       320
                 |         |
2-H06     YHLYPSCNPATDPLCVANVV
2-F11     YLRYPNCDPRVDPYCAY---
2-J       YDPYDFNQDLYDPFRHAAPA
```

Figure 9. Details on repeats in 2-H06 and 2-F11 peptide sequences.

The alignment shows a central region of repeats of 9 amino acids in the two peptide sequences, 2-H06 and 2-F11 with cysteines flanking each side; each repeat is thought to form a loop and the repeats may stack on each other to form fibrils. The cysteines are highlighted in blue while the other amino acids in the central region of the repeats namely, proline and aspartic acid are highlighted in pink and yellow respectively.

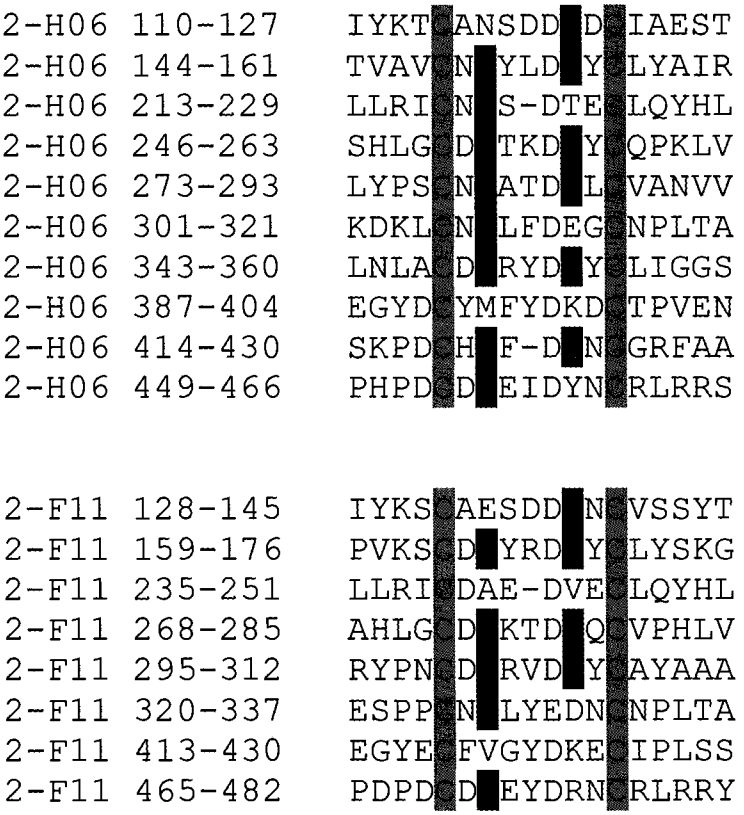
2-H06 110-127 IYKTCANSDDNDCIAEST
2-H06 144-161 TVAVCNNYLDNYCLYAIR
2-H06 213-229 LLRICNNS-DTECLQYHL
2-H06 246-263 SHLGCDNTKDNYCQPKLV
2-H06 273-293 LYPSCNNATDNLCVANVV
2-H06 301-321 KDKLCNNLFDEGCNPLTA
2-H06 343-360 LNLACDNRYDNYCLIGGS
2-H06 387-404 EGYDCYMFYDKDCTPVEN
2-H06 414-430 SKPDCHNF-DNNCGRFAA
2-H06 449-466 PHPDCDNEIDYNCRLRRS
2-F11 128-145 IYKSCAESDDNNCVSSYT
2-F11 159-176 PVKSCDNYRDNYCLYSKG
2-F11 235-251 LLRICDAE-DVECLQYHL
2-F11 268-285 AHLGCDNKTDNQCVPHLV
2-F11 295-312 RYPNCDNRVDNYCAYAAA
2-F11 320-337 ESPPCNNLYEDNCNPLTA
2-F11 413-430 EGYECFVGYDKECIPLSS
2-F11 465-482 PDPDCDNEYDRNCRLRRY

12.5%. The fibrillar domain of collagens (type I and III) is very rich in proline as well (Miles *et al.*, 2000; Ricard-Blum & Ruggiero, 2005). Proline residues have been shown to cause kinks in helices and when found at regular intervals might lead to a fibrillar structure (Bella *et al.*, 2006).

Both the 2-H06 and 2-F11 peptide sequences are tyrosine-rich as well. The tyrosine content of 2-H06 is 5.72% and of 2-F11 is 8.09%. Elastoidin fibrils, as mentioned earlier in the introduction section, are known to be very rich in tyrosine. The tyrosine content of col1a1 is only 0.62% while elastoidin has 7.15% tyrosine content (Damodaran *et al.*, 1956). All these analyses taken together suggest strong similarities of 2-H06 and 2-F11 to the fibril forming elastoidin component of the actinotrichia.

3.5. Details on protein alignments with orthologs in other teleosts

Database searches using BLAST (http://www.ncbi.nlm.nih.gov/BLAST/) with standard search parameters revealed no significant similarity of the zebrafish 2-H06 and 2-F11 proteins with proteins of any tetrapod species. This suggests that there may not be any orthologs of these proteins in tetrapod species. Moreover, no similarities were found between the two proteins and the proteins of invertebrate, fungi, protozoan and plant species.

However, high levels of similarities with the proteins exist when compared with the proteins of other teleosts like the pufferfish *Takifugu rubripes* (fugu) (Figure 10), *Tetraodon nigroviridis* (Green spotted pufferfish), and *Oryzias latipes* (Medaka), that are as zebrafish, bony fish. The alignment of the two zebrafish peptide sequences with the two corresponding fugu sequences reveals 45.53% similar residues between all four

Figure 10. Alignment of the two zebrafish and two *Takifugu rubripes* (fugu) peptide sequences.

The two *Takifugu rubripes* (fugu) peptide sequences corresponding to the two zebrafish peptide sequences 2-H06 and 2-F11 are named F-H06 and F-F11, respectively. The conserved cleavage sites for convertases are depicted in green. The identical amino acids are in red and the yellow boxed region depicts the peptide chosen for antibody production from the conserved region in all four peptide sequences. The positions of the 9 aa repeats conserved between all the sequences are underlined in each sequence.

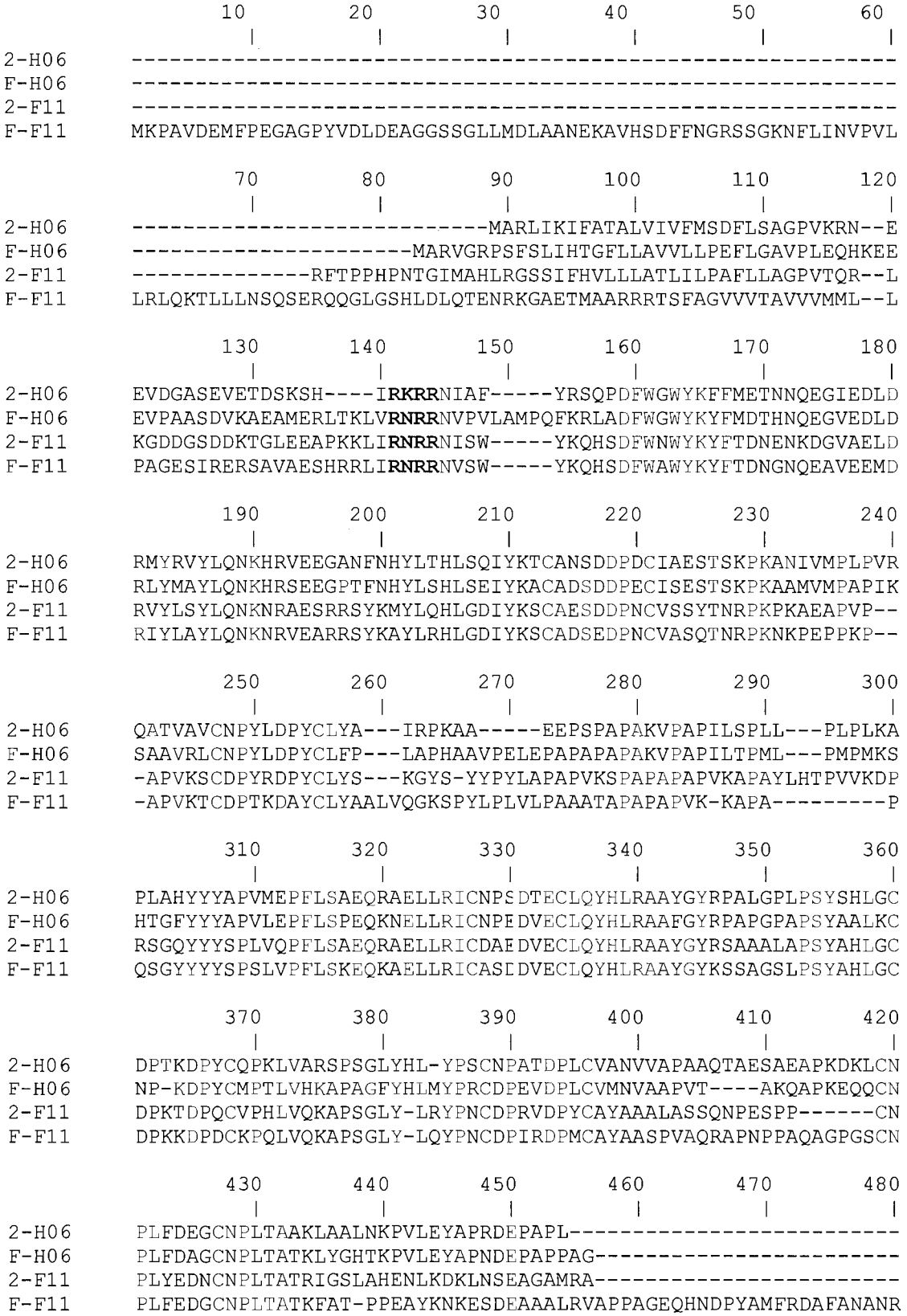
10 20 30 40 50 60
2-H06 ----------
F-H06 ----------
2-F11 ----------
F-F11 MKPAVDEMFPEGAGPYVDLDEAGGSSGLLMDLAANEKAVHSDFFNGRSSGKNFLINVPVL
70 80 90 100 110 120
2-H06 ----------MARLIKIFATALVIVFMSDFLSAGPVKRN--E
F-H06 ----------MARVGRPSFSLIHTGFLLAVVLLPEFLGAVPLEQHKEE
2-F11 ----------RFTPPHPNTGIMAHLRGSSIFHVLLLATLILPAFLLAGPVTQR--L
F-F11 LRLQKTLLLNSQSERQQGLGSHLDLQTENRKGAETMAARRRTSFAGVVVTAVVVMML--L
130 140 150 160 170 180
2-H06 EVDGASEVETDSKSH----IRKRRNIAF-----YRSQPDFWGWYKFFMETNNQEGIEDLD
F-H06 EVPAASDVKAEAMERLTKLVRNRRNVPVLAMPQFKRLADFWGWYKYFMDTHNQEGVEDLD
2-F11 KGDDGSDDKTGLEEAPKKLIRNRRNISW-----YKQHSDFWNWYKYFTDNENKDGVAELD
F-F11 PAGESIRERSAVAESHRRLIRNRRNVSW-----YKQHSDFWAWYKYFTDNGNQEAVEEMD
190 200 210 220 230 240
2-H06 RMYRVYLQNKHRVEEGANFNHYLTHLSQIYKTCANSDDPDCIAESTSKPKANIVMPLPVR
F-H06 RLYMAYLQNKHRSEEGPTFNHYLSHLSEIYKACADSDDPECISESTSKPKAAMVMPAPIK
2-F11 RVYLSYLQNKNRAESRRSYKMYLQHLGDIYKSCAESDDPNCVSSYTNRPKPKAEAPVP--
F-F11 RIYLAYLQNKNRVEARRSYKAYLRHLGDIYKSCADSEDPNCVASQTNRPKNKPEPPKP--
250 260 270 280 290 300
2-H06 QATVAVCNPYLDPYCLYA---IRPKAA-----EEPSPAPAKVPAPILSPLL---PLPLKA
F-H06 SAAVRLCNPYLDPYCLFP---LAPHAAVPELEPAPAPAPAKVPAPILTPML---PMPMKS
2-F11 -APVKSCDPYRDPYCLYS---KGYS-YYPYLAPAPVKSPAPAPAPVKAPAYLHTPVVKDP
F-F11 -APVKTCDPTKDAYCLYAALVQGKSPYLPLVLPAAATAPAPAPVK-KAPA---------P
310 320 330 340 350 360
2-H06 PLAHYYYAPVMEPFLSAEQRAELLRICNPSDTECLQYHLRAAYGYRPALGPLPSYSHLGC
F-H06 HTGFYYYAPVLEPFLSPEQKNELLRICNPEDVECLQYHLRAAFGYRPAPGPAPSYAALKC
2-F11 RSGQYYYSPLVQPFLSAEQRAELLRICDAEDVECLQYHLRAAYGYRSAAALAPSYAHLGC
F-F11 QSGYYYYSPSLVPFLSKEQKAELLRICASEDVECLQYHLRAAYGYKSSAGSLPSYAHLGC
370 380 390 400 410 420
2-H06 DPTKDPYCQPKLVARSPSGLYHL-YPSCNPATDPLCVANVVAPAAQTAESAEAPKDKLCN
F-H06 NP-KDPYCMPTLVHKAPAGFYHLMYPRCDPEVDPLCVMNVAAPVT----AKQAPKEQQCN
2-F11 DPKTDPQCVPHLVQKAPSGLY-LRYPNCDPRVDPYCAYAAALASSQNPESPP------CN
F-F11 DPKKDPDCKPQLVQKAPSGLY-LQYPNCDPIRDPMCAYAASPVAQRAPNPPAQAGPGSCN
430 440 450 460 470 480
2-H06 PLFDEGCNPLTAAKLAALNKPVLEYAPRDEPAPL----------
F-H06 PLFDAGCNPLTATKLYGHTKPVLEYAPNDEPAPPAG----------
2-F11 PLYEDNCNPLTATRIGSLAHENLKDKLNSEAGAMRA----------
F-F11 PLFEDGCNPLTATKFAT-PPEAYKNKESDEAAALRVAPPAGEQHNDPYAMFRDAFANANR

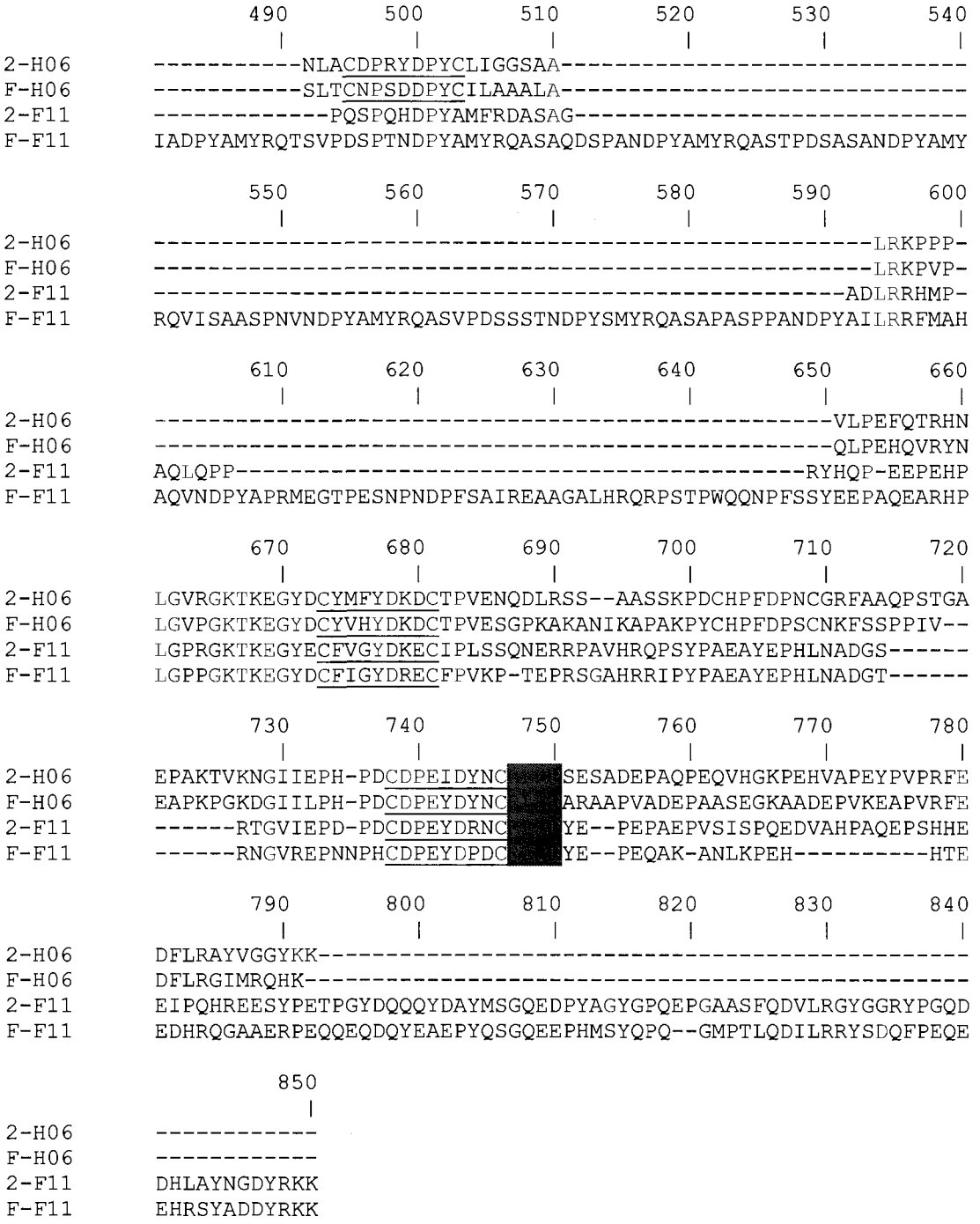
490 500 510 520 530 540
2-H06 ----------NLACDPRYDPYCLIGGSAA----------
F-H06 ----------SLTCNPSDDPYCILAAALA----------
2-F11 ----------PQSPQHDPYAMFRDASAG----------
F-F11 IADPYAMYRQTSVPDSPTNDPYAMYRQASAQDSPANDPYAMYRQASTPDSASANDPYAMY
550 560 570 580 590 600
2-H06 ----------LRKPPP-
F-H06 ----------LRKPVP-
2-F11 ----------ADLRRHMP-
F-F11 RQVISAASPNVNDPYAMYRQASVPDSSSTNDPYSMYRQASAPASPPANDPYAILRRFMAH
610 620 630 640 650 660
2-H06 ----------VLPEFQTRHN
F-H06 ----------QLPEHQVRYN
2-F11 AQLQPP----------RYHQP-EEPEHP
F-F11 AQVNDPYAPRMEGTPESNPNDPFSAIREAAGALHRQRPSTPWQQNPFSSYEEPAQEARHP
670 680 690 700 710 720
2-H06 LGVRGKTKEGYDCYMFYDKDCTPVENQDLRSS--AASSKPDCHPFDPNCGRFAAQPSTGA
F-H06 LGVPGKTKEGYDCYVHYDKDCTPVESGPKAKANIKAPAKPYCHPFDPSCNKFSSPPIV--
2-F11 LGPRGKTKEGYECFVGYDKECIPLSSQNERRPAVHRQPSYPAEAYEPHLNADGS------
F-F11 LGPPGKTKEGYDCFIGYDRECFPVKP-TEPRSGAHRRIPYPAEAYEPHLNADGT------
730 740 750 760 770 780
2-H06 EPAKTVKNGIIEPH-PDCDPEIDYNC SESADEPAQPEQVHGKPEHVAPEYPVPRFE
F-H06 EAPKPGKDGIILPH-PDCDPEYDYNC ARAAPVADEPAASEGKAADEPVKEAPVRFE
2-F11 ------RTGVIEPD-PDCDPEYDRNC YE--PEPAEPVSISPQEDVAHPAQEPSHHE
F-F11 ------RNGVREPNNPHCDPEYDPDC YE--PEQAK-ANLKPEH----------HTE
790 800 810 820 830 840
2-H06 DFLRAYVGGYKK----------
F-H06 DFLRGIMRQHK----------
2-F11 EIPQHREESYPETPGYDQQQYDAYMSGQEDPYAGYGPQEPGAASFQDVLRGYGGRYPGQD
F-F11 EDHRQGAAERPEQQEQDQYEAEPYQSGQEEPHMSYQPQ--GMPTLQDILRRYSDQFPEQE
850
2-H06 ----------
F-H06 ----------
2-F11 DHLAYNGDYRKK
F-F11 EHRSYADDYRKK

sequences. Also, both the potential convertase cleavage sites are conserved in all the four sequences (Figure 10). The peptide sequence analysis shows very high levels of conservation of the central region of the repeats in both the *Takifugu* rubripes (fugu) (Figure. 10) as well as tetraodon protein sequences (data not shown). Hence, these two genes seem to be specific to teleost fish.

3.6. Expression analysis in embryos, larvae and regenerating fins

The spatial distribution of the transcripts of *2-H06* and *2-F11* in developing embryos was examined using *in situ* hybridization of antisense RNA probes and immuno-histochemical techniques were used to establish the possible domains of the protein expression during early development.

For the preparation of RNA probes, sequences less than 400 bases often give very weak signals. Consequently, we used the zebrafish EST clones fa96e08 and fa99d09 corresponding to *2-H06* and *2-F11* respectively for probe preparation (Padhi *et al.*, 2004). To examine the spatial distribution of *2-H06* and *2-F11* mRNAs during development, I prepared two *in vitro* synthesized antisense RNA probes specific to *2-H06* and *2-F11* to identify expressing cells in whole mount embryos and sections of embryos using the ISH technique (Figures 11, 12 and 13). The antisense RNA probes were synthesized by RT-PCR using total RNA obtained from 48hpf embryos (as described in section 2.5). Sense RNA probes for *2-H06* and *2-F11* were used as negative controls whereas antisense RNA probes for genes with known expression patterns were used as positive controls for the ISH technique (data not shown).

Figure 11. During embryogenesis, *2-H06* and *2-F11* expression is restricted to the developing fin buds.

In both **A** and **B**, the top panels show *2-H06* expression and bottom panels *2-F11* expression. **A**. The expression of both genes is restricted to the median fin fold at 19-24hpf, 30-32hpf and 48hpf. **B** Dorsal view of 72hpf larvae in the left panels while the right panels show a close-up of the pectoral fin buds hybridized with the two probes. Scale bars in **A** (a-f): 100 μm. Scale bars in **B**: 50 μm.

A

2-H06

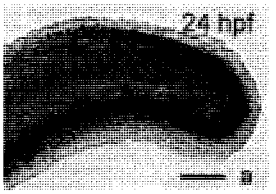

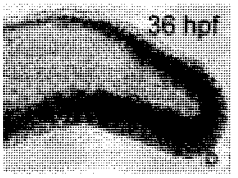

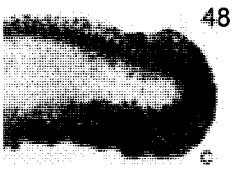

2-F11

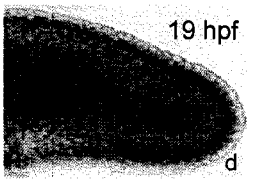

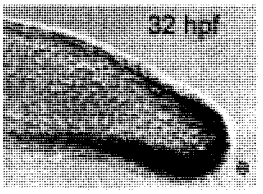

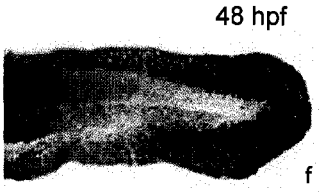

B

2-H06

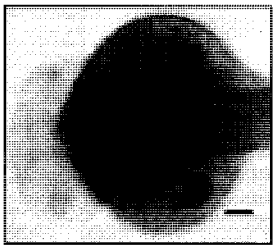

72 hpf

2-F11

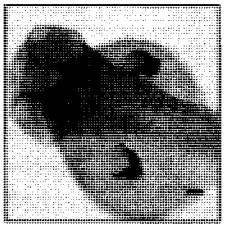

72 hpf

3.6.1. Spatial distribution of *2-H06* and *2-F11* mRNAs in developing embryos and larvae using *in situ* hybridization technique

I performed a detailed time-course analysis of the pattern of expression of both genes in embryos and larvae at various developmental stages: 6, 8 and 10 hpf, 12 hpf, 16 hpf, 18 hpf as well as 24 hpf.

No expression of either gene was detected in the whole mount embryos at 6hpf, 8hpf, 10hpf, 16hpf and 18hpf (data not shown). A detailed study of the expression patterns in embryos and larvae, at the 1, 2 and 4dpf stages (Figures 11, 12, 13A and 13B), hybridized with each probe reveals that the expression of both genes is activated during fin formation at approximately 19hpf at the onset of the formation of the median fin fold. The expression is first seen at the posterior tip of the embryo. At that stage, the pattern of expression of both genes is very similar and is restricted to the posterior part of the embryo, in cells located lateral to the median fin fold (Figure 11A).

It was observed that at 3dpf as the fin fold develops the number of cells expressing *2-H06* and *2-F11* increases and the expression becomes localized to the entire fin fold (Figure 11). By 48hpf, the pectoral fin buds have already started to develop but its only when the fin fold is forming that the expression appears in the pectoral fin buds. The expression in the pectoral fin fold is very similar to what is seen in the median fin fold and persists at least until 6dpf (Figure 12). Furthermore, the expression is always located in the fin folds and is not seen in the central core region of the pectoral fin buds

Figure 12. Expression of *2-H06* and *2-F11* in the pectoral fin buds of whole mount embryos and larvae.

A and **B.** Expression of *2-H06* and of *2-F11*, respectively, at stages ranging between 22hpf to 6dpf. Dorsal views of the embryos and larvae with the head to the left. The arrow in the top right panel indicates the expression in purple. Scale bars: 200 μm.

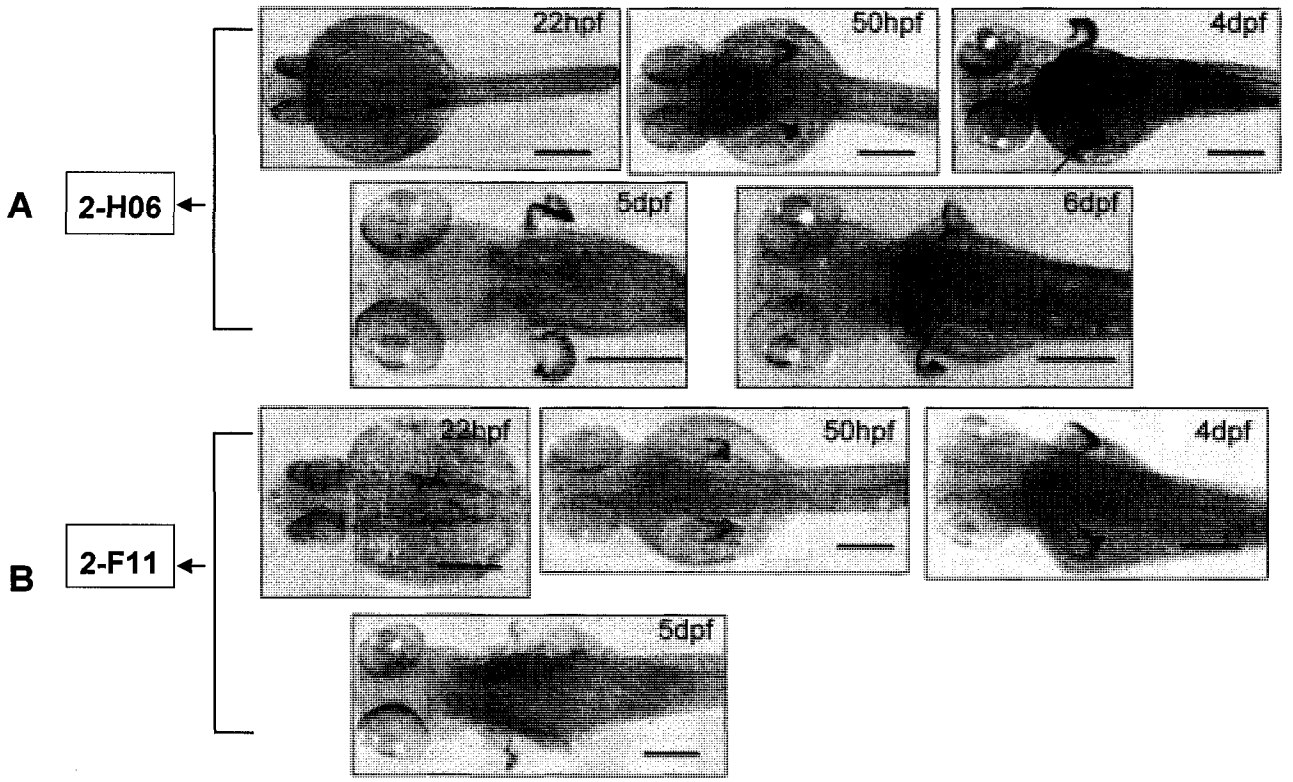
A
2-H06
22hpf
50hpf
4dpf
5dpf
6dpf
B
2-F11
22hpf
50hpf
4dpf
5dpf

Figure 13. Expression patterns seen in transverse sections of embryos and larvae.

A and **B** show the expression patterns of *2-H06* and *2-F11*, respectively, in embryos at 28hpf (top panels), 48hpf (middle panels) and 4dpf larvae (bottom panels). The sections shown from left to right are rostral to caudal. Dorsal is at the top of the panels and ventral is to the bottom. The solid lines indicate the approximate region the sections are from while the expression is seen in blue. Scale bars in **A.** 1, 2 and 3: 200 μm; a-e, g-i and k-m: 50 μm; f, j, n: 25 μm. Scale bars in **B.** 1, 2 and 3: 200 μm; a-c, f-h, j-l: 50 μm; d,e: 25 μm. Abbreviations: y,yolk; ff, fin fold; d, dorsal; v,ventral; nc, notochord; nt, neural tube.

2-H06

A

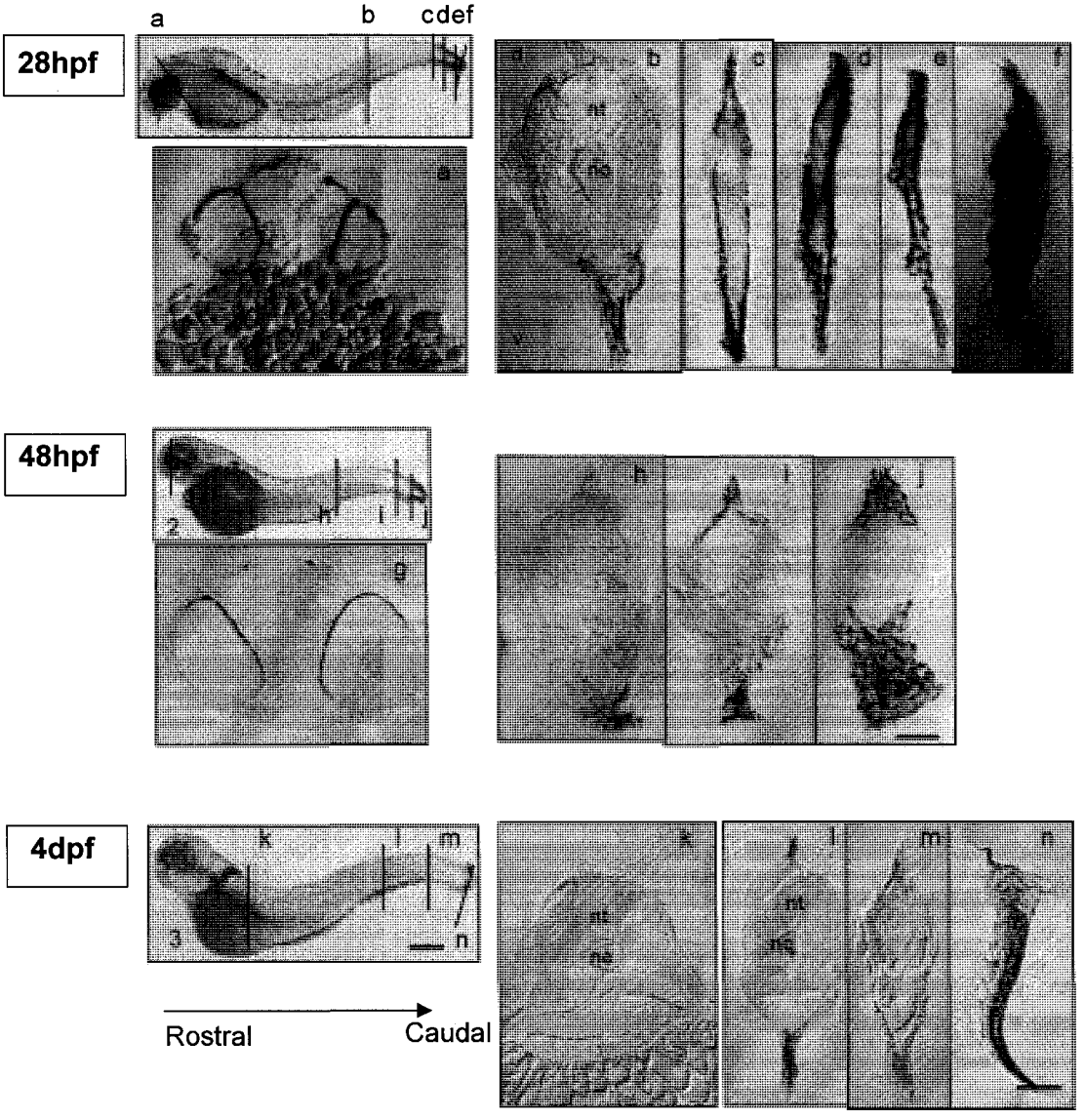

2-F11

B

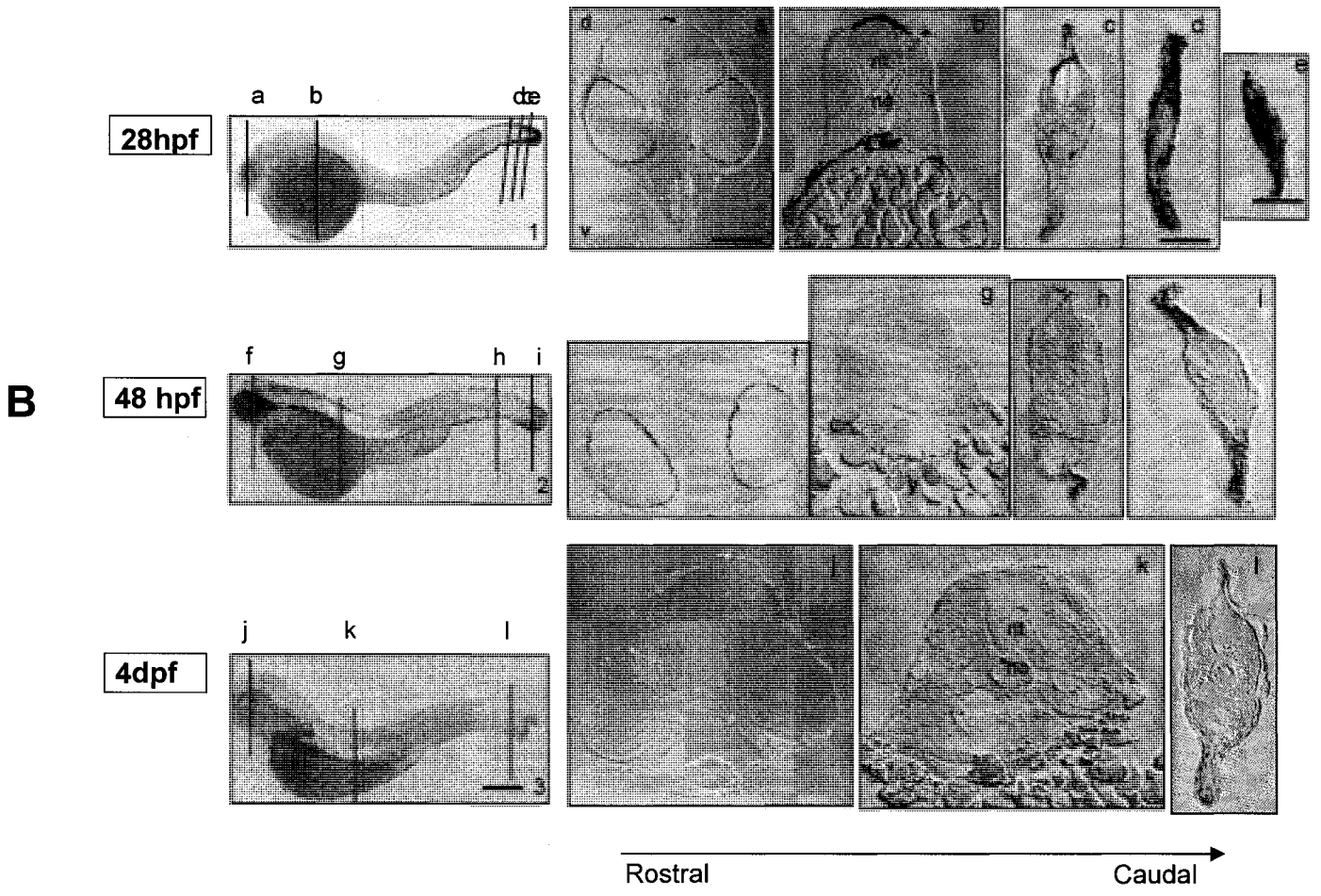

where the endochondral bones are forming. No expression is detected in other structures besides the fin folds; this is more evident upon analyzing sections of *in situ* hybridized embryos and larvae (Figure 13A and 13B).

Upon transversely sectioning the 1, 2 and 4dpf embryos and larvae, hybridized with the *2-H06* (Figure 13A) and *2-F11* (Figure 13B) anti-sense RNA probes, it was found that the expression of both genes at 28hpf and after is restricted to the epidermis as well as the mesenchymal cells in the caudal part of the fin folds. In all the cases the expression was absent in the periderm and from all the structures besides the fin buds.

The analysis of sections of 1, 2 and 4dpf embryos and larvae hybridized with *2-H06* and *2-F11* probes shows that the two genes have a very similar pattern of expression and this expression is restricted to the developing fin folds of the pectoral fin buds and the median fin fold. An antisense RNA probe for the *2-J* gene (cloned in our laboratory) was also prepared to compare its expression pattern using ISH with those seen for *2-H06* and *2-F11*, and it was seen that in the fin fold the expression patterns at 3dpf were very similar (data not shown).

3.6.2. Expression analysis of *2-H06* and *2-F11* in fin regenerates

As the two genes were isolated from a screen for genes up-regulated during fin regeneration, I performed a detailed analysis of their expression during the regeneration process of the caudal fin. *In situ* hybridizations first performed on whole mount fin regenerates using the *2-H06* (Figure 14) and *2-F11* (Figure 15C and data not shown) probes between 1dpa to 14dpa revealed extremely similar patterns of expression.

Figure 14. Expression pattern of *2-H06* in fin regenerates (whole mounts).

The expression of *2-H06* is seen in whole-mount caudal fin regenerates hybridized with anti-sense RNA probes. **a-i** in situ hybridizations were performed on 2, 3, 4, 5, 6, 7, 8, 10 and 14 dpa whole mount WT fish fin regenerates. The expression was limited to the distal part of each fin ray. The black arrows indicate the expression domain at the distal end of each ray regenerate. The brown dots are the pigments in the regenerate, not to be confused with the gene expression in purple. The white dotted line in a-c shows the level of amputation. Scale bars in a-i: 80μm.

Abbreviations: r, ray.

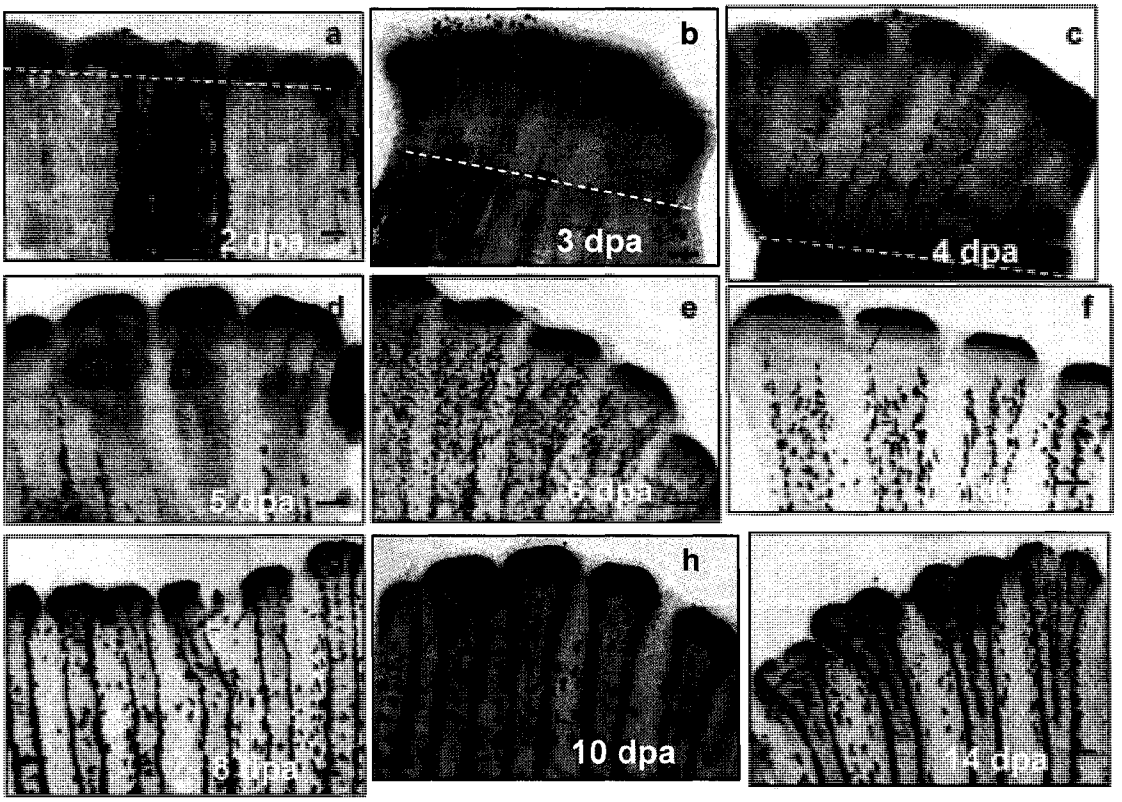
a
2 dpa
b
3 dpa
c
4 dpa
d
5 dpa
e
6 dpa
f
h
10 dpa

Transcripts of both genes were undetectable at 1 dpa or in intact fins. Starting at 1.5dpa, the expression of *2-H06* and *2-F11* was limited to the distal part of each fin ray.

As the fin regenerated, the expression became more and more restricted to the distal-most tip of the fin regenerate in the rapidly proliferating part of the regenerate. As shown in Figure 15A, the bone in each fin ray known as the lepidotrichia bifurcates into two sister ray branches. At the distal most tip of each fin ray there are the thin, collagenous fibrils also known as the actinotrichia. At 6 dpa and after that stage both *2-H06* and *2-F11* show an extremely similar expression pattern where the strongest expression is seen in the distal-most tip of the regenerating fin where the actinotrichia are present and around the bifurcating fin rays (Figures 15B and 15C). As shown in Figure 15B, a cross-shaped expression pattern was noticed, for *2-H06* gene expression, while looking down at the distal tip of the 8dpa regenerating fin samples. A similar pattern was observed for *2-F11* (data not shown). This expression may indicate that the genes are involved in fin ray bifurcation.

In situ hybridization on longitudinal sections of a 4dpa regenerating fin ray reveal very subtle differences in the expression patterns of *2-H06* and *2-F11* in fin regenerates that were not visible in the whole mount in situ studies. *2-H06* expression was observed in the blastema and was stronger in the subset of cells in the highly proliferating part of the regenerate. No expression was observed in the scleroblasts or bone-forming cells (Figure 16A). *2-F11* presents a similar pattern of expression to *2-H06* in the proliferating blastema with the exception of the most distal cells. As *2-H06,* it is also expressed in a subset of cells in the differentiating part of the regenerate but not in the scleroblasts. In

Figure 15. Expression of *2-H06* and *2-F11* at the level of the bifurcation of fin rays after 6dpa in whole mount caudal fin regenerates.

A. Schematic of the skeleton of one fin ray showing the lepidotrichia bifurcating into two sister ray branches. At the distal-most tip of the fin rays are the actinotrichia. **B** and **C** Expression of *2-H06* (**B**) and *2-F11* (**C**) is observed at the distal tip of the regenerate around the bifurcating fin ray as indicated by the black arrows. **B. a** and **b** show the same 8dpa fin regenerate **a.** lateral view **b.** view from the top of the fin regenerate allows to observe the cross shaped pattern of expression for *2-H06*, indicated by the white block arrow, located at the level where the sister branches are separating. **C.** A lateral view of the *2-F11* expression pattern at the distal most tip of 6dpa to 10dpa regenerating fins show staining around the bifurcating fin rays. Scale bars: 80μm.

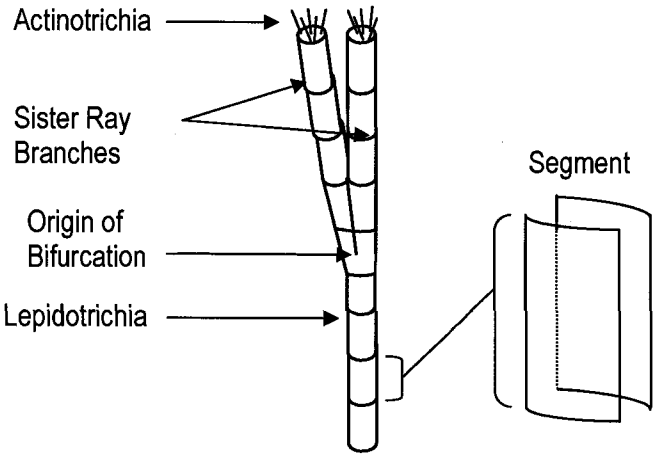
Actinotrichia
Sister Ray Branches
Origin of Bifurcation
Lepidotrichia
Segment

A

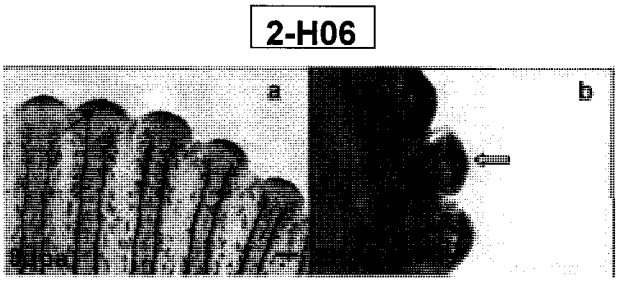
2-H06
a
b

B

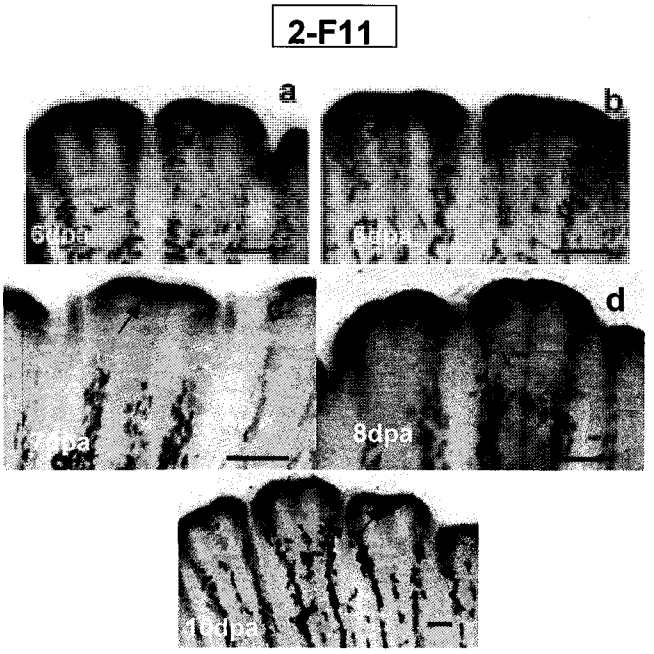
2-F11
a
b
d
8dpa

C

Figure 16. Expression of *2-H06* and *2-F11* in longitudinal sections of 4dpa regenerating fins.

A. *2-H06* is expressed in the blastema (b). There is no expression in the bone-forming cells (scleroblasts: scl). **B.** *2-F11* is expressed in the basal layer of epidermis (ble). It is also expressed in the blastema (b) with the exception of the most distal cells of the blastema (db). Moreover, it is expressed in a subset of cells in the differentiating part of the regenerate but not in the scleroblasts. Scale bar for **A** and **B**: 20 μm.

Abbreviations: b, blastema; scl, scleroblasts; ble, basal layer of epidermis; db, distal blastema.

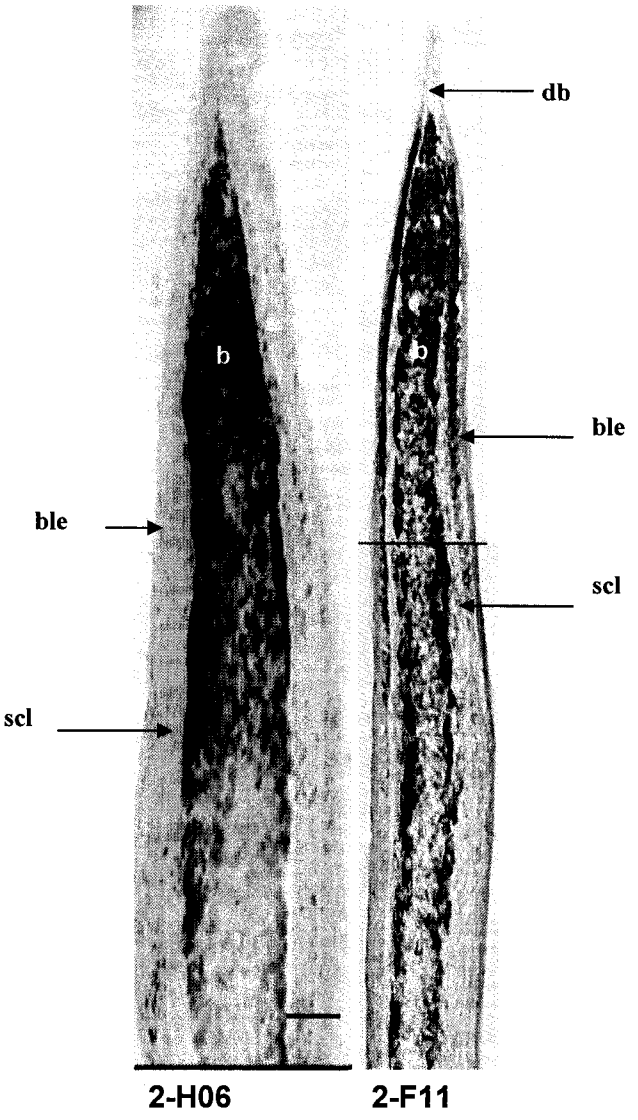
db
b
b
ble
ble
scl
scl
2-H06
2-F11
A
B

contrast to *2-H06, 2-F11* is also expressed in a subset of cells of the basal layer of the epidermis (Figure 16B).

The rostral to caudal transverse sections of a 7dpa regenerating caudal fin hybridized with the two probes revealed that *2-H06* expression is found in the rapidly proliferating region of the blastema in the cells located between the inner boundaries of the actinotrichia (Figure 17A). In the case of *2-F11*, the expression was restricted to the cells lining the inner margins of the actinotrichia (Figure 17B). This expression at the RNA level suggests that these two genes could encode for a protein that is playing a role in the formation of these actinotrichia.

3.7. 2-H06 and 2-F11 protein expression analysis in developing embryos and regenerating fins

The polyclonal antibody, anti-2-F11, raised against a peptide DVECLQYHLRAAYGYR chosen from a region conserved in the zebrafish and fugu 2-F11 and 2-H06 proteins, was ordered from *Open biosystems* (Figure 10). This antibody was used as the primary antibody and an anti-rabbit antibody was used as the secondary antibody in immunoblotting and immunostaining experiments.

Total protein extracts from 24hpf, 48hpf embryos and 7dpf larvae were separated by SDS-PAGE (12% acrylamide) and immunoblotted with the anti-2-F11 antibody. At all three stages a band corresponding to the molecular weight of the two proteins 2-H06 (45.6kD) and 2-F11 (46.2kD) after cleavage was detected (data not shown). This band was not detected with proteins extracted from 10hpf embryos (data not shown).

Since *in situ* hybridization shows the expression of the two proteins restricted

Figure 17. Transverse sections through 7dpa fin hybridized with the *2-H06* and *2-F11* probes.

A. Expression of *2-H06*. The approximate levels of the transverse sections of a 7dpa regenerating fin are indicated in (**i**) by the horizontal lines. The sections go from the more distal to the more proximal from **i**, **ii** and the most proximal in **iii**. *2-H06* expression is restricted to the cells of the rapidly proliferating region of the blastema located between the inner boundaries of the actinotrichia (**ii**, **iii** and **iv**). **B.** Expression of *2-F11*. The approximate levels of the transverse sections of the fin sample are shown by the solid horizontal lines in (**v**) while the dotted line indicates the level of amputation. The sections go from distal (**i**) to proximal (**iii**). *2-F11* expression was restricted to the cells lining the inner margins of the actinotrichia. Scale bars in i-iii and vi-viii: 10 μm.

Abbreviations: a, actinotrichia; bv, blood vessel; b, blastema; db, distal blastema; ble, basal layer of epidermis; e, epidermis; i, interray; l, lepidotrichia.

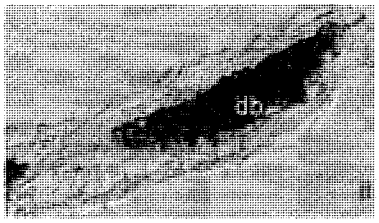

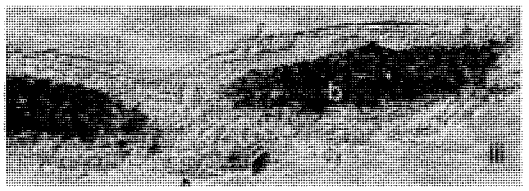

2-H06

A

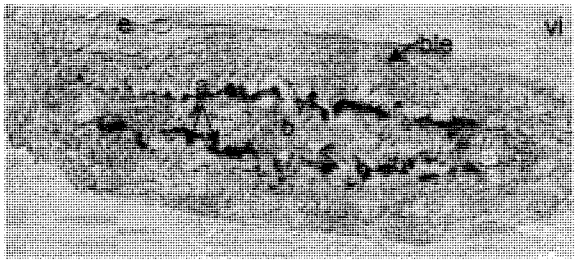

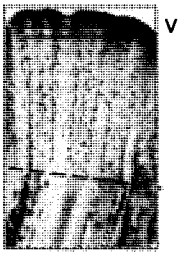

7 dpa Wt

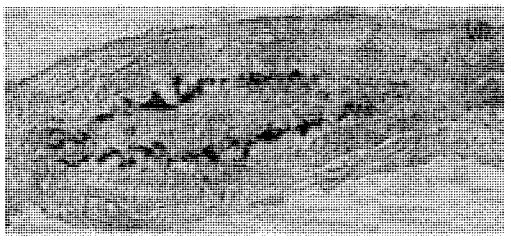

2-F11

B

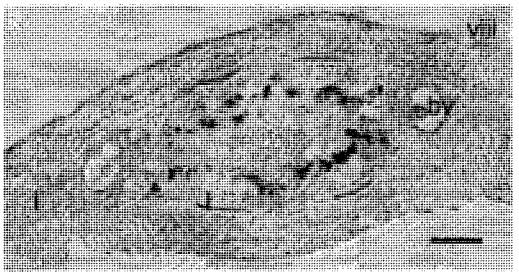

only to the developing fin folds. Proteins were extracted from the posterior half of the embryos excluding the yolk (to avoid any possible interference by the highly abundant yolk proteins). Proteins extracted from the head of the 3dpf larvae were also immuno-blotted along with the proteins from the tail region of the 3dpf larvae in a separate lane; the band at 50kD was preserved in the proteins from the tail region while it was missing from the lanes which had proteins from the head (Figure 18A).

Moreover, immuno-blotting of total protein extracts from intact as well as 3dpa regenerating fins with the 2-F11 antibody revealed a band at 50kD corresponding to the two proteins (Figure 18B). The detection of a band at 50kD in proteins extracted from embryos, embryo tail halves and regenerating fins suggests that the proteins are most likely cleaved as expected by convertases. The specificity of the anti-2-F11 antibody was determined by peptide competition. The 50kD band is absent when excess of the antigen, 2-F11 peptide (50-fold antibody), is used to neutralize the binding of anti-2-F11 antibody to the total protein extracts of the 3dpf larvae tails (Figure 18C).

Immunostaining using the affinity purified 2-F11 antibody, on whole mount larvae at 4dpf stage and on whole mount 4dpa regenerating fin as well as cryosections of both types of samples was unsuccessful, most likely because of technical problems (see discussion).

To conclude, the analyses by ISH revealing the temporal and spatial expression of the two genes, the immunoblotting results as well as the sequence analysis revealing the presence of orthologs of the two genes only in teleost fish species suggest that the two gene products might be playing an important role both during fin development as well as

Figure 18. Temporal expression of 2-H06 and 2-F11 proteins in 3dpa regenerating fins and 3dpf WT.

A. Total proteins from 3dpf WT larvae heads and tails were separated using SDS-PAGE (12% acrylamide) and immunoblotted with anti-2-F11 antibody. **B.** Total proteins from 3dpf WT larvae tails and 3dpa regenerating fin were immunoblotted with anti-2-F11 antibody. **C.** The specificity of the anti-2-F11 antibody was determined by peptide blocking. The 50kD band is absent when excess of 2-F11 peptide is used to neutralize the binding of anti-2-F11 antibody to the total protein extracts of the 3dpf larvae tails.

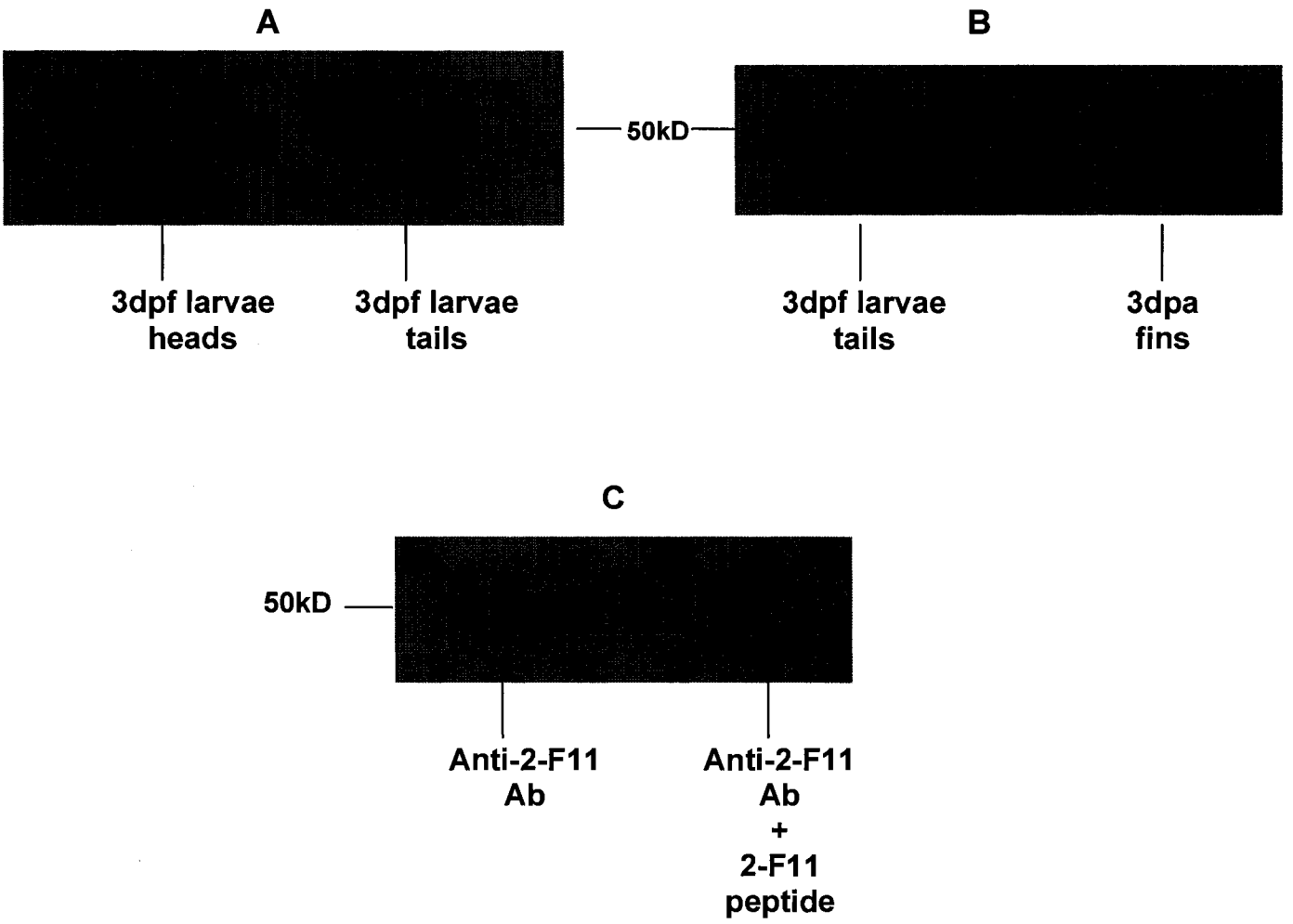
A
B
50kD
3dpf larvae heads
3dpf larvae tails
3dpf larvae tails
3dpa fins
C
50kD
Anti-2-F11 Ab
Anti-2-F11 Ab + 2-F11 peptide

during fin regeneration. Moreover, similarities with collagen and elastoidin make them good candidates for the components of the actinotrichia.

3.8. Functional analysis of 2-H06 and 2-F11 proteins during zebrafish embryogenesis

The functional analysis of the *2-H06* and *2-F11* genes during embryogenesis was performed using a gene "knockdown" approach based on the injection of morpholino oligonucleotides in 1-cell-stage zebrafish embryos. Morpholinos are short modified oligonucleotides that can block the initiation of translation in the cytosol if they are targeted to the 5' UTR of a given mRNA or can modify pre-mRNA splicing in the nucleus if they are targeted to splice junctions. They have a nucleic acid base, a non-ionic phosphorodiamidate inter-subunit linkage and a 6-member morpholine ring instead of 5-member ribose backbone which makes them more stable than other oligonucleotides in living systems. Morpholinos were made against each gene and were injected in embryos individually and together. The results of each type of injection will be discussed in detail below.

The zebrafish 2-H06 morpholino (2-H06-MO) and 2-F11 morpholino (2-F11-MO) (Gene Tools, LLC) are targeted to block the translation initiation of zebrafish *2-H06* and *2-F11* mRNAs, respectively. To verify the efficiency of the morpholino injections, the 2-F11 morpholino was designed with a fluorescein tag. The fluorescence helps to determine whether the morpholino has successfully been incorporated in the embryo after injection. This aided not only the 2-F11-MO injections but also in the co-injections and only those embryos with similar fluorescence levels were taken in the calculations.

The standard non-specific morpholino (Gene Tools, LLC) and uninjected embryos were used as controls. The phenotypic morphology of the *2-H06* and *2-F11* knockdown embryos (or morphants) and control embryos was compared at various developmental stages to obtain clues about the role of the two proteins during development. The morphant embryos were analyzed for size, survival rates, overall morphology and gene expression to gain more insights into the differences with wild type embryos.

3.8.1. Choices of the MO concentrations used for the functional analysis

As choosing the right concentration of morpholinos for injections is a trial and error method, seven different amounts of the *2-H06* and *2-F11* morpholinos 40ng, 10ng, 5ng, 2ng, 1ng, 0.5ng and 0.1ng were injected into the 1-cell zygote.

Following these, the survival rates and the various defects of the morphant embryos were analyzed. Due to the high mortality (90%, n=150) seen upon injecting the two highest doses of 40ng and 10ng, it was concluded that they were toxic to the embryos. Hence the four other concentrations ranging from 5ng to 0.1ng were used for subsequent analysis. The same amounts of standard non-specific morpholino were injected into embryos as controls and some embryos were left uninjected. The survival rates of embryos injected with the standard control morpholino were high in all the control injections, 10ng (70.14%, n=200), 2ng (82.31%, n=180), 1ng (79.12%, n=150), 0.4ng (81.67%, n=200), 0.1ng (80.91%, n=200). No significant defects were seen in the standard control injected morphants when compared with wild type embryos.

Injections performed at 1.5ng for the 2-H06-MO and 3.5ng for the 2-F11-MO were used in further experiments are these amounts gave the highest survival rate with minimal detectable defects.

3.8.2. Effects of the individual injection of 2-H06-MO

During the preliminary stages of the *2-H06* gene knockdown it was observed, that even at the lower non-toxic concentrations of 5ng/embryo and 2ng/embryo for *2-H06* morpholino, although the survival rate was high (73%, n=210), there were many different defects affecting not only the fins, as was expected, but other structures such as the heart, head, eyes and the overall growth and pigmentation. All these defects were drastically reduced when 1.75ng of 2-H06-MO was injected in the embryos (Figure 19). At this dosage the morphants showed reduced pectoral fin buds and a reduced median fin fold.

The actinotrichia were present and were only slightly smaller in size when compared to the WT embryos. The morphants had a smaller overall size and their development was slightly delayed. Pigmentation defects such as the presence of pigment cells in regions not usually expected (yolk sac and fin folds) as well as excessive pigments in regions such as the head and trunk were still widely observed and about 79% of the morphants still had a smaller head. There were no defects in the somites but there was still a 5% occurrence of pericardial edema after 4dpf and 99% of the embryos showed a delay in development. These results are shown in a tabulated form in Table 1.

Figure 19. Comparison of 3dpf WT and 3dpf morphant phenotypes.

The figure shows the lateral view of the entire larvae at 3dpf in the left panels (a-e). The middle panels (f-j) show the lateral view of the median fin folds and the right panels (k-o) show the dorsal view of the head and pectoral fins. The horizontal panels from top to bottom show WT, 2-H06-MO (1.5ng) injected, 2-F11-MO (3.5ng) injected, CO-MO (1.5ng 2-H06 and 3.5ng 2-F11) injected and standard control-MO (3.5ng) injected larvae at 3dpf, respectively. The arrow in panel (n) of the 3dpf co-injected morphant points out the absence of the pectoral fin buds while the circled region in panel (o) of the std. control injected morphants shows the presence of the fin buds. Scale bar for a-e: 250 μm.

3dpf WT

3dpf 2-H06-MO

3dpf 2-F11-MO

3dpf CO-MO

3dpf Std.cont-MO

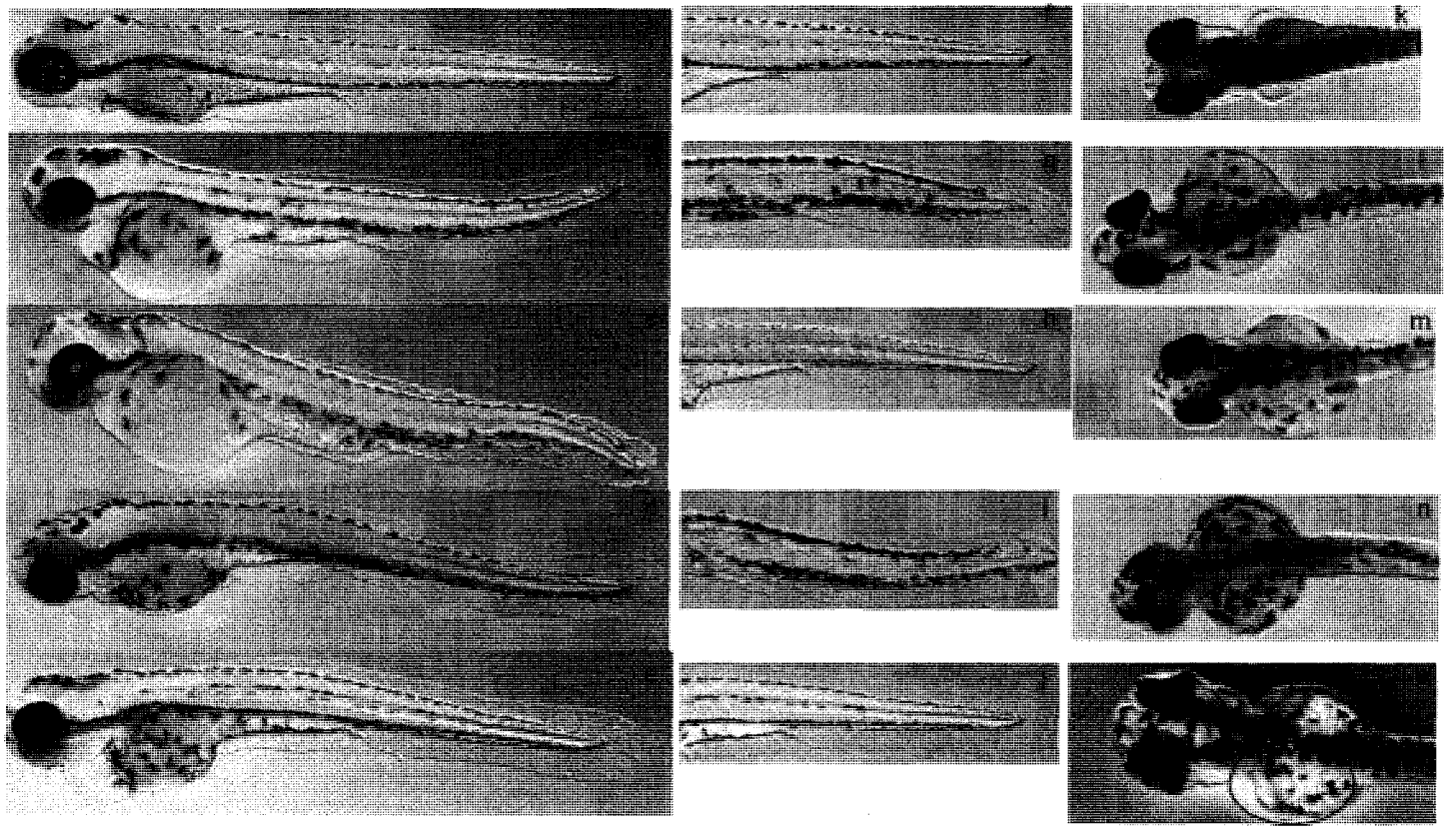

Table 1. Effects of *2-H06* and/or *2-F11* morpholino injections on zebrafish development.

Defects observed at 72hpf following injection of each morpholino	**WT (n=350)**	**2-H06 Morphants (n=358)**	**2-F11 Morphants (n=310)**	**Co-injected Morphants (n=372)**
Reduced pectoral fin buds	0%	87%	5%	99%
Reduced median fin fold	0%	85%	80%	90%
Absence of actinotrichia	0%	2%	0%	97%
Pericardial edema	0%	5%	2%	5%
Smaller overall size	1%	95%	95%	99%
Smaller head / craniofacial defects	0%	79%	81%	87%
Delay in development	1%	99%	97%	99%
Pigmentation defects	0%	92%	93%	97%
Defects in pattern of somites	0%	0%	0%	0%

Dosage injected
1.75ng/embryo of 2-H06-MO
3.5ng/embryo of 2-F11-MO
1.75ng/embryo and 3.5ng/embryo of CO-MO

3.8.3. Effects of the individual injection of 2-F11-MO

The morpholino for the *2-F11* gene was designed with a fluorescein tag to aid examination of the injected embryos. The initial doses that were injected for this morpholino (0.1 and 2ng) did not seem to have any effect on the developing fin buds when compared with the WT phenotype. When the dosage was changed to 5ng a smaller head and craniofacial defects (65%, n=150) as well as defects in pigmentation (75%, n=150) and possible defects in the hindbrain and forebrain regions were observed. Hence, a final dosage of 3.5ng that generated fewer defects was selected for all further analysis.

At this dosage, the median fin fold as well as the pectoral fin buds appeared to be developing normally but the dorsal portion of the median fin fold seemed less developed. The actinotrichia were visible and were the same size as the actinotrichia of the WT uninjected control embryos. The morphants were smaller in size (95%) when compared with the WT embryos and there was a very slight delay in their development (97%). These results are shown in Figure 19 and Table 1.

3.8.4. Effects of the coinjection of both morpholinos

Upon the co-injection of both morpholinos at 4ng of each morpholino, many defects affecting not only the fins, as was expected, but also other structures such as the heart, head, eyes, overall growth and pigmentation were evident in the co-injected morphants. The morphants showed severe craniofacial defects, with a small head and eyes developing very close to each other. Subsequent injections with a reduced concentration of the 2-H06-MO to 1.75ng and of the 2-F11-MO to 3.5ng not only increased the rate of survival of the morphants but also decreased the different types and

frequency of defects affecting structures other than the fins (Figure 19). The rate of pericardial edema after 4dpf was drastically reduced (1%, n=300), but even at the lower doses the morphants seemed to be slightly smaller and there was a slight delay in their development. There were pigmentation defects (10%, n=200) but repeated injections of standard control morpholino also showed these pigmentation defects (8%, n=350) and delay in development as well as a smaller overall size (1%, n=300), hence these could be non-specific defects. A closer study of the fin folds of these morphants revealed a delay in development and the fin folds seemed smaller than the fin folds of wild type embryos of the same clutch. As mentioned earlier, the actinotrichia in the *2-H06* and *2-F11* single morphants seemed to be developing normally when compared to the wild type and standard control morpholino injected embryos. In contrast, following the co-injection of both morpholinos, embryos showed a complete absence of actinotrichia, which lead to the fin fold losing its structural integrity (Figures 20 and 21). In the coinjected morphants, the fin fold was distinctly granular in appearance when compared with the WT and *2-H06* or *2F11* morphants (Figure 20). This could be due to the cell processes of the migrating cells in the fin fold not being aligned in the absence of the actinotrichia. The fin fold seemed to be very delicate (tore frequently during fixation), less supported and curled up easily in these morphants. This supports the hypothesis that the two genes encode for structural components of the actinotrichia.

To clearly examine the fin fold and actinotrichia defects in the morphants, Picrosirius red staining was used. This staining protocol allows the easy visualization of the collagenous fibrils (Bechara *et al.*, 2000). The various collagen-containing structures appear bright red when stained with picrosirius red. Thus, it clearly showed the

Figure 20. Comparison of 4dpf WT and morphant median fin folds.

Lateral view of the caudal part of 4dpf WT uninjected larva (a), larva injected with 2-H06-MO alone (b), 2-F11-MO alone (c) and co-injected with 2-H06 and 2-F11-MOs (d). The dotted line in (a) represents one actinotrichial fibril. An absence of the actinotrichia is observed only in larvae co-injected with the two morpholinos. Rostral is to the left and caudal to the right. Scale bar in a-d: 25 μm.

Abbreviations: a, actinotrichia; mff, median fin fold.

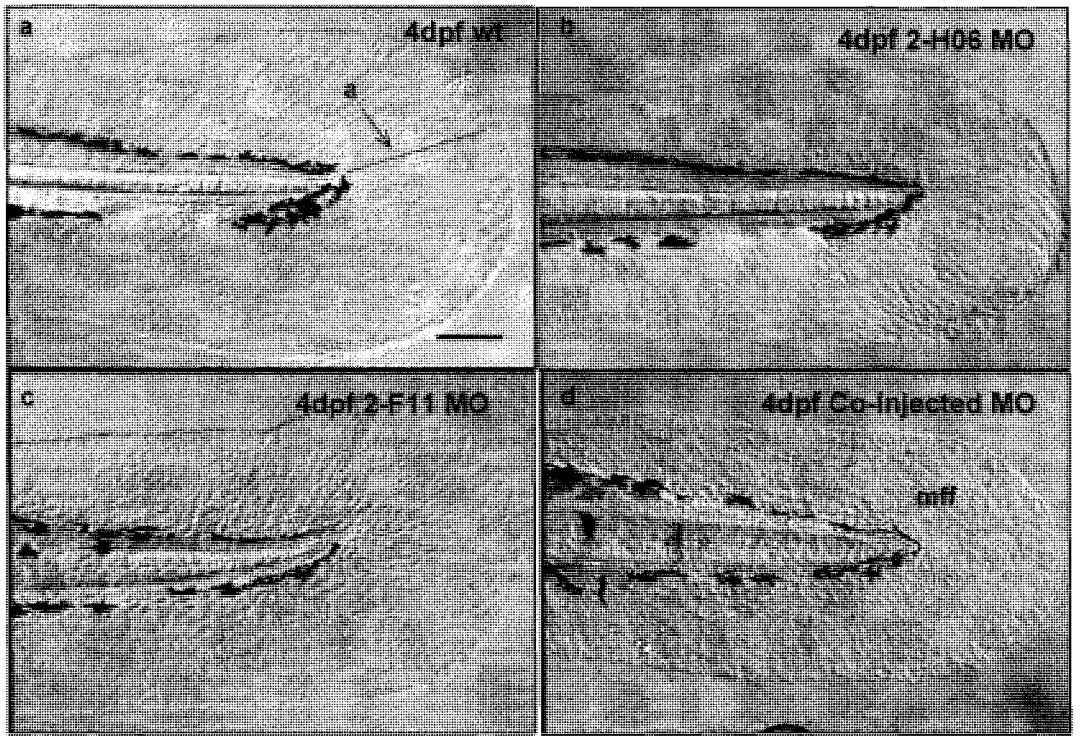
a
4dpf wt
d
b
4dpf 2-H06 MO
c
4dpf 2-F11 MO
d
4dpf Co-Injected MO
mff

Figure 21. Picrosirius red staining of 4dpf WT and morphant median fin folds showing the absence of actinotrichia in the co-injected morphants.

Lateral view of the caudal part of (**a**) 4dpf WT median fin fold; (**b**) and (**c**) the median fin folds of larvae injected with 2-H06-mo and 2-F11-MO respectively; (**d**) median fin fold of CO-MO injected larvae. The dotted line in (**a**) represents one actinotrichial fibril. The actinotrichial fibrils are only missing in the coinjected embryos. Scale bar in a-d: 10 μm. Abbreviations: a, actinotrichia; mff, median fin fold.

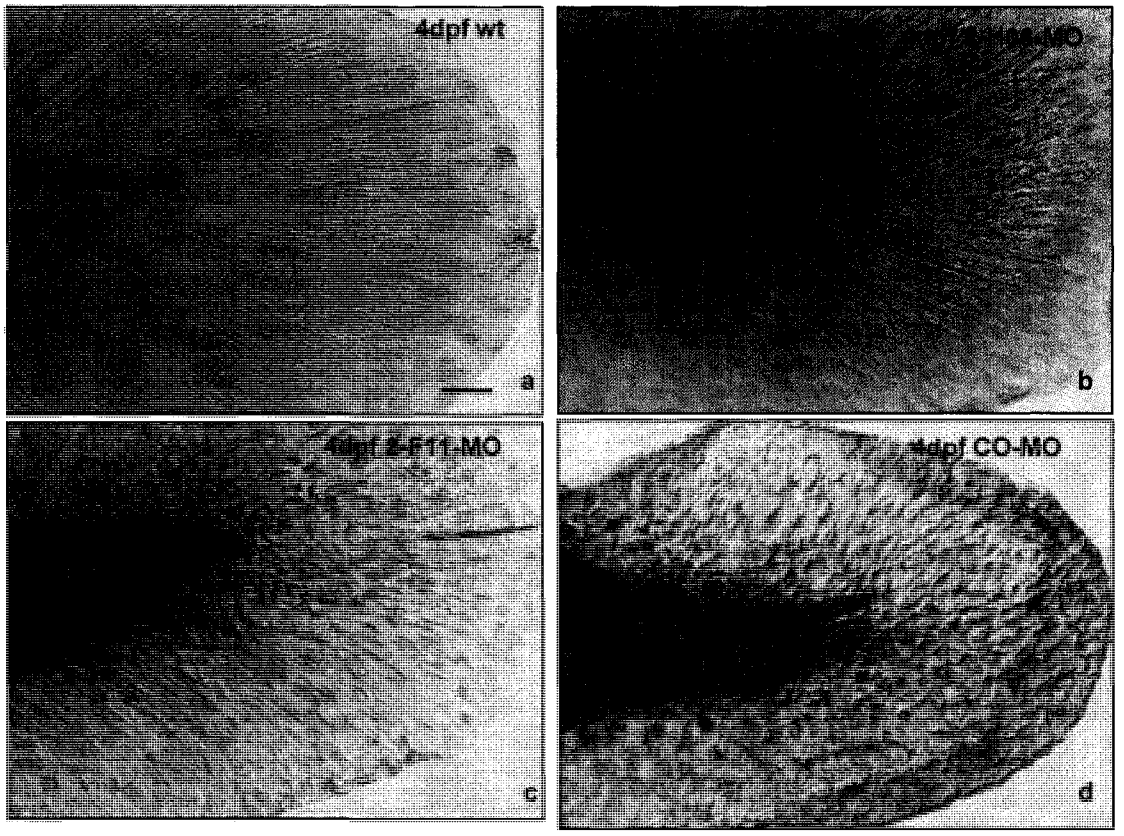
4dpf wt
a
b
4dpf δ-F11-MO
c
4dpf CO-MO
d

actinotrichial defects seen in the co-injected morphants (Figure 21).The pectoral fin buds seemed to be very deformed at the higher concentration of 4ng of each morpholino and were stump-like but at the lower dose of 1.75ng 2-H06-MO and 3.5ng of 2-F11-MO, the fin buds were developing normally but with smaller fin folds (data not shown).

3.9. Expression of *2-H06* and *2-F11* in morphant and control embryos

The expression of *2-H06* and *2-F11* transcripts in the morphants was analyzed by ISH.

ISH on *2-F11* morphants with *2-H06* antisense-RNA probe showed no evident difference in expression when compared with the expression of *2-H06* in WT embryos, whereas the expression of *2-H06* in the 2-H06-MO injected morphants was greatly reduced and was almost absent in the co-injected morphants (Figure 22).

A similar scenario was seen for the *2-F11* antisense-RNA probe. There was no difference in the expression of the *2-F11* probe on the 2-H06-MO injected morphants, but the expression of the *2-F11* in the 2-F11-MO injected morphants was severely reduced in comparison with its expression in the WT counterparts and was absent in the coinjected morphants (Figure 22).

3.10. Protein analysis of morphant and control embryos:

To verify the efficiency of the morpholinos, proteins were extracted from 3dpf larvae, both WT and morphants (1.75ng 2-H06-MO, 3.5ng 2-F11-MO and embryos coinjected with 1.75ng 2-H06-MO and 3.5ng 2-F11-MO). The proteins were separated by SDS-PAGE and were immunoblotted using the anti-2-F11 antibody. The immunoblot for

Figure 22. Absence of *2-H06* and *2-F11* transcripts in the coinjected 3dpf morphant larvae.

(a-d) 3dpf larvae hybridized with the *2-H06* probe and (e-h) 3dpf larvae hybridized with the *2-F11* probe. The arrows in (a) and (e) show expression of *2-H06* and *2-F11,* respectively. The arrows in (d) and (h) indicate the region in the median fin fold of the coinjected morphants that shows no expression of the respective probes.

Scale bar in a-h: 200 μm.

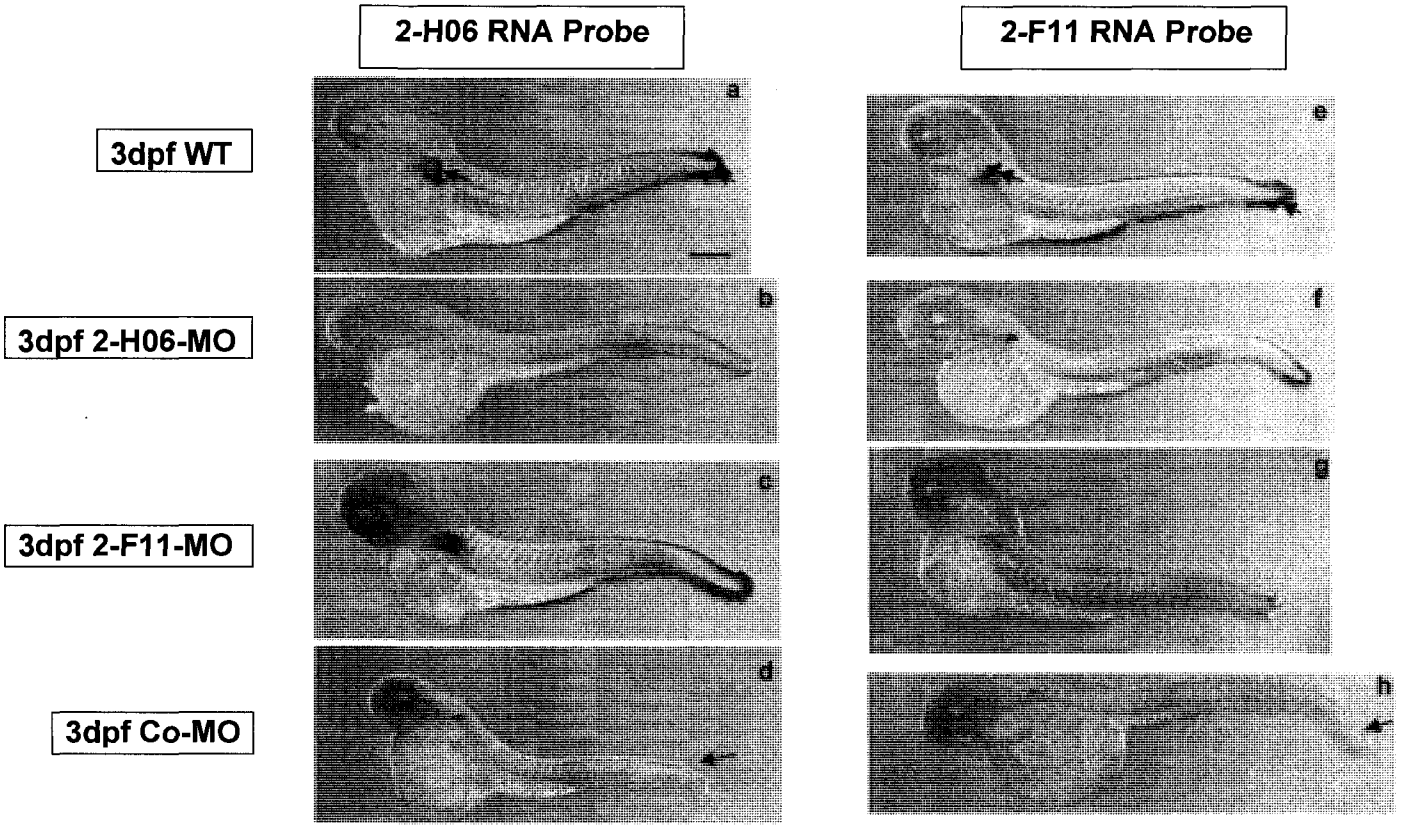
2-H06 RNA Probe
2-F11 RNA Probe
3dpf WT
3dpf 2-H06-MO
3dpf 2-F11-MO
3dpf Co-MO
a
b
c
d
e
f
g
h

proteins from 3dpf WT larvae tails showed a distinct band at around 50kD. The immunoblot with the proteins from the 2-H06 and 2-F11 single morphants still showed a band at 50kD, in spite of the knock down. This result was expected as the antibody is against a peptide chosen from a region conserved in both proteins. In contrast, this band was absent in protein extracts from coinjected morphants (Figure 23). This confirms that the knock-down of both genes accomplished by co-injecting the two morpholinos blocked the translation of both mRNAs.

3.11. Observations after the morpholinos are no longer effective

It has been shown that morpholinos have an effect up to 4-5dpf ("Special morpholino issue" of Genesis vol. 30(3), 2001). Some observations were made after 4dpf and are detailed below.

3.11.1. Growth of Actinotrichia

We observed that the actinotrichia gradually started to grow in the fin folds of the coinjected morphants at 5dpf suggesting that the morpholinos lose their effectiveness after 5dpf (Figure 24). The actinotrichia in the coinjected morphants were similar to the WT counterparts at approximately 7dpf. This is also a confirmation of the fact that the absence of actinotrichia is a result of the morpholino coinjections.

3.11.2. Expression of *2-H06* and *2-F11* transcripts in coinjected morphants

In situ hybridizations were performed on the median fin folds of the morphants at 3, 4, 5, 6 and 7dpf using antisense-RNA probes for *2-F11* and *2-H06*. At 3dpf and 4dpf,

Figure 23. Expression of 2-H06 and 2-F11 proteins in 3dpf morphant larvae.

Total proteins from 3dpf morphant larvae tails were separated using SDS-PAGE (12% acrylamide) and immunoblotted with anti-2-F11 antibody. The 50kD band is present in embryos following injection of 2-H06-MO or 2-F11-MO but is absent in the 3dpf coinjected morphants.

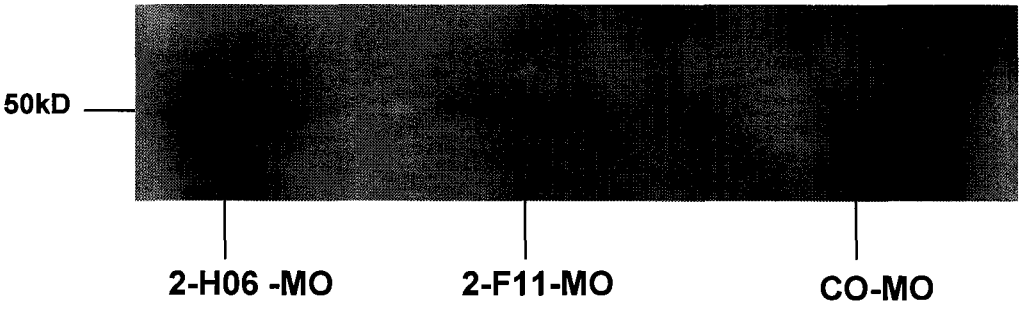
50kD
2-H06 -MO
2-F11-MO
CO-MO

Figure 24. Growth of the actinotrichial fibrils after 5dpf in the coinjected morphants.

(**A**) Absence of actinotrichial fibrils in the lateral view of the median fin fold of 4dpf coinjected morphants. (**B**) Growth of the actinotrichia in the fin fold of 5.5dpf coinjected morphants. The arrow points to the gradually growing actinotrichia. The dotted white lines indicate the length of the actinotrichia in the fin fold. Scale bars: 5 μm.

Abbreviations: a, actinotrichia; mff, median fin fold.

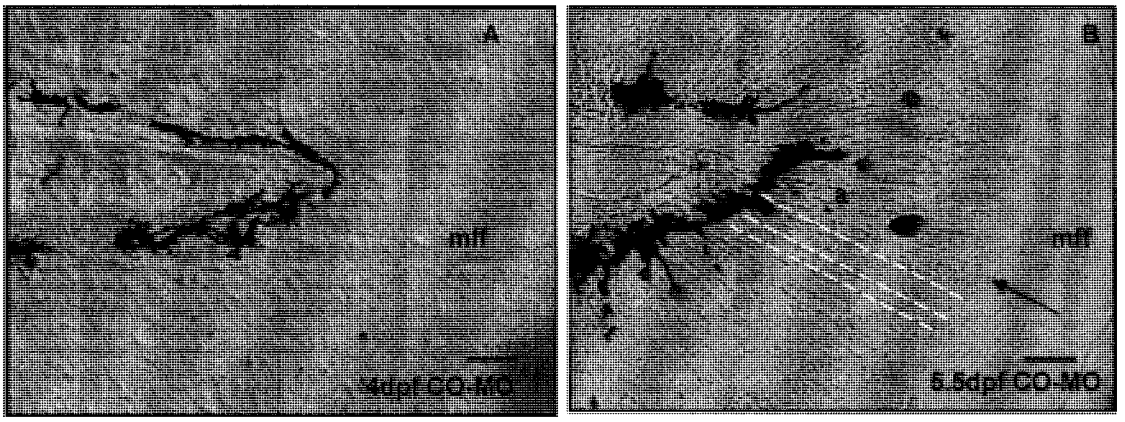
A
mlf
4dpf CO-MO
B
mlf
5.5dpf CO-MO

there was no expression of *2-F11* and *2-H06*. However, when ISH was performed at 5dpf and 6dpf on the coinjected morphants, I observed expression of both *2-H06* and *2-F11* with a stronger hybridization signal at 6dpf than at 5dpf (Figure 25). The ISH was performed exactly in the same conditions and the samples were stained for the same amount of time. The expression of *2-H06* and *2-F11* further suggests that the morpholinos are no longer effective after 4dpf. Furthermore, this expression correlating with the appearance of the actinotrichia at the same stages confirms the role of 2-H06 and 2-F11 in the formation of the actinotrichia (Figure 25).

3.12. Rescue of morphants by *2-H06* and *2-F11* mRNA injection

To rescue the phenotype observed with the coinjection of both morpholinos, 16ng, 8ng and 4ng of *2-H06* or *2-F11* mRNA was coinjected along with the morpholinos. The highest survival rate of the rescued morphants was obtained with the injection of 4ng of *2-H06* mRNA (59.29%) or 4ng *2-F11* mRNA (62.64%). Each mRNA individually rescued the absence of actinotrichia phenotype (Table 2) but neither was able to rescue the pigmentation and craniofacial defects to a great degree.

The actinotrichia in the rescued morphants were developing at a rate similar to their WT counterparts. Rescue analysis performed by injection of single stranded mRNA (*2-H06* or *2-F11* mRNA) in the coinjected morphant embryos confirmed that the absence of actinotrichia was a defect specific to the knockdown of both *2-H06* and *2-F11* genes.

Figure 25. Gradual increase of expression of *2-H06* and *2-F11* transcripts in the median fin fold of the 5 and 6dpf coinjected morphant larvae.

Lateral view of the median fin fold of 4, 5 and 6dpf larvae hybridized with the *2-H06* probe (a-c) and the *2-F11* probe (d-f). (a, d) WT larvae at 4dpf, (b, e) and (c, f) morphant larvae at 5dpf and 6dpf, respectively.

Scale bar in a-f: 100 μm.

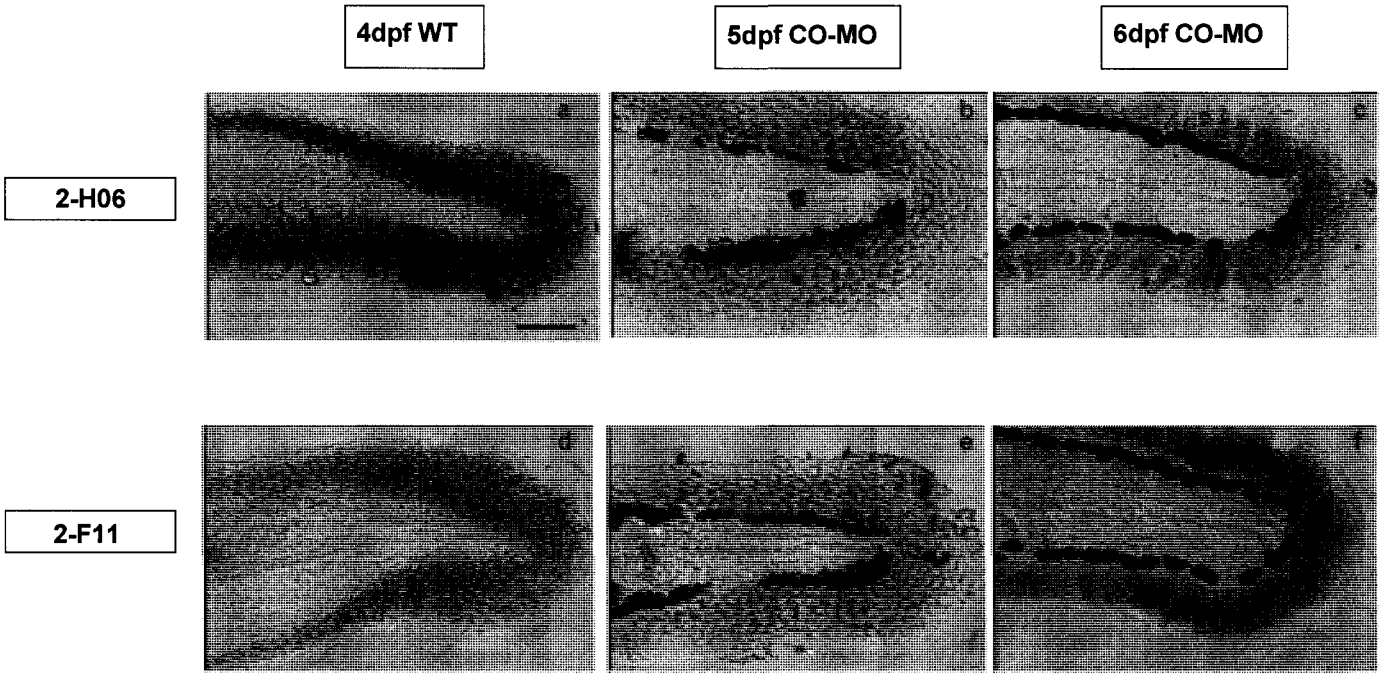
4dpf WT
5dpf CO-MO
6dpf CO-MO
2-H06
2-F11
a
b
c
d
e
f

Table 2. The percentage of the rescue of the absence of actinotrichia defect in the coinjected morphants. The absence of actinotrichia was rescued in 85.29% and 92.64% of morphants by injection of *2-H06* or *2-F11* mRNA, respectively.

Table 2: Percentage of the rescue of the absence of actinotrichia defect in the co-injected morphants

Concentration of mRNA/ Name of mRNA	4ng
2-H06	85.29
2-F11	92.64

n = approx. 250 embryos/ solution

3.13. Comparison of expression pattern of *2-H06* and *2-F11* with *col1a1* and *col1a3*:

The collagen component of the actinotrichial fibrils is collagen type I (Montes *et al.*, 1982; Kimura *et al.*, 1986). ISH reveals that *col1a2* is not expressed in the fin folds (Fisher *et al.*, 2003). In addition to the collagen α1(I) and α2(I) subunits common to all vertebrates, many teleost fish have a third collagen subunit, α3(I), which has not been found in any other vertebrates (Kimura *et al.*, 1987; Kimura *et al.*, 1991; Kimura, 1992). The properties of the *col1a3* are closely related to those of *col1a1*. ISH were performed with the *col1a1* and *col1a3* antisense RNA probes (cloned in our laboratory). We observed high levels of expression of *col1a1* and *col1a3* in the median fin fold and the pectoral fin buds reminiscent to that of *2-H06* and *2-F11* expression in 3dpf WT embryos (Figure 26).

Figure 26. Expression of *col1a1*, *col1a3*, *2-H06* and *2-F11* in 3dpf larvae.

In situ hybridization revealed similar in the expression patterns in the developing fin folds. The larvae are 3dpf and are shown in a lateral view with rostral to the left and caudal to the right. The arrows indicate similar expression patterns in the median fin folds of the 3dpf larvae. Scale bar: 200 μm.

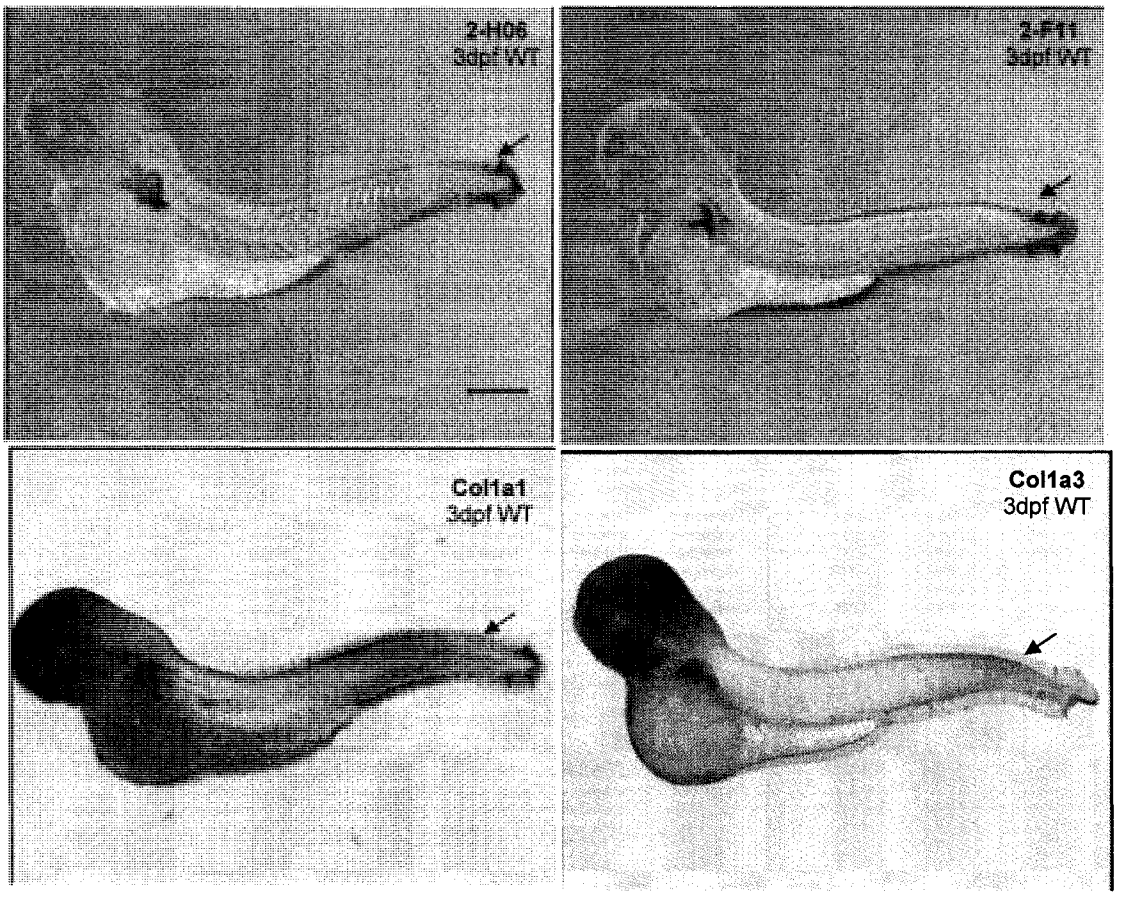
2-H06
3dpf WT
2-F11
3dpf WT
Col1a1
3dpf WT
Col1a3
3dpf WT

4. DISCUSSION

The zebrafish (*Danio rerio*) is an excellent animal model for the study of vertebrate development and regeneration. The major part of the developing zebrafish fins is made up of a fin fold which is supported by the endoskeleton. The first components of the exoskeleton are rigid fibrils known as the actinotrichia. Later the main exoskeletal component of the rays, the lepidotrichia appear and they are made of dermal bone (Grandel & Schulte-Merker, 1998). Our initial hypothesis based on the expression analysis data and sequence alignments was that the two newly identified genes, *2-H06* and *2-F11*, were good candidates for components of the actinotrichia.

4.1. Similarities between actinotrichial elastoidin and the 2-F11 protein family at the biochemical level

The composition of the actinotrichial fibrils has been debated since the late 19th century. It is now known that actinotrichia are formed of elastoidin, a complex consisting of a collagenous and a non-collagenous component (Kimura & Kubota, 1966). The collagenous component of elastoidin is made of col1a1 protein (Montes *et al.*, 1982) while the non-collagenous component has not yet been characterized. Type I collagen serves the main supporting function in all vertebrates (Kimura *et al.*, 1987; Kimura *et al.*, 1991). The elastoidin forms the actinotrichial fibrils are responsible for the structural integrity of the fin fold, holding it stretched, yet elastic enough to help the fish swim. The actinotrichia appear before lepidotrichia, early in fin development and regeneration (Géraudie & Singer, 1992; Becerra *et al.*, 1996). As the lepidotrichia grow in length, the

arrays of actinotrichia become confined to the distal tip of the lepidotrichia remaining always distally located in a constant polymerization-depolymerization balance (Marí-Beffa *et al.*, 1989). This spatial relationship suggests that actinotrichia may possibly guide the location of lepidotrichia and the tip of the fin may remain structurally rigid in the absence of bone (Géraudie & Landis, 1982)

In the 1950's and 60's many biochemical studies were performed on elastoidin fibers. It was found that collagenase from *Clostridium histolyticum*, which showed a high specific activity on both native and denatured collagen, hydrolyzed only 5% of the elastoidin fiber indicating that the elastoidin complex contains collagen and a non-collagenous part (Gross & Dumsha, 1958; Kimura & Kubota, 1966). Moreover, the collagen moiety of elastoidin, unlike its non-collagenous counterpart, was readily released by pepsin treatment in the native state (Kimura & Kubota, 1966). Based on these findings it has been suggested that the interaction between the collagen molecule and the non-collagenous protein would be responsible for the formation of the insoluble elastoidin fiber, which would then reject the action of collagenase. It has also been hypothesized that cross-linkages such as disulfide linkage and a peroxide linkage formed by oxidation of two tyrosine residues, may possibly explain the peculiar hydrothermal behavior and insolubilization of elastoidin (Kimura & Kubota, 1966). A more recent study has also discussed how a high content of tyrosine in the N-terminal domains of collagens is likely to mechanically stabilize a fibrillar complex (Snellman *et al.*, 2007). Early biochemical studies conducted on elastoidin showed that it is very rich in tyrosine, 7.15% by weight as compared to 1% for collagens (Kimura & Kubota, 1969). Elastoidin also has low hydroxy-proline content similar to that of fish collagens (Damodaran *et al.*,

1956). Both 2-H06 and 2-F11 have high tyrosine contents similar to the tyrosine content of the non-collagenous component of elastoidin. 2-H06 has 5.72% tyrosine residues and 2-F11 has 8.09%. It is possible that 2-H06 and 2-F11 provide tensile strength to the actinotrichial fibrils by hetero-typically cross-linking to col1a1 and forming a multi-component fibril in this fashion.

Cysteine residues are assumed to be essential in the trimerization of the collagen molecule by forming disulfide bonds between the alpha chains (Dubois *et al.*, 2002; Snellman *et al.*, 2007). The 9 aa repeats found in both, 2-H06 and 2-F11, peptide sequences are flanked by cysteine on each side and are hypothesized to stack upon each other aided by the cysteine bonds and then form rod-like structures. This corroborates the hypothesis that the two proteins, 2-H06 and 2-F11 play a role in fibril formation.

4.2. Expression analysis of the *2-F11* gene family in regenerating fins and developing embryos at the mRNA level

The onset of expression of *2-H06* and *2-F11* is seen at 24hpf, just preceding the time point at which the actinotrichia become visible in the median fin fold (at around 28hpf). A recent search of the Sanger Institute database revealed two genes, *2-J* and a fourth gene, encoding for much shorter protein sequences. Expression analyses done in our laboratory reveal that the expression patterns of transcripts of the two short genes in the developing fin buds of the zebrafish embryos are very similar to those of *2-H06* and *2-F11* suggesting that all the four genes belong to the same gene family.

In regenerating fins, the *2-H06* and *2-F11* transcripts are found in the cells lining the actinotrichial arrays. Moreover, the expression of the transcripts in regenerating fins

is seen after blastema formation and not during the initiation of fin regeneration. This expression seen at the time and at the level of the actinotrichia in regenerating fins suggests that the genes play a role in actinotrichia formation during adult fin regeneration.

Expression patterns for *2-H06* and *2-F11* transcripts are clearly restricted to the developing fin buds. Moreover, their expression is seen at the time of formation and at the level of the actinotrichia in the regenerating fin samples. These expression patterns seen both in developing embryos and in regenerating fins of adult fish suggest a possible role of these proteins in the formation of the actinotrichia. It has long been debated whether cells of mesenchymal or epidermal origin are responsible for actinotrichia formation. Studies in the 70's and 80's hypothesized that the origin of the actinotrichial fibrils was in the mesenchymal region below the developing epidermal fold (Géraudie, 1977; Géraudie & Landis, 1982; Géraudie, 1985). In 1991, Peter Thorogood suggested that the actinotrichia originate from the epithelium and grow lengthways by distal extension (Thorogood, 1991). Our results suggest that cells of both mesenchymal and epidermal origins are responsible for actinotrichia formation.

4.3. Knockdown of *2-H06* and *2-F11* genes in developing embryos leads to an absence of actinotrichia

Individual gene knockdowns of *2-H06* and *2-F11* did not show any major defect in the fin morphology when compared with the WT embryos and control morpholino injected embryos. Only the double knockdown after the coinjection of both the morpholinos showed an absence of actinotrichia. The absence of effect following single

gene knockdown might be due to the compensation effect of the protein of the same family that is not knocked down and therefore might mask the effect of the absence of the one that is knocked down. These results suggest that the two proteins might be cooperating to make the elastoidin protein complex.

Studies conducted on cultured embryonic fins and intact embryos showed that shortly after maximal fin fold extension is attained, the most distal mesenchymal cells at the base of the fin bud start to migrate distalward into the extracellular space of the fold (Thorogood, 1991). This coincides with the emergence of a number of aligned filopodia on the distal aspect of the migrating mesenchymal cells. Ultrastructural and morphometric analyses revealed that both filopodia and cell bodies of these migrating cells use the actinotrichia almost exclusively as a migration substratum (Wood & Thorogood, 1984). Thus, the actinotrichia not only support the fin fold but also elicit a guided response from the invading mesenchymal cells and thereby were proposed to set up the cell organization and geometry for the formation of the definitive dermal skeleton of the functional fin (Thorogood, 1991). In the double knockdown morphants, the absence of actinotrichia leads to the formation of a less developed and smaller median fin fold that curls, easily tears and has lost its structural integrity. This demonstrates the important function of the actinotrichia as a support structure keeping the fin fold elastic yet stretched. Moreover, as the cell processes in the fin fold are not aligned, it is possible that the absence of the actinotrichia leads to disrupted migration of mesenchymal cells in the developing fin fold.

Recently, the mapping and molecular characterization of the *chihuahua (chi)* mutation in zebrafish revealed a defect in the gene encoding collagen I (α1) (*col1a1*)

(Fisher *et al.*, 2003). It is interesting to note that these mutants have defective fin folds. It was observed in some heterozygous *chi/+* larvae that the fin growth was slower than its wild type counterparts and the fins showed 80% of the width of WT fins. Both these phenotypes were observed in the double knock down morphants by co-injection of 2-H06-MO and 2-F11-MO. col1a1 is present in actinotrichia therefore allowing the hypothesis that the *chi* mutants could possibly lack actinotrichia. Further morphological analysis of these *chi* mutants and expression analysis could also shed light on the relationship of 2-H06 and 2-F11 with col1a1. Future studies could also focus on confirming the binding of the proteins of this gene family to collagen type I. This can be studied *in vitro* using 2-F11+GST and 2-H06+GST fusion proteins in a collagen binding assay in plates coated with collagen Type I protein.

Non-antisense effects of the morpholinos can result from undesirable interactions between the morpholino and proteins or nucleic acid sequences, even when rigorous controls are in place (Corey & Abrams, 2001). Hence, it is suggested that gene knockdowns should be followed up by mRNA rescue experiments to validate results (Ekker, 2000). The rescue experiments revealed that only the absence of actinotrichia defect was completely recovered after the individual injection of the *2-H06* or *2-F11* mRNAs. These results further suggest that the two genes probably have similar and complementary functions during early development. Other defects that were not rescued by mRNA injections might be non-specific. However, one cannot rule out the possibility that the expression of the two genes exclusively seen in the developing fins is due to a lack of sensitivity of the ISH and over-staining the samples might reveal their expression in other tissues. In this case it is possible that the other defects observed in the single and

double knockdown morphants could be specific.

The efficiency of the double knockdown was confirmed by immunoblotting using the anti-2-F11 antibody. In accordance with the expression analysis results, immunoblotting also revealed that both proteins, 2-H06 and 2-F11, are expressed during early development specifically at the level of the developing fin folds and are absent from the head region. However, immunohistochemistry on tissue samples from both embryos and fin regenerates, using the anti-2-F11 antibody did not detect any signal. Nevertheless, it is possible that immunohistochemistry might not have worked due to technical problems. For example, it is not excluded that with the technique of fixation of the tissue samples may not be appropriate. This procedure can be further tested using a shorter or longer fixation time or a different fixation buffer.

ISH on *2-F11* morphants with the *2-H06* antisense-RNA probe showed no evident difference in *2-H06* expression when compared with its expression in WT embryos, whereas the *2-H06* expression in the 2-H06-MO injected morphants was greatly reduced. A similar scenario was seen with the *2-F11* antisense-RNA probe, with no difference in the *2-F11* expression in the 2-H06-MO injected morphants; but *2-F11* expression was severely reduced in the 2-F11-MO injected morphants. There was no expression of *2-H06* or *2-F11* in the coinjected morphants. The down-regulation of the *2-H06* and *2-F11* transcripts in the single morphants is an interesting aspect of the knockdown experiments. It may suggest a positive feedback mechanism wherein the 2-H06 and 2-F11 protein products regulate the transcription of the respective genes. In zebrafish presomitic mesoderm, oscillatory genes include *her1* and *her7,* transcriptional repressors whose expression is thought to be enhanced by Notch signaling (Cinquin, 2007). Her1 and Her7

were initially hypothesized to be involved in a direct negative auto-regulatory loop (Lewis, 2003) but morpholino blocking of *her1* or *her7* mRNA translation leads to down-regulation of their respective transcription (Cinquin, 2007). Her1 and Her7 are basic-Helix-Loop-Helix proteins, a family whose members normally function as dimers, and knockdown phenotypes can be explained by taking into account the formation of Her dimers that repress transcription (Cinquin, 2007).

The eventual recovery of actinotrichial growth correlates with the morpholinos losing their effectiveness (at around 4 dpf) and a complete recovery is observed by 8-12dpf suggesting that the disrupted gene activity is essential for actinotrichia formation. The absence of actinotrichia for the first 4pdf does not seem to affect the later development of either the actinotrichia or the fin folds. It is possible that within this window of developmental time, the affected tissues are competent and open to respond to the disruption of gene activities.

4.4. An evolutionary perspective on the loss of the *2-F11* gene family from tetrapod species

The paired fins of teleost fish are phylogenetically related to the limbs of higher vertebrate species. The early stages of formation of teleost paired fins and tetrapod limbs are controlled by similar molecular mechanisms. The zebrafish pectoral fin buds become structurally distinct from tetrapod limb buds only after 48 hours of development when fin fold formation occurs (Grandel *et al.*, 2000). Tetrapods do not develop any structure homologous to the fin fold and actinotrichia do not exist in the tetrapod limb buds. Interestingly, we show that the *2-F11* gene family is only present in fishes and absent

from tetrapod species. There are two possible reasons for this absence. One possibility is that the gene family has been lost in the tetrapod species during evolution after the separation of the teleost fish from the tetrapod lineage. The other explanation is that the gene family has been acquired in teleosts following the divergence from the tetrapod lineage.

Cartilaginous fishes (sharks, rays, skates and chimaeras) are one of the oldest phylogenetic groups of jawed vertebrates and owing to their phylogenetic position, they provide a critical reference for our understanding of vertebrate genome evolution. A survey sequencing genome analysis of the chimaerid holocephalian, elephant shark (*Callorhinchus milii*) was recently conducted (Venkatesh *et al.*, 2007). Fragments of approximately 15,000 elephant shark genes reveal specific examples of genes that have been lost differentially during the evolution of tetrapod and teleost fish lineages (Venkatesh *et al.*, 2007). BLAST searches performed in our lab revealed the presence of orthologs of *2-H06* and *2-F11* in the elephant shark. The presence of orthologs of *2-H06* and *2-F11* in cartilaginous fish, a much older phylogenetic group, suggests that the gene family has been lost in tetrapods. It is interesting to note that the loss of this gene family correlates with the loss of a fin fold in the tetrapod species and with the formation of a limb bud. Therefore, it is possible that the loss of the fish-specific *2-F11* gene family during tetrapod evolution maybe one of the causes or consequences of the transition from fins to limbs.

4.5. Some directions for future studies

The genetic mechanism of median fin fold extension is largely uncharacterized in

zebrafish. At this time, no regulatory elements driving the expression of genes in the fin fold have been characterized. The restricted expression of *2-H06* and *2-F11* in embryonic fins offers the opportunity to use the regulatory regions of these genes to specifically target transgene expression in developing fins and to analyze the effects of gene misexpression on fin buds without affecting any other developmental processes. Thus, identification of such regulatory elements for *2-H06* and *2-F11* will provide unique tools to manipulate gene expression. The ectopic expression of a number of genes known to play an important role in fin and limb development can be investigated; for example, the *hoxd* complex, *bmps,* etc. In mouse limb buds and zebrafish fin buds the expression domain of the 5' members of the *hoxd* complex genes, *hoxd11*, *hoxd12* and *hoxd13* is first restricted to the posterior mesenchymal region on the developing limb/fin buds (Sordino *et al.*, 1995). As the mouse limb develops, the domain of expression of these *hoxd* genes changes and lines the antero-posterior border of the bud (Sordino *et al.*, 1995). As this change in expression is not observed in the zebrafish fin buds, it has been proposed to be necessary for patterning the digital arch of the mouse limb bud, an event thought to have driven the transition from fins to limbs (Sordino *et al.*, 1995; Metscher *et al.*, 2005).

Generation of a zebrafish transgenic line expressing one of the 5' members of the *hoxd* complex (*hoxd11/12/13*) under the control of the regulatory elements of *2-F11* should extend the expression of this gene along the antero-posterior axis in the late fin bud. One can expect that such misexpression may induce patterning defects of the fin buds, perhaps ectopic cartilaginous nodules that may allow us to test the hypothesis of the role of the 5' *hoxd* genes in the formation of the digital arch.

The bone morphogenetic proteins, Bmp2 (bmp2b in zebrafish) and Bmp4, are expressed in the distal mesenchyme and in the AER of the developing limb buds and fin buds (Francis *et al.*, 1994; Neumann *et al.*, 1999). In chicks, experimental inhibition of BMP signaling results in persistence of the AER and excess soft-tissue growth between the digits (Pizette & Niswander, 1999; Panman & Zeller, 2003). This suggests that BMPs negatively regulate the AER and is necessary for the normal regression of the AER (Pizette & Niswander, 1999; Panman & Zeller, 2003). However, in fin buds, instead of regressing, the AER becomes the fin fold that elongates while bmp2b and bmp4 are still expressed (Neumann *et al.*, 1999). Chordin binds to and antagonizes the function of bmps (Piccolo *et al.*, 1996; Bachiller *et al.*, 2003; Nakayama *et al.*, 2004). Generation of transgenic lines ectopically expressing Chordin under the control of the regulatory elements of *2-F11* should inhibit Bmp signaling in the distal part of the fin bud. The expression of Chordin will be induced at the time corresponding to the regression of the AER and not from the very beginning of the fin bud development. This could possibly lead to a persistence of the AER and no fin fold formation.

4.6. CONCLUDING REMARKS

The results from the study conducted on these two novel genes, *2-H06* and *2-F11*, provide evidence that they are members of a fish-specific gene family, which are components of the elastoidin complex involved in the formation of the actinotrichia. Further study of this gene family during fin bud development and fin regeneration could not only lead to a better understanding of the molecular mechanism underlying the process of formation of the actinotrichia and the composition of elastoidin but also in understanding the evolutionary fin-to-limb transition.

5. REFERENCES

Abe, G., Ide, H., & Tamura, K. (2007). Function of fgf signaling in the developmental process of the median fin fold in zebrafish. *Dev Biol, 304*(1), 355-366.

Ahn, D. G., Kourakis, M. J., Rohde, L. A., Silver, L. M., & Ho, R. K. (2002). T-box gene *tbx5* is essential for formation of the pectoral limb bud. *Nature, 417*(6890), 754-758.

Akimenko, M.-A., Johnson, S. L., Westerfield, M., & Ekker, M. (1995). Differential induction of four *msx* homeobox genes during fin development and regeneration in zebrafish. *Development, 121*, 347-357.

Akimenko, M. A., & Ekker, M. (1995). Anterior duplication of the sonic hedgehog expression pattern in the pectoral fin buds of zebrafish treated with retinoic acid. *Dev Biol, 170*(1), 243-247.

Akimenko, M. A., Ekker, M., Wegner, J., Lin, W., & Westerfield, M. (1994). Combinatorial expression of three zebrafish genes related to distal-less: Part of a homeobox gene code for the head. *J Neurosci, 14*(6), 3475-3486.

Akimenko, M. A., Marí-Beffa, M., Becerra, J., & Géraudie, J. (2003). Old questions, new tools, and some answers to the mystery of fin regeneration. *Dev Dyn, 226*(2), 190-201.

Altabef, M., Clarke, J. D., & Tickle, C. (1997). Dorso-ventral ectodermal compartments and origin of apical ectodermal ridge in developing chick limb. *Development, 124*(22), 4547-4556.

Avaron, F., Hoffman, L., Guay, D., & Akimenko, M. A. (2006). Characterization of two new zebrafish members of the hedgehog family: Atypical expression of a zebrafish indian hedgehog gene in skeletal elements of both endochondral and dermal origins. *Dev Dyn, 235*(2), 478-489.

Bachiller, D., Klingensmith, J., Shneyder, N., Tran, U., Anderson, R., Rossant, J., *et al.* (2003). The role of chordin/bmp signals in mammalian pharyngeal development and Digeorge syndrome. *Development, 130*(15), 3567-3578.

Bauer, D., Muller, H., Reich, J., Riedel, H., Ahrenkiel, V., Warthoe, P., *et al.* (1993). Identification of differentially expressed mRNA species by an improved display technique (DDRT-PCR). *Nucleic Acids Res, 21*(18), 4272-4280.

Becerra, J., Junqueira, L. C., Bechara, I. J., & Montes, G. S. (1996). Regeneration of fin rays in teleosts: A histochemical, radioautographic, and ultrastructural study. *Arch Histol Cytol, 59*(1), 15-35.

Becerra, J., Montes, G. S., Bexiga, S. R. R., & Junqueira, J. C. U. (1983). Structure of the tail fin in teleosts. *Cell Tissue Res., 230*, 127-137.

Bechara, I. J., Joazeiro, P. P., Marí-Beffa, M., Becerra, J., & Montes, G. S. (2000). Collagen-affecting drugs impair regeneration of teleost tail fins. *J. Submicrosc. Cytol. Pathol., 32*, 273-280.

Beis, D., & Stainier, D. Y. (2006). In vivo cell biology: Following the zebrafish trend. *Trends Cell Biol, 16*(2), 105-112.

Bella, J., Liu, J., Kramer, R., Brodsky, B., & Berman, H. M. (2006). Conformational effects of gly-x-gly interruptions in the collagen triple helix. *J Mol Biol, 362*(2), 298-311.

Bernhard, Y. M., & Wagner, G. P. (1992). Regeneration in *salaria pavo* (blenniidae, teleostei). *Anat. Embryol., 186*, 153-165.

Brockes, J. P., & Kumar, A. (2002). Plasticity and reprogramming of differentiated cells in amphibian regeneration. *Nat Rev Mol Cell Biol, 3*, 566-574.

Bullock, A., Marks, R., & Roberts, R. (1978). The cell kinetics of teleost fish epidermis: Epidermal mitotic activity in relation to wound healing at varying temperatures in plaice (*pleuronectes platessa*). *J. of Zoology, 185*, 197-204.

Capdevila, J., & Izpisua Belmonte, J. C. (2001). Patterning mechanisms controlling vertebrate limb development. *Annu Rev Cell Dev Biol, 17*, 87-132.

Chandross, R. J. (1982). Structure and packing of dry elastoidin: A collagen phase change. *Coll Relat Res, 2*(4), 331-348.

Chandross, R. J., & Bear, R. S. (1979). Comparison of mammalian collagen and elasmobranch elastoidin fiber structures, based on electron density profiles. *J. Mol. Biol., 130*, 215-229.

Cinquin, O. (2007). Repressor dimerization in the zebrafish somitogenesis clock. *PLoS Comput Biol, 3*(2), e32.

Coimbra, R. S., Weil, D., Brottier, P., Blanchard, S., Levi, M., Hardelin, J. P., *et al.* (2002). A subtracted cDNA library from the zebrafish (*Danio rerio*) embryonic inner ear. *Genome Res, 12*(6), 1007-1011.

Corey, D. R., & Abrams, J. M. (2001). Morpholino antisense oligonucleotides: Tools for investigating vertebrate development. *Genome Biol, 2*(5), 1015.

Crossley, P. H., & Martin, G. R. (1995). The mouse *fgf-8* gene encodes a family of polypeptides and is expressed in regions that direct outgrowth and patterning in the developing embryo. *Development, 121*, 439-451.

Crossley, P. H., Minowada, G., McArthur, C. A., & Martin, G. R. (1996). Roles for fgf8 in the induction, initiation and maintenance of chick limb development. *Cell, 84*, 127-136.

Damodaran, M., Sivaraman, C., & Dhavalikar, R. S. (1956). Amino acid composition of elastoidin. *Biochem J, 62*(4), 621-625.

Dane, P. J., & Tucker, J. B. (1985). Modulation of epidermal cell shaping and extracellular matrix during caudal fin morphogenesis in the zebrafish *brachydanio rerio*. *J. Embryol. Exp. Morph., 87*, 145-162.

Diatchenko, L., Lau, Y. F., Campbell, A. P., Chenchik, A., Moqadam, F., Huang, B., *et al.* (1996). Suppression subtractive hybridization: A method for generating differentially regulated or tissue-specific cDNA probes and libraries. *Proc Natl Acad Sci U S A, 93*(12), 6025-6030.

Draper, B. W., Stock, D. W., & Kimmel, C. B. (2003). Zebrafish fgf24 functions with fgf8 to promote posterior mesodermal development. *Development, 130*(19), 4639-4654.

Driever, W., Stemple, D., Schier, A., & Solnica-Krezel, L. (1994). Zebrafish: Genetic tools for studying vertebrate development. *Trends Genetics, 10*, 152-159.

Dubois, G. M., Haftek, Z., Crozet, C., Garrone, R., & Le Guellec, D. (2002). Structure and spatio temporal expression of the full length DNA complementary to RNA coding for alpha2 type I collagen of zebrafish. *Gene, 294*(1-2), 55-65.

Ekker, M., Akimenko, M.-A., Bremiller, R., & Westerfield, M. (1992). Regional expression of three homeobox transcripts in the inner ear of zebrafish embryos. *Neuron, 9*, 27-35.

Ekker, S. C. (2000). Morphants: A new systematic vertebrate functional genomics approach. *Yeast, 17*, 302-306.

Ekker, S. C., & Larson, J. D. (2001). Morphant technology in model developmental systems. *Genesis, 30*(3), 89-93.

Ferretti, P., & Géraudie, J. (1995). Retinoic acid-induced cell death in the wound epidermis of regenerating zebrafish fins. *Dev Dyn, 202*(3), 271-283.

Fischer, S., Draper, B. W., & Neumann, C. J. (2003). The zebrafish fgf24 mutant identifies an additional level of fgf signaling involved in vertebrate forelimb initiation. *Development, 130*, 3515-3524.

Fisher, S., Jagadeeswaran, P., & Halpern, M. E. (2003). Radiographic analysis of zebrafish skeletal defects. *Dev Biol, 264*(1), 64-76.

Francis, P. H., Richardson, M. K., Brickell, P. M., & Tickle, C. (1994). Bone morphogenetic proteins and a signalling pathway that controls patterning in the developing chick limb. *Development, 120*, 209-218.

Fürthauer, M., Thisse, C., & Thisse, B. (1997). A role for fgf-8 in the dorsoventral patterning of the zebrafish gastrula. *Development, 124*, 4253-4264.

Geisler, R., Rauch, G.-J., Baier, H., van Bebber, F., Brob, L., dekens, M. P. S., *et al.* (1999). A radiation hybrid map of the zebrafish genome. *Nature Genetics, 23*, 86-89.

Géraudie, J. (1977). Initiation of the actinotrichial development in the early fin bud of the fish, *salmo. J. Morphol., 151*, 353-361.

Géraudie, J. (1980). Mitotic activity in the pseudoapical ridge of the trout pelvic fin bud, *salmo gairdneri. J. Exp. Zool., 214*, 311-316.

Géraudie, J. (1985). Innervation of the early pelvic fin bud of the trout embryo, *salmo gairdneri. J. Morphol., 184*, 61-73.

Géraudie, J., & François, Y. (1973). [first stages of the formation of the pelvic fin anlage in the trout (*Salmo fario* and *Salmo gairdneri*). I. Anatomical study]. *J Embryol Exp Morphol, 29*(1), 221-237.

Géraudie, J., & Landis, W. J. (1982). The fine structure of the developing pelvic fin dermal skeleton in the trout *Salmo gairdneri. Am J Anat, 163*(2), 141-156.

Géraudie, J., & Singer, M. (1992). The fish fin regenerate. In C. H. Taban & B. Boilly (Eds.), *Fishes and amphibians.* (Vol. 23, pp. 62-72). Basel: S. Karger.

Géraudie, J., Brulfert, A., Monnot, M.-J., & Ferretti, P. (1994). Teratogenic and morphogenetic effects of retinoic acid on the regenerating pectoral fin in zebrafish. *J. Exp. Zool., 269*, 12-22.

Géraudie, J., Monnot, M. J., Brulfert, A., & Ferretti, P. (1995). Caudal fin regeneration in wild type and long-fin mutant zebrafish is affected by retinoic acid. *Int J Dev Biol, 39*(2), 373-381.

Géraudie, J., & Ferretti, P. (1997). Correlation between RA-induced apoptosis and patterning defects in regenerating fins and limbs. *Int. J. Dev. Biol., 41*, 529-532.

Géraudie, J., & Ferretti, P. (1998). Gene expression during amphibian limb regeneration. *Int Rev Cytol, 180*, 1-50.

Goss, R. J. (1969). Regeneration in fishes. In R. J. Goss (Ed.), *Principles of regeneration.* (pp. 113-139.): New York: Academic Press Inc.

Goss, R. J., & Stagg, M. W. (1957). The regeneration of fins and fin rays in *Fundulus heteroclitus. J. Exp. Zool., 136*, 487-508.

Grandel, H., & Schulte-Merker, S. (1998). The development of the paired fins in the zebrafish (*Danio rerio*). *Mechanisms of Dev., 79*, 99-120.

Grandel, H., Draper, B. W., & Schulte-Merker, S. (2000). Dackel acts in the ectoderm of the zebrafish pectoral fin bud to maintain AER signaling. *Development, 127*(19), 4169-4178.

Gross, J., & Dumsha, B. (1958). Elastoidin: A two component member of the collagen class. *Biochim Biophys Acta, 28*(2), 268-270.

Hukriede, N., Fisher, D., Epstein, J., Joly, L., Tellis, P., Zhou, Y., *et al.* (2001). The Ln54 radiation hybrid map of zebrafish expressed sequences. *Genome Res, 11*(12), 2127-2132.

Hukriede, N. A., Joly, L., Tsang, M., Miles, J., Tellis, P., Epstein, J. A., *et al.* (1999). Radiation hybrid mapping of the zebrafish genome. *Proc. Natl. Acad. Sci. USA, 96*, 9745-9750.

Johnson, R. L., Riddle, R. D., & Tabin, C. J. (1994). Mechanisms of limb patterning. *Curr Opin Genet Dev, 4*(4), 535-542.

Johnson, S. L., & Bennett, P. (1999). Growth control in the ontogenetic and regenerating zebrafish fin. *Methods Mol Biol, 59*, 301-311.

Jones, B. B., Ohno, C. K., Allenby, G., Boffa, M. B., Levin, A. A., Grippo, J. F., *et al.* (1995). New retinoid x receptor subtypes in zebrafish (*Danio rerio*) differentially modulate transcription and do not bind 9-cis retinoic acid. *Mol. Cell. Biol., 15*, 5226-5234.

Junqueira, L. C., Montes, G. S., Kaupert, D., Shigihara, K. M., Bolonhani, T. M., & Krisztan, R. M. (1981). Morphological and histochemical studies on the collagen in neurinomas, neurofibromas, and fibromas. *J Neuropathol Exp Neurol, 40*(2), 123-133.

Kawakami, A., Fukazawa, T., & Takeda, H. (2004). Early fin primordia of zebrafish larvae regenerate by a similar growth control mechanism with adult regeneration. *Dev Dyn, 231*(4), 693-699.

Kimmel, C. B., Ballard, W. W., Kimmel, S. R., Ullmann, B., & Schilling, T. F. (1995). Stages of embryonic development of the zebrafish. *Developmental Dynamics, 203*, 253-310.

Kimura, S. (1992). Wide distribution of the skin type I collagen alpha 3 chain in bony fish. *Comp Biochem Physiol B, 102*(2), 255-260.

Kimura, S., & Kubota, M. (1966). Studies on elastoidin. I. Some chemical and physical properties of elastoidin and its components. *J Biochem (Tokyo), 60*(6), 615-621.

Kimura, S., & Kubota, M. (1969). Tyrosine derivatives in a structural protein, elastoidin. *J Biochem (Tokyo), 65*(1), 141-143.

Kimura, S., Miyauchi, Y., & Uchida, N. (1991). Scale and bone type I collagens of carp (*Cyprinus carpio*). *Comp Biochem Physiol B, 99*(2), 473-476.

Kimura, S., Ohno, Y., Miyauchi, Y., & Uchida, N. (1987). Fish skin type I collagen: Wide distribution of an alpha 3 subunit in teleosts. *Comp Biochem Physiol B, 88*(1), 27-34.

Kimura, S., Uematsu, Y., & Miyauchi, Y. (1986). Shark (*Prionace glauca*) elastoidin: Characterization of its collagen as [alpha 1(E)]3 homotrimers. *Comp Biochem Physiol B, 84*(3), 305-308.

Knapik, E. W., Goodman, A., Ekker, M., Chevrette, M., Delgado, J., Neuhauss, S., *et al.* (1998). A microsatellite genetic linkage map for zebrafish (*Danio rerio*). *Nat Genet, 18*(4), 338-343.

Krauss, S., Concordet, J. P., & Ingham, P. W. (1993). A functionally conserved homolog of the *Drosophila* segment polarity gene *hh* is expressed in tissues with polarizing activity in zebrafish embryos. *Cell, 75*(7), 1431-1444.

Laforest, L., Brown, C. W., Poleo, G., Géraudie, J., Tada, M., Ekker, M., *et al.* (1998). Involvement of the *sonic hedgehog, patched 1* and *bmp2* genes in patterning of the zebrafish dermal fin rays. *Development, 125*, 4175-4184.

Lewis, J. (2003). Autoinhibition with transcriptional delay: A simple mechanism for the zebrafish somitogenesis oscillator. *Curr Biol, 13*(16), 1398-1408.

Liang, P., & Pardee, A. B. (1992). Differential display of eukaryotic messenger RNA by means of the polymerase chain reaction. *Science, 257*(5072), 967-971.

Marí-Beffa, M., Carmona, M. C., & Becerra, J. (1989). Elastoidin turn-over during tail fin regeneration in teleosts. A morphometric and radioautographic study. *Anat Embryol (Berl), 180*(5), 465-470.

Marí-Beffa, M., Mateos, I., Palmqvist, P., & Becerra, J. (1996a). Cell to cell interactions during teleosts fin regeneration. *Int J Dev Biol, Suppl 1*, 179S-180S.

Marí-Beffa, M., Palmqvist, P., Marin-Giron, F., Montes, G. S., & Becerra, J. (1999). Morphometric study of the regeneration of individual rays in teleost tail fins. *J. Anat., 195*, 393-405.

Marí-Beffa, M., Santamaría, J. A., Fernandez-Llebrez, P., & Becerra, J. (1996b). Histochemically defined cell states during tail fin regeneration in teleost fishes. *Differentiation, 60*, 139-149.

Marigo, V., Scott, M. P., Johnson, R. L., Goodrich, L. V., & Tabin, C. J. (1996). Conservation in *hedgehog* signaling: Induction of a chicken *patched* homolog by *sonic hedgehog* in the developing limb. *Development, 122*, 1225-1233.

Metscher, B. D., Takahashi, K., Crow, K., Amemiya, C., Nonaka, D. F., & Wagner, G. P. (2005). Expression of hoxa-11 and hoxa-13 in the pectoral fin of a basal ray-finned fish, *Polyodon spathula*: Implications for the origin of tetrapod limbs. *Evol Dev, 7*(3), 186-195.

Michaud, J. L., Lapointe, F., & Le Douarin, N. M. (1997). The dorsoventral polarity of the presumptive limb is determined by signals produced by the somites and by the lateral somatopleure. *Development, 124*(8), 1453-1463.

Miles, C. A., Sionkowska, A., Hulin, S. L., Sims, T. J., Avery, N. C., & Bailey, A. J. (2000). Identification of an intermediate state in the helix-coil degradation of collagen by ultraviolet light. *J Biol Chem, 275*(42), 33014-33020.

Montes, G. S., Becerra, J., Toledo, O. M. S., Gordilho, M. A., & Junqueira, L. C. U. (1982). Fine structure and histochemistry of the tail fin rays in teleosts. *Histochemistry, 75*, 363-376.

Morgan, T. H. (1900). Regeneration in teleosts. *Arch. Entw. Mech. Org, 10*, 120-131.

Morgan, T. H. (1902). Further experiments on the regeneration of the tail of fishes. *Arch. Entw. Mech. Org, XIV*, 539-561.

Moss, M. L. (1963). The biology of acellular teleost bone. *Ann. Nat. Acad. Sci., 109*, 337-350.

Mullins, M. C., & Nüsslein-Volhard, C. (1993). Mutational approaches to studying embryonic pattern formation in the zebrafish. *Curr. Opin. Genet. Dev., 3*, 648-654.

Muneoka, K., & Bryant, S. V. (1982). Evidence that patterning mechanisms in developing and regenerating limbs are the same. *Nature, 298*(5872), 369-371.

Muneoka, K., & Sassoon, D. (1992). Molecular aspects of regeneration in developing vertebrate limbs. *Developmental Biology, 152*, 37-49.

Nakayama, N., Han, C. Y., Cam, L., Lee, J. I., Pretorius, J., Fisher, S., *et al.* (2004). A novel chordin-like bmp inhibitor, chl2, expressed preferentially in chondrocytes of developing cartilage and osteoarthritic joint cartilage. *Development, 131*(1), 229-240.

Nasevicius, A., & Ekker, S. C. (2000). Effective targeted gene 'knockdown' in zebrafish. *Nat Genet, 26*(2), 216-220.

Nechiporuk, A., & Keating, M. (2002). A proliferation gradient between proximal and msxb-expressing distal blastema directs zebrafish fin regeneration. *Development, 129*, 2607-2617.

Neumann, C. J., Grandel, H., Gaffield, W., Schulte-Merker, S., & Nusslein-Volhard, C. (1999). Transient establishment of antero-posterior polarity in the zebrafish pectoral fin bud in the absence of *sonic hedgehog* activity. *Development, 126*, 4817-4826.

Ng, J. K., Kawakami, Y., Buscher, D., Raya, A., Itoh, T., Koth, C. M., *et al.* (2002). The limb identity gene *tbx5* promotes limb initiation by interacting with *wnt2b* and *fgf10*. *Development, 129*(22), 5161-5170.

Ng, J. K., Tamura, K., Buscher, D., & Izpisua-Belmonte, J. C. (1999). Molecular and cellular basis of pattern formation during vertebrate limb development. *Curr Top Dev Biol, 41*, 37-66.

Nili, E., Cojocaru, G. S., Kalma, Y., Ginsberg, D., Copeland, N. G., Gilbert, D. J., *et al.* (2001). Nuclear membrane protein lap2beta mediates transcriptional repression alone and together with its binding partner gcl (germ-cell-less). *J Cell Sci, 114*(Pt 18), 3297-3307.

Niswander, L., & Martin, G. R. (1992). Fgf-4 expression during gastrulation, myogenesis, limb and tooth development in the mouse. *Development, 114*(3), 755-768.

Nomura, R., Kamei, E., Hotta, Y., Konishi, M., Miyake, A., & Itoh, N. (2006). Fgf16 is essential for pectoral fin bud formation in zebrafish. *Biochem Biophys Res Commun, 347*(1), 340-346.

Norton, W. H., Ledin, J., Grandel, H., & Neumann, C. J. (2005). Hspg synthesis by zebrafish *ext2* and *extl3* is required for fgf10 signalling during limb development. *Development, 132*(22), 4963-4973.

Nuesslein-Volhard, C., & Dahm, R. (2002). *Zebrafish* (First ed.). Oxford: Oxford University Press.

Nusslein-Volhard, C., & Dahm, R. (2002). Zebrafish - a practical approach: Oxford University Press.

Nye, H. L. D., Cameron, J. A., Chernoff, E. A. G., & Stocum, D. L. (2003). Regeneration of the urodele limb: A review. *Developmental Dynamics, 226*, 280-294.

Odelberg, S. J., Kollhoff, A., & Keating, M. T. (2000). Dedifferentiation of mammalian myotubes induced by msx1. *Cell, 103*, 1099-1109.

Padhi, B. K., Joly, L., Tellis, P., Smith, A., Nanjappa, P., Chevrette, M., *et al.* (2004). Screen for genes differentially expressed during regeneration of the zebrafish caudal fin. *Dev Dyn, 231*(3), 527-541.

Panman, L., & Zeller, R. (2003). Patterning the limb before and after shh signalling. *J.Anat., 202*, 3-12.

Piccolo, S., Sasai, Y., Lu, B., & De Robertis, E. M. (1996). Dorsoventral patterning in *Xenopus*: Inhibition of ventral signals by direct binding of chordin to bmp-4. *Cell, 86*(4), 589-598.

Pillai, R., Coverdale, L. E., Dubey, G., & Martin, C. C. (2004). Histone deacetylase 1 (hdac1) required for the normal formation of craniofacial cartilage and pectoral fins of zebrafish. *Developmental Dynamics, 231*, 647-654.

Pizette, S., & Niswander, L. (1999). Bmps negatively regulate structure and function of the apical ectodermal ridge. *Development, 126*, 883-894.

Poleo, G., Brown, C. W., Laforest, L., & Akimenko, M.-A. (2001). Cell proliferation and movement during early fin regeneration in zebrafish. *Dev. Dynamics, 221*, 380-390.

Poss, K. D., Keating, M. T., & Nechiporuk, A. (2003). Tales of regeneration in zebrafish. *Developmental Dynamics, 226*, 202-210.

Ramachandran, L. K. (1962). Elastoidin--a mixture of three proteins. *Biochem Biophys Res Commun, 6*, 443-448.

Reifers, F., Bohli, H., Walsh, E. C., Crossley, P. H., Stainier, D. Y. R., & Brand, M. (1998). *Fgf8* is mutated in zebrafish *acerebellar* (*ace*) mutants and is required for maintenance of midbrain-hindbrain boundary development and somitogenesis. *Development, 125*, 2381-2395.

Ricard-Blum, S., & Ruggiero, F. (2005). The collagen superfamily: From the extracellular matrix to the cell membrane. *Pathol Biol (Paris), 53*(7), 430-442.

Riddle, R. D., Johnson, R. L., Laufer, E., & Tabin, C. (1993). *Sonic hedgehog* mediates the polarizing activity of the ZPA. *Cell, 75*, 1401-1416.

Riley, B. B., Savage, M. P., Simandl, B. K., Olwin, B. B., & Fallon, J. F. (1993). Retroviral expression of fgf-2 (bfgf) affects patterning in chick limb bud. *Development, 118*(1), 95-104.

Roy, S., & Levesque, M. (2006). Limb regeneration in axolotl: Is it superhealing? *ScientificWorldJournal, 6*, 12-25.

Sambrook, J., & Russell, D. (2001). *Molecular cloning* (Third Edition). Cold Spring Harbor, New York: Cold Spring Harbor Laboratory Press.

Santamaria, J., & Becerra, J. (1991). Tail fin regeneration in teleosts: Cell-extracellular matrix interaction in blastemal differentiation. *J. Anat., 176*, 9-21.

Santamaria, J. A., Marí-Beffa, M., & Becerra, J. (1992). Interactions of the lepidotrichial matrix components during tail fin regeneration in teleosts. *Differentiation, 49*(3), 143-150.

Santamaría, J. A., Marí-Beffa, M., & Becerra, J. (1992). Interactions of the lepidotrichial matrix components during tail fin regeneration in teleosts. *Differentiation, 49*, 143-150.

Santamaria, J. A., Marí-Beffa, M., Santos-Ruiz, L., & Becerra, J. (1996a). Incorporation of bromodeoxyuridine in regenerating fin tissue of the goldfish *Carassius auratus*. *J Exp Zool, 275*(4), 300-307.

Santamaria, J. A., Santos Ruiz, L., & Becerra, J. (1996b). An antiserum against ceratotrichia (selachian) recognizes actinotrichia in teleost regenerating fins. *Int. J. Dev. Biol., Suppl 1*, 175S-176S.

Santos Ruiz, L., Santamaria, J. A., & Becerra, J. (1996). Cell proliferation in fin fish regeneration. *Int J Dev Biol, Suppl 1*, 183S-184S.

Sastry, L. V., & Ramachandran, L. K. (1965). The protein components of elastoidin. *Biochim Biophys Acta, 97*, 281-287.

Saunders, J. W., & Gasseling, M. T. (1968). *Ectodermal-mesenchymal interactions in the origin of limb symmetry.* Baltimore: Williams & Wilkins.

Saunders, J. W., Jr. (1998). Apical ectodermal ridge in retrospect. *J Exp Zool, 282*(6), 669-676.

Schoft, V. K., Beauvais, A. J., Lang, C., Gajewski, A., Prufert, K., Winkler, C., *et al.* (2003). The lamina-associated polypeptide 2 (lap2) isoforms beta, gamma and omega of zebrafish: Developmental expression and behavior during the cell cycle. *J Cell Sci, 116*(Pt 12), 2505-2517.

Simon, H. G., Kittappa, R., Khan, P. A., Tsilfidis, C., Liversage, R. A., & Oppenheimer, S. (1997). A novel family of t-box genes in urodele amphibian limb development and regeneration: Candidate genes involved in vertebrate forelimb/hindlimb patterning. *Development, 124*(7), 1355-1366.

Snellman, A., Tuomisto, A., Koski, A., Latvanlehto, A., & Pihlajaniemi, T. (2007). The role of disulfide bonds and alpha-helical coiled-coils in the biosynthesis of type XIII collagen and other collagenous transmembrane proteins. *J Biol Chem, 282*(20), 14898-14905.

Sordino, P., van der Hoeven, F., & Duboule, D. (1995). *Hox* gene expression in teleost fins and the origin of vertebrate digits. *Nature, 375*, 678-681.

Special morpholino issue genesis. (2001). *The Journal of Genetics and Development, 30*(3).

Strähle, U., Blader, P., Adam, J., & Ingham, P. W. (1994). A simple and efficient procedure for non-isotopic in situ hybridization to sectioned material. *Trends Genet, 10*(3), 75-76.

Stringer, H. W., and Highton, T. C. (1960). The shrinkage temperature of skin collagen. *Australasian Journal of Dermatology, 5*(4), 230-234.

Summerbell, D. (1974). Interaction between the proximo-distal and antero-posterior co-ordinates of positional value during the specification of positional information in the early development of the chick limb-bud. *J Embryol Exp Morphol, 32*(1), 227-237.

Summerbell, D., Lewis, J. H., & Wolpert, L. (1973). *Nature, 224*, 492-496.

Summerton, J. (1999). Morpholino antisense oligomers: The case for an RNase-H-independent structural type. *Biochem. Biophys. Acta, 1489*, 141-158.

Summerton, J., & Weller, D. (1997). Morpholino antisense oligomers: Design, preparation, and properties. *Antisense & nucleic acid drug development., 7*, 187-195.

Suzuki, H. R., Sakamoto, H., Yoshida, T., Sugimura, T., Terada, M., & Solursh, M. (1992). Localization of hsti transcripts to the apical ectodermal ridge in the mouse embryo. *Dev Biol, 150*(1), 219-222.

Thisse, B., Heyer, V., Lux, A., Alunni, V., Degrave, A., Seiliez, I., *et al.* (2004). Spatial and temporal expression of the zebrafish genome by large-scale in situ hybridization screening. *Methods Cell Biol, 77*, 505-519.

Thorogood, P. (1991). The development of the teleost fin and implications for our understanding of tetrapod limb evolution. In J. R. Hinchliffe (Ed.), *Developmental patterning of the vertebrate limb* (pp. 347-353). New York: Plenum Press.

Thorpe, C. J., Weidinger, G., & Moon, R. T. (2005). Wnt/beta-catenin regulation of the sp1-related transcription factor sp5l promotes tail development in zebrafish. *Development, 132*(8), 1763-1772.

Tsonis, P. A., Del Rio-Tsonis, K., Wallace, J. L., Burns, J. C., Hofmann, M. C., Millan, J. L., *et al.* (1996). Can insights into urodele limb regeneration be achieved with cell cultures and retroviruses? *Int J Dev Biol, 40*(4), 813-816.

van de Loo, J. W., Creemers, J. W., Bright, N. A., Young, B. D., Roebroek, A. J., & Van de Ven, W. J. (1997). Biosynthesis, distinct post-translational modifications, and functional characterization of lymphoma proprotein convertase. *J Biol Chem, 272*(43), 27116-27123.

Venkatesh, B., Kirkness, E. F., Loh, Y. H., Halpern, A. L., Lee, A. P., Johnson, J., *et al.* (2007). Survey sequencing and comparative analysis of the elephant shark (*Callorhinchus milii*) genome. *PLoS Biol, 5*(4), e101.

Vogel, A., & Tickle, C. (1993). Fgf-4 maintains polarizing activity of posterior limb bud cells in vivo and in vitro. *Development, 119*(1), 199-206.

Westerfield, M. (1995). *The zebrafish book.* Eugene: University of Oregon Press.

White, J. A., Boffa, M. B., Jones, B., & Petkovich, M. (1994). A zebrafish retinoic acid receptor expressed in the regenerating caudal fin. *Development, 120*, 1861-1872.

Wood, A. (1982). Early pectoral fin development and morphogenesis of the apical ectodermal ridge in the killifish, *Aphyosemion scheeli. Anat Rec, 204*(4), 349-356.

Wood, A., & Thorogood, P. (1984). An analysis of in vivo cell migration during teleost fin morphogenesis. *J. Cell Sci., 66*, 205-222.

Yamaguchi, K., Francis-West, P. H., Shiraishi, K., & Akita, K. (2004). Premature regression of the leg apical ectodermal ridge in the japanese chick wingless mutant. *Anat Embryol (Berl), 208*(6), 487-497.

Yan, Y. L., Willoughby, J., Liu, D., Crump, J. G., Wilson, C., Miller, C. T., *et al.* (2005). A pair of sox: Distinct and overlapping functions of zebrafish sox9 co-orthologs in craniofacial and pectoral fin development. *Development, 132*(5), 1069-1083.